HHS Public Access

Author manuscript

Chem Res Toxicol. Author manuscript; available in PMC 2017 December 19.

Published in final edited form as:

Chem Res Toxicol. 2016 December 19; 29(12): 2008–2039. doi:10.1021/acs.chemrestox.6b00265.

Occurrence, Biological Consequences, and Human Health Relevance of Oxidative Stress-Induced DNA Damage

Yang Yu[†], **Yuxiang Cui**[†], **Laura J. Niedernhofer**[§], and **Yinsheng Wang**[*,†,‡]

[†]Environmental Toxicology Graduate Program, University of California, Riverside, California 92521, United States

[‡]Department of Chemistry, University of California, Riverside, California 92521, United States

[§]Department of Metabolism and Aging, The Scripps Research Institute Florida, Jupiter, Florida 33458, United States

Abstract

A variety of endogenous and exogenous agents can induce DNA damage and lead to genomic instability. Reactive oxygen species (ROS), an important class of DNA damaging agents, are constantly generated in cells as a consequence of endogenous metabolism, infection/inflammation, and/or exposure to environmental toxicants. A wide array of DNA lesions can be induced by ROS directly, including single-nucleobase lesions, tandem lesions, and hypochlorous acid (HOCl)/hypobromous acid (HOBr)-derived DNA adducts. ROS can also lead to lipid peroxidation, whose byproducts can also react with DNA to produce exocyclic DNA lesions. A combination of bioanalytical chemistry, synthetic organic chemistry, and molecular biology approaches have provided significant insights into the occurrence, repair, and biological consequences of oxidatively induced DNA lesions. The involvement of these lesions in the etiology of human diseases and aging was also investigated in the past several decades, suggesting that the oxidatively induced DNA adducts, especially bulky DNA lesions, may serve as biomarkers for exploring the role of oxidative stress in human diseases. The continuing development and improvement of LC-MS/MS coupled with the stable isotope-dilution method for DNA adduct quantification will further promote research about the clinical implications and diagnostic applications of oxidatively induced DNA adducts.

Graphical abstract

[*]Corresponding Author Tel: 951-827-2700. Yinsheng.Wang@ucr.edu.

Notes: The authors declare no competing financial interest.

Special Issue: Mass Spectrometry and Emerging Technologies for Biomarker Discovery in the Assessment of Human Health and Disease

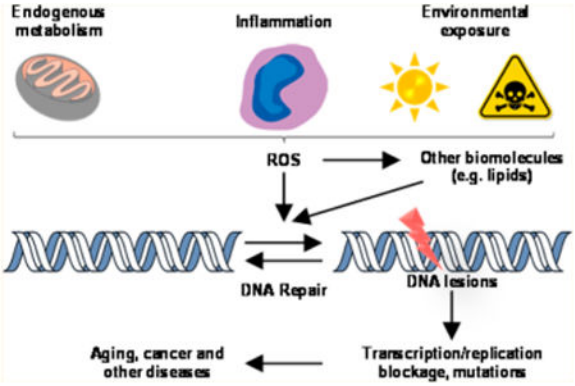

1. Oxidative Stress and ROS

The human genome is constantly exposed to a variety of endogenous and exogenous agents that can generate DNA damage, which may compromise genomic integrity.[1] Reactive oxygen species (ROS) constitute an important class of DNA damaging agents, and they are continuously generated in cells as a consequence of endogenous metabolism and/or exposure to environmental toxicants.[2] ROS encompass a variety of chemical species, e.g., superoxide anion radical ($O_2^{-\bullet}$), hydrogen peroxide (H_2O_2), hydroxyl radical ($^{\bullet}OH$), and singlet oxygen ($^1O_2$). In this vein, mitochondrion is considered a major source of ROS production in cells, where electrons leaking from the electron transport chain during mitochondrial respiration can combine with molecular oxygen to generate $O_2^{-\bullet}$, which can be subsequently converted to H_2O_2 by superoxide dismutase (SOD).[3] H_2O_2, which diffuses freely in the cellular environment, may react with the reduced-state transition metal ions to give $^{\bullet}OH$ via the Fenton-type reactions:[4]

$$Cu^{+}/Fe^{2+}+H_2O_2 \rightarrow Cu^{2+}/Fe^{3+}+{}^{\bullet}OH+OH^{-}$$

Oxidation of biomolecules depends on the location of ROS production and the redox potential of the biomolecules. Some of the aforementioned ROS, such as $O_2^{-\bullet}$ and $^{\bullet}OH$, are extremely unstable, whereas others, like H_2O_2, are relatively long-lived.[2,5,6]

Infection and inflammation activate inflammatory cells, which induce and activate various oxidant-generating enzymes.[7] Activated inflammatory cells produce $O_2^{-\bullet}$ through nicotinamide adenine dinucleotide phosphate (NADPH) oxidase complexes or xanthine oxidase, and these cells release high concentrations of oxidant-generating enzymes such as myeloperoxidase and eosinophil peroxidase through degranulation.[7–11] These enzymes produce high concentrations of reactive oxygen, nitrogen, and halogen species such as superoxide anion, nitric oxide, peroxynitrite, hydrogen peroxide, hypochlorous acid, and hypobromous acid at sites of inflammation.[7,12] Although intended to neutralize invading pathogens, these reactive chemical species can result in collateral DNA damage of host cells.

Aside from damaging DNA directly, ROS may also lead to DNA damage indirectly, through reaction with lipids, proteins, and other cellular components to produce electrophilic species

that can react with DNA.[13,14] In particular, peroxidation of polyunsaturated fatty acids (PUFA) can give rise to a multitude of reactive aldehydes that can conjugate with DNA to yield DNA adducts.[13,14] In this vein, DNA is susceptible to electrophilic attack because it contains many nucleophilic sites, including the *N*1, N^2, *N*3, *N*7, and O^6 of guanine; the *N*1, *N*3, N^6, and *N*7 of adenine; the O^2, *N*3, and O^4 of thymine; and the O^2, *N*3, and N^4 of cytosine.[15,16]

In this review, we will discuss common types of oxidatively induced DNA lesions, including single-nucleobase lesions and tandem lesions that arise from direct ROS attack, as well as indirect ROS-induced DNA damage, such as those induced by inflammation and byproducts of lipid peroxidation. The emphasis is placed on their chemical mechanisms of formation, biological consequences, and human health relevance. In addition, we will discuss cellular replication and transcription studies of these lesions as well as their repair pathways and detection.

2. Chemistry of Oxidative Stress-Induced DNA Damage

2.1. Direct ROS-Induced DNA Lesions

2.1.1. Single-Nucleobase Lesions—•OH is highly reactive toward DNA; it can readily abstract a hydrogen atom from 2-deoxyribose or methyl group on nucleobases or be added to double bonds of purine and pyrimidine bases. Addition of hydroxyl radical to guanine leads to the formation of adduct radicals on the C4, C5, and C8 atoms, which have been previously reviewed.[17] One-electron oxidation of the resulting C8-OH adduct radical gives rise to the formation of 8-oxo-7,8-dihydro-2′-deoxyguanosine (8-oxo-dG, Figure 1), which was first reported in the 1980s.[18] The C8-OH adduct radical of guanine can also undergo an intramolecular ring opening of its imidazole moiety by the cleavage of the C8–N7 bond, followed by one-electron reduction, to yield 2,6-diamino-4-hydroxy-5-formamidopyrimidine 2′-deoxynucleoside (Fapy-dG, Figure 1). Alternatively, one-electron reduction may also occur prior to the imidazole ring-opening process, generating 7-hydro-8-hydroxy-2′-deoxyguanosine, which subsequently undergoes ring-opening to form Fapy-dG.[19,20] Similarly, the reaction between 2′-deoxyadenosine (dA) and hydroxyl radical gives 8-oxo-7,8-dihydro-2′-deoxyadenosine (8-oxo-dA)[21] and 4,6-diamino-5-formamidopyrimidine 2′-deoxynucleoside (Fapy-dA).[20] Apart from hydroxyl radical attack, singlet oxygen ($^1O_2$) may also oxidize dG to yield 8-oxo-dG. In this vein, ^{18}O-labeled 8-oxo-dG could be detected in DNA isolated from cells incubated with water-soluble ^{18}O-labeled nonionic 1,4-endoperoxide *N*,*N*′-di(2,3-dihydroxypropyl)-1,4-naphthalene-dipropanamide (DHPN$^{18}O_2$), whose thermal decomposition gives ^{18}O-labeled singlet oxygen.[22] The above-mentioned DNA adducts have already been detected at appreciable levels *in vivo* and summarized in previous reviews.[23–28]

Guanine is the most easily oxidized among the four nucleobases in DNA, and a reduction potential of 1.29 V vs NHE was reported for guanosine.[29] Compared to dG, 8-oxo-dG has an even lower reduction potential (0.74 V vs NHE).[30] Indeed, it has been demonstrated that 8-oxo-dG can be readily oxidized by various oxidizing agents including Na_2IrCl_6, γ rays, peroxynitrite, Fenton-like reagents, hypochlorous acid (HOCl), etc.[31–36] One-electron oxidation of 8-oxo-dG can give rise to a radical cation, which can undergo hydration,

deprotonation, and another one-electron oxidation to produce 5-hydroxy-substituted derivative of 8-oxo-dG (5-OH-8-oxo-dG).[31,34] Subsequent oxidation of 5-OH-8-oxo-dG leads to the formation of guanidinohydantoin 2′-deoxynucleoside (dGh), spiroiminodihydantoin 2′-deoxynucleoside (dSp), and various other oxidation products.[31,34] The distributions of these products depend on the reaction context (e.g., nucleoside, single-stranded DNA, double-stranded DNA, and base pairing),[37] oxidizing agents,[32] and reaction conditions (e.g., pH and temperature).[38] Generally speaking, the formation of dGh is favored in duplex DNA, while the formation of dSp is preferred in nucleosides, single-stranded DNA, and G-quadruplex DNA.[39] dGh is the predominant product at acidic pH, while dSp is the major product at higher pH.[40] Under physiological pH, especially within cells where nucleosides, ssDNA, and dsDNA are available, the formation of both dGh and dSp are feasible.

The pyrimidine bases are also prone to attack by free radicals.[15] For instance, the hydroxyl radical can be added to the C5═C6 double bond of thymine and cytosine to yield C5-OH- and C6-OH-adduct radicals (Figure 2).[17] The C5-OH- and C6-OH-adduct radicals can lead to the formation of 5,6-dihydroxy-5,6-dihydrothymidine (thymidine glycol) via different reaction pathways in the presence or absence of O_2 (Figure 2), which was reviewed by Dizdaroglu and Jaruga[41] and Teoule.[42] Similar mechanisms may account for the formation of 5-methyl-2′-deoxycytidine (5-mdC) glycol, which can undergo deamination to yield thymidine glycol.[43–47] The formation of 5-mdC glycol may be involved in the C → T transition mutations occurring at CpG dinucleotide sites, a type of mutation ubiquitously found in human cancers.[48,49] Exposure to ionizing radiation[50,51] and reaction with oxidizing agents, including $KMnO_4$, OsO_4,[52] and Fenton reagents,[47] can result in the formation of thymidine glycol in DNA.

The hydroxyl radical can also abstract a hydrogen atom from the 5-methyl group of thymine and 5-methylcytosine to produce the 5-methyl radical of the two pyrimidine bases (Figures 2 and 3).[17] In addition, the 5-methyl radical may also form from one-electron oxidation of the pyrimidine bases followed by deprotonation.[53,54] The 5-methyl radical can be transformed to produce 5-hydroxymethyl-2′-deoxyuridine (5-hmdU) and 5-formyl-2′-deoxyuridine (5-fdU),[41,42,55] 5-hydroxymethyl-2′-deoxycytidine (5-hmdC), and 5-formyl-2′-deoxycytidine (5-fdC).[53] Along this line, it was found recently that the oxidation of 5-mdC could also be catalyzed by Fe(II)- and 2-oxoglutarate (2-OG)-dependent ten-eleven translocation (TET) family dioxygenases.[56–58] The resulting 5-hmdC, 5-fdC, and 5-carboxyl-2′-deoxycytidine (5-cadC) can be considered as epigenetic marks (Figure 3a).[58–63] In addition, the removal of 5-fdC and 5-cadC by the base excision repair (BER) machinery is thought to play an important role in active cytosine demethylation in mammalian systems.[60,64] Aside from being an oxidation product of thymidine, 5-hmdU may also arise from the deamination of 5-hydroxymethyl-2′-deoxycytidine (5-hmdC).[65,66] In addition, Pfaffeneder et al.[67] reported that TET enzymes could catalyze directly the formation of 5-hmdU from thymidine in the DNA of mouse embryonic stem cells (mESCs), and they also found that the deamination of 5-hmdC did not contribute significantly to the 5-hmdU level in mESCs (Figure 3b).[67] 5-fdU can be formed from thymidine upon exposure to ionizing radiation, one-electron photooxidation, and Fenton-type reactions, and its yield was similar or somewhat lower than that of 8-oxo-dG.[55,68–71]

2.1.2. Tandem Lesions—Apart from the above-mentioned single-nucleobase lesions, ROS may also induce the formation of bulky DNA lesions. In this context, exposure to ROS from a variety of experimental systems was found to induce CC → TT and mCG → TT tandem base substitutions, suggesting that ROS may induce the formation of intrastrand cross-link lesions.[72–75] In addition, Randerath et al.,[76,77] by using thin-layer chromatography (TLC) analysis of ^{32}P-postlabeled DNA digestion products, demonstrated the existence of I (indigenous)-compounds, the bulky DNA modifications which increase markedly with aging in tissues of healthy laboratory animals and are derived from DNA-reactive intermediates arising from nutrient and oxygen metabolism. Especially, the type II I-compounds include several bulky DNA lesions, which are enhanced in kidney DNA of rodents treated with pro-oxidant carcinogen ferric nitrilotriacetate (Fe-NTA) and are identical to these lesions generated in DNA or oligodeoxyribonucleotides (ODNs) treated with Fenton reagents *in vitro*.[76]

Later, a modified ^{32}P-postlabeling assay demonstrated that four type II I-compounds in mammalian tissue DNA are dinucleotides containing the bulky 5′*S* diastereomer of 8,5′-cyclo-2′-deoxyadenosine (cdA) as the 3′ nucleoside.[78] The dinucleotides arise from the incomplete hydrolysis of the phosphodiester bond on the 5′ side of the modified nucleoside with the enzymes used in the ^{32}P-postlabeling assay.[78]

The formation of purine cyclonucleosides (cPus) was proposed to arise from a single hydroxyl radical attack via a two-step mechanism (Figure 4).[79,80] In this respect, the hydroxyl radical abstracts a hydrogen atom from the C5′ of 2-deoxyribose, yielding a carbon-centered radical, which attacks the C8 of adenine or guanine to form a new C–C bond. The resulting conjugate can lose an electron and a proton to give cdA and cdG. Molecular oxygen can inhibit this reaction by directly reacting with the C5′ radical, thereby preventing intramolecular cyclization.[81,82] The above cyclization reaction yields two diastereomers at similar frequencies in calf thymus DNA exposed to ionizing radiation under anaerobic conditions.[83] However, the 5′R diastereomers of cdA and cdG were induced in calf thymus DNA by Fenton-type reagents at markedly higher levels than the 5′S counterparts, with cdG being produced at a higher yield than cdA.[84] Moreover, the cPus could be detected at appreciable levels in cells and animal tissues.[23,85–91]

The ROS-induced tandem DNA lesions with the adjacent nucleobases in the same DNA strand being covalently bonded were also investigated in the past few decades. Earlier studies by Box et al.[92–95] showed the formation of intrastrand nucleobase–nucleobase cross-link lesions with guanine being covalently bonded with its adjacent thymine or cytosine when aqueous solutions of synthetic di- or tetranucleotides were exposed to X or γ rays under anaerobic conditions.

By introducing a photolabile precursor of the 5-methyl radical of thymine and 5-methylcytosine in synthetic dinucleoside monophosphates and ODNs, it was later found that the 5-methyl radical of the two pyrimidine bases can couple with the C8 position of its neighboring guanine and/or adenine to yield intrastrand cross-link lesions.[96–99] Additionally, Zhang et al.[100,101] revealed that an independently generated 5-hydroxy-5,6-dihydrothymidin-6-yl radical can conjugate with the C8 of guanine to give an intrastrand

cross-link lesion in dinucleoside monophosphates and ODNs, though the formation of this lesion in duplex DNA was minimal. These studies provided important mechanistic insights into the ROS-induced formation of the intrastrand cross-link lesions. Furthermore, Zeng et al.[102–104] and Hong et al.[105] found that the UVB irradiation of duplex DNA containing a site-specifically inserted 5-bromocytosine or 5-bromouracil could give rise to efficient formation of intrastrand cross-link products with the C5 position of the pyrimidine base being covalently bonded with the C8 or N^2 position of its neighboring guanine or with the C2, N^6, and C8 position of its adjacent adenine. Together, these photochemical approaches offered a facile synthetic route for the generation of ODNs harboring site-specifically inserted and structurally defined intrastrand cross-link lesions, which are necessary for the characterizations of the repair of these lesions as well as their impact on DNA replication and transcription.

Further investigations were conducted about the formation of nucleobase–nucleobase intrastrand cross-links *in vitro* and *in vivo*. Along this line, Gu et al.[106] showed that exposure of synthetic duplex DNA with γ rays under anaerobic conditions could give rise to the formation of the d(G[8–5]C) intrastrand cross-link. In addition, Zhang et al.[98] observed that treatment of d(5mCG) with γ rays under anoxic conditions could lead to the formation of the d(5mC[5m-8]G) intrastrand cross-link. By using LC-MS/MS, Hong et al.[71] further observed a dose dependent induction of d(G[8–5m]T) in calf thymus DNA upon treatment with the Fenton reagent, with a yield that is 2–3 orders of magnitude lower than that of common single-nucleobase lesions like 8-oxo-dG,5-hmdU and 5-fdU. Moreover, d(G[8–5]C) and d(G[8–5m]T) (Figure 5) could be detected in HeLa S3 cells upon exposure to γ rays, and the yields for these two lesions increase with the dose of γ rays.[107] It was also observed that d(G[8–5m]5mC) (Figure 5)was formed at a higher yield than d(5mC[5m-8]G) in synthetic double-stranded DNA upon treatment with Fenton-type reagents.[108] In addition to the above-mentioned intrastrand cross-links involving two adjacent nucleobases, Crean et al.[109] demonstrated the induction of a nonadjacent intrastrand cross-link lesion between guanine and thymine bases separated by a cytosine in the single-stranded 5′-d(GpCpT)-3′ ODN exposed to a $CO_3^{\bullet-}$ radical. Similarly, the generation of nonadjacent and adjacent cross-link lesions between the C8 of guanine and the *N*3 of thymidine (d(G[8-*N*3]T)) (Figure 5) was observed in 5′-d(GpT)-3′ and 5′-d(GpCpT)-3′ ODN or calf thymus DNA treated with peroxynitrite/carbon dioxide/bicarbonate, in addition to the nitration/oxidation products of guanine such as 8-nitro-2′-deoxyguanosine (8-nitro-dG), 5-guanidino-4-nitroimidazole 2′-deoxynucleoside (dNIm), 8-oxo-dG, and dSp.[110] Further study also demonstrated the formation of these two d(G[8-*N*3]T) lesions in HeLa cells upon one-electron oxidation initiated by intense nanosecond 266 nm laser irradiation.[111]

2.2. Inflammation-Induced DNA Damage

Chronic inflammation is an established risk factor for different types of cancers.[112,113] Inflammatory responses protect human bodies from adverse effects inflicted by pathogens and damaged cells through the generation of reactive oxygen, nitrogen, and halogen species.[12,114] These reactive chemical entities damage proteins and DNA of invaders as well as nearby healthy cells and tissues.[12,112–114] The heme enzyme myeloperoxidase, which is secreted by activated neutrophils and monocytes, employs hydrogen peroxide (H_2O_2) and

chloride ion as substrates to yield hypochlorous acid (HOCl) as the initial product (Figure 6).[115,116] Likewise, eosinophil peroxidase, a structurally related heme protein released by activated eosinophils, preferentially oxidizes bromide to give hypobromous acid (HOBr, Figure 6).[117] In addition, myeloperoxidase-induced production of HOCl is also involved in the formation of brominating species (Figure 6).[117,118]

HOCl and HOBr may lead to mutagenesis by damaging the nucleotide pool or reacting directly with DNA. In this vein, reactions of HOCl and HOBr with uracil produce 5-chlorouracil (5-ClU) and 5-bromouracil (5-BrU, Figure 6),[117,118] respectively, which can be further converted to 5-chloro-2′-deoxyuridine (5-Cl-dU) and 5-bromo-2′-deoxyuridine (5-Br-dU) by thymidine phosphorylase.[119,120] Both 5-Cl-dU and 5-Br-dU are dT analogues, and they can be converted to their corresponding nucleoside triphosphates and incorporated into DNA.[121,122] In addition, bromination of 2′-deoxycytidine leads to the formation of 5-bromo-2′-deoxycytidine (5-Br-dC, Figure 6), which can undergo deamination before being incorporated into DNA as 5-Br-dU.[117,118] Major products arising from the reaction of HOCl with DNA include 5-chloro-2′-deoxycytidine (5-Cl-dC), 5-Cl-dU, 8-chloro-2′-deoxyguanosine (8-Cl-dG), and 8-chloro-2′-deoxyadenosine (8-Cl-dA).[118,123–127] Reaction of HOBr with DNA can lead to the formation of 8-bromo-2′-deoxyguanosine (8-Br-dG), 8-bromo-2′-deoxyadenosine (8-Br-dA), and 5-Br-dU (Figure 6).[118,128–130] Among these halogenated nucleosides, 5-Cl-dC has been the most extensively studied and is considered a biomarker for chronic inflammation.[131,132]

During immune response, activated neutrophils and macrophages can also secrete other reactive chemical species, such as nitric oxide (•NO), which can further react with superoxide ($O_2^{-\bullet}$), leading to the formation of peroxynitrite ($ONOO^-$).[12,133–136] Peroxynitrite is highly reactive toward DNA and may contribute to the cytotoxicity and carcinogenesis associated with excess generation of •NO and $O_2^{-\bullet}$ during chronic inflammation.[137] $ONOO^-$ was found to react preferentially with dG, at a reaction rate that is at least 9 times higher than that of dA, dC, and dT in the nucleoside form.[138] Along this line, previous *in vitro* experiments demonstrated that $ONOO^-$ induced the formation of dNIm (Figure 1) in synthesized ODNs and calf thymus DNA.[110,139] Other *in vitro* studies also illustrated that the nitrogen dioxide radical ($^\bullet NO_2$), produced from photolysis of nitrate with 308 nm nanosecond XeCl laser, could react with guanine neutral radicals (G(-H)•) in aqueous solution of ODNs and calf thymus DNA, leading to the formation of dNIm.[140]

2.3. DNA Damage Formed from Byproducts of Lipid Peroxidation

ROS can also attack biomolecules other than DNA. Specifically, the hydroxyl radical initiates the peroxidative degradation of lipids by abstracting a hydrogen atom from polyunsaturated fatty acids (PUFA).[13,141–148] The resulting lipid radical (L•)is first converted to a lipid peroxyl radical (LOO•) in the presence of O_2, leading to the formation of a lipid hydroperoxide (LOOH) via hydrogen atom abstraction, and finally to an alkoxyl radical (LO•) by the transition metal ion-catalyzed Fenton-type reaction. Further fragmentations of peroxyl and alkoxyl radicals give rise to reactive aldehydes, including malondialdehyde (MDA), acrolein, crotonaldehyde, 2-hexenal, 4-hydroxy-2-hexenal (HHE), 4-hydroxy-2-nonenal (HNE), 4-oxo-2-nonenal (ONE), 4-hydroperoxy-(2*E*)-nonenal

(HPNE), 9,12-dioxo-(10*E*)-dodecenoic acid (DODE), 5,8-dioxo-(10*E*)-octenoic acid (DOOE), 2,4-decadienal (DDE), 4,5-epoxy-(2*E*)-decenal (EDE), etc. (Figure 7)[13,14,148]

The aldehydes formed from lipid peroxidation can react with DNA to generate a variety of DNA adducts (Figure 7).[13,14,148] In this vein, malondialdehyde reacts with guanine, adenine, and cytosine in DNA to form exocyclic pyrimido-[1,2-*α*]purine-10(3*H*)-one-2′-deoxyribose (M_1dG), linear N^6-(3-oxopropenyl)-2′-deoxyadenosine (M_1dA), and N^4-(3-oxopropenyl)-2′-deoxycytidine (M_1dC), respectively (Figure 7).[13] The *α*,*β*-unsaturated LPO products, such as acrolein, crotonaldehyde, and HNE, can lead to the formation of different diastereomers of exocyclic six-membered ring propano adducts in DNA with or without substituted alkyl side chains. The *α*,*β*-unsaturated aldehydes can undergo Michael addition with the N^2-amino group of dG to give N^2-(3-oxopropyl)-dG adducts, followed by cyclization of *N*1 with the aldehyde moiety to generate the corresponding exocyclic 1,N^2-propano-dG products (Acr-dG, Cro-dG, and HNE-dG, etc.).[149] This cyclization is reversible, and the ensuing release of the aldehyde functionality can induce the generation of DNA interstrand cross-links and DNA–protein cross-links.[14,150,151] Along this line, it is worth noting that the unsubstituted Cro-dG can also arise from consecutive reactions of guanine with two molecules of acetaldehyde.[152]

Another type of LPO-induced DNA adduct, etheno adduct, possesses unsaturated five-membered exocyclic rings fused with heterocyclic nucleobases. Previous studies proposed a putative mechanism for the formation of etheno adducts from HNE-derived epoxide intermediate, where the *α*,*β*-unsaturated HNE can be converted to reactive intermediate 2,3-epoxy-4-hydroxynonanal by auto-oxidation or by oxidation with H_2O_2.[143,144,153,154] The resulting reactive epoxy aldehyde can further react with DNA to yield the etheno adducts with or without substituted alkyl side chains, such as 1,N^6-etheno-2′-deoxyadenosine (*ε*dA), 3,N^4-etheno-2′-deoxycytidine (*ε*dC), 1,N^2-etheno-2′-deoxyguanosine (1,N^2-*ε*dG), and N^2,3-etheno-2′-deoxyguanosine (N^2,3-*ε*dG), etc.[143,144,153,154] N^2,3-*ε*dG can also be induced in DNA from exposure to carcinogen vinyl chloride via a similar epoxide initiation mechanism.[155] Additionally, Lee et al.[156,157] demonstrated possible HNE-independent pathways for the formation of 1,N^2-*ε*dG initiated from either another LPO product EDE or HNE precursor HPNE, suggesting the existence of probable controversies concerning the mechanism for the formation of etheno DNA adducts *in vivo*. The above-mentioned DNA adducts emanating from products of LPO could be detected at appreciable levels *in vivo*.[88,152,158–174]

3. Repair and Biological Consequences of Oxidative Stress-Induced DNA Lesions

To minimize mutation induction and to maintain genome integrity, cells are equipped with multiple DNA repair systems to enable efficient removal of DNA lesions from the genome. Unrepaired DNA lesions may elicit cytotoxic and mutagenic effects by perturbing the accuracy and efficiency of DNA replication and transcription. Chemical synthesis of ODNs harboring site-specifically inserted and structurally defined DNA lesions, along with *in vitro* biochemical assay and shuttle vector-based cellular experiments, has provided important

insights into how the oxidative stress-induced DNA lesions are repaired and how they compromise the flow of genetic information by inhibiting DNA replication and transcription and inducing mutations in these processes.[175,176] Tables 1 and 2 summarize the key findings made from studies about how oxidative stress-induced DNA lesions perturb the efficiencies and fidelities of DNA replication and transcription in cells. Tables 3 and 4 provide information about the detection and repair mechanisms of oxidatively induced DNA modifications.

3.1. Direct ROS-Induced DNA Lesions

3.1.1. Single-Nucleobase Lesions—It has been illustrated that owing to the 8-oxo-dG:dA mispairing, replicative bypass of 8-oxo-dG leads to G → T transversion and that misincorporation of 8-oxodGTP formed in the nucleotide pool into DNA gives rise to A → C substitutions.[177–179] 8-oxo-dA induces A → G transitions and A → C transversions in mammalian cells.[180] Fapy-dG can mispair with dA, which can induce G → T transversion (~8–30% frequency).[181,182] Fapy-dA is weakly mutagenic (0.4% frequency) and induces A → C transversion *in vivo*.[181]

In vitro experiments showed that 8-oxo-dG only slightly perturbed T7 RNA polymerase (T7RNAP)-mediated transcription, with bypass efficiency being up to 95%.[183] *E. coli* RNA polymerase can efficiently bypass 8-oxo-dG *in vivo*, where the lesion induces C → A transversion and single-nucleotide deletion at frequencies of 33% and 26%, respectively.[184,185] In addition, this lesion transiently paused transcription mediated by mammalian RNA polymerase II and led to a similar C → A transversion mutation,[183,186] and Saxowsky et al.[187] found that 8-oxo-dG induced one-nucleotide deletion and C → A transversion in transcripts in mouse embryonic fibroblasts (MEFs). Moreover, elevated levels of mutant transcripts were generated in the *Ogg1*$^{-/-}$ MEFs and *Csb*$^{-/-}$*Ogg1*$^{-/-}$ MEFs, indicating the involvement of transcription-coupled repair and DNA glycosylase in the removal of 8-oxo-dG.[187] The major known proteins and pathways for the repair of the aforementioned oxidatively induced nucleobase lesions were previously reviewed.[188–190]

A number of replication and repair studies have been conducted for dGh and dSp. These two lesions strongly block DNA polymerases, and once bypassed, they can be highly mutagenic and yield G → C and G → T transversions,[191,192] and the frequencies of the dGh-induced mutations are pH-dependent.[39] In addition, dGh and dSp adducts were found to be substrates for both BER and NER pathways. While neither lesion could be repaired by human hOGG1,[193,194] both were found to be substrates for *E. coli* DNA glycosylases MutM, Nth and Nei,[195–197] yeast yOGG1, yOGG2,[193] murine NEIL1 and NEIL2,[197] and human hNEIL1,[198] where the repair mediated by hNEIL1 seems to be stereoselective.[198] McKibbin et al.[194] demonstrated the excision of dGh, dSp, and dSp-amine adducts by Nei, Fpg, NEIL1 (BER glycosylases), as well as the UvrABC system (bacterial NER pathway). It is worth noting that the authors demonstrated that bulky dSp-amine adducts (including dSp-Lys, dSp-GlcN, and dSp-GPRPGP) can be repaired by the BER pathway, indicating the presence of overlapping mechanisms for the removal of hydantoin and hydantoin-amine adducts.[194] Shafirovich et al.[199] also observed the formation of both BER and NER products when the dGh- and dSp-containing ODNs were treated with human cell extracts. The

involvement of NER was further substantiated by the observation that the lack of XPA or XPC diminished the repair activity, whereas complementation of extracts of XPC-deficient cells with XPCRAD23B restored the NER activity.[199] Comprehensive investigations into how BER and NER pathways are involved in the removal of dGh and dSp lesions *in vivo* will paint a more complete picture about the repair of these lesions.

Thymidine glycol effectively blocks DNA polymerases *in vitro*,[200] while resulting in cell death *in vivo*.[189,201] Although generally regarded as not highly mutagenic on its own,[202] thymidine glycol was found to modulate the mutagenic properties of other closely placed DNA lesions. One example is that thymine glycol can form as part of clustered DNA damage with a neighboring 8-oxo-dG, where the presence of a neighboring thymidine glycol significantly increased the mutagenic potential of 8-oxo-dG.[203] As noted elsewhere in this review, thymidine glycol can also arise from the deamination of 5-methyl-2′-deoxycytidine glycol;[46,47] thus, the thymidine glycol/8-oxo-dG tandem lesion may be induced at methylated CpG sites upon ROS attack, thus contributing to CpG mutagenesis.[47,48] When thymidine glycol is located opposite to an apurinic/apyrimidinic (AP) site, DNA double-strand breaks (DSBs) can be formed through a BER mechanism or at replication fork.[204] When thymidine glycol is opposite to 8-oxo-dG, the DSB formation decreased, but mutation frequency of 8-oxo-dG increased compared to that found for 8-oxo-dG present as an isolated lesion.[204] In addition, Almohaini and co-workers[205] reported that the presence of a thymidine glycol at the first or second position from one 3′ terminus of a blunt-end DSB significantly impeded nonhomologous end-joining, while BER of thymidine glycol located at the fifth position from the blunt end interfered with the DSB ligation.

Thymidine glycol is mainly repaired via the BER pathway, and the lesion was found to be a substrate for a number of DNA glycosylases. These include endonucleases III (Endo III; Nth) and VIII (Endo VIII; Nei) in *E. coli*, yNTG1 (Ntg1) and yNTG2 (Ntg2) in *S. cerevisiae*, as well as NTH1, NEIL1, NEIL2, and NEIL3 in mammalian cells.[189,201,206] In this context, it is worth noting that ADAR1-dependent adenosine-to-inosine editing of pre-mRNA of human *NEIL1* gene yields a different form of NEIL1 protein with lysine 242 being converted to an arginine, and the edited form exhibits differential activity from its corresponding unedited form toward the removal of thymine glycol in duplex DNA.[207] Both forms of NEIL1 can promote tautomerization of thymine glycol, thereby facilitating the recognition and removal of the lesion.[208] Besides BER, some NER activity was also observed for the removal of thymidine glycol in *E. coli* and human systems,[209–212] though the lesion is unlikely a substrate for the mismatch repair pathway in *E. coli*.[213] 5-hmdU formed from dT oxidation pairs with dA, while 5-hmdU produced by oxidation and deamination of 5-mdC pairs with dG. Earlier studies of 5-hmdU focused on its role as an oxidatively induced DNA lesion from dT and revealed that the modified nucleoside is weakly mutagenic,[214] does not block DNA polymerases,[215] pairs with dA in Watson–Crick geometry,[216] and even replaces thymidine in bacteriophage DNA.[217] The excision activity of 5-hmU in 5-hmU:A pair was much lower than that in 5-hmU:G pair by human cell extracts.[218] 5-hmU:G can be excised by TDG, SMUG1, MBD4,[219–222] and with some weak activity by NEIL1.[221] SMUG1 was also found to remove 5-hmU:A, albeit with lower activity.[219] These attributes of 5-hmdU are in agreement with the recent hypothesis that this

modified nucleoside may assume an epigenetic role.[67,223] The occurrence, repair, and biological consequences of 5-hmdU were previously reviewed.[189,224]

5-fdU does not strongly block DNA polymerases.[225] Although high-fidelity DNA polymerases can incorporate any of the four dNTPs opposite the lesion *in vitro*, 5-fdU is weakly mutagenic (0.01–0.04% mutation frequencies in double-stranded vectors), and it induces T → G and T → A transversions in simian COS-7 cells.[226] 5-fdU is predominantly repaired by the BER pathway. AlkA in *E. coli*[227–229] and SMUG1 in mammalian cells[230–232] are the major enzymes for the removal of 5-fdU from DNA. Nth, Fpg, and Nei in *E. coli*, SpNth1 in *Schizosaccharomyces pombe* (a homologue of *E. coli* endonuclease III), human Nth1 and Mbd4, and mouse Nth1 and Tdg can also excise 5-fdU from DNA.[230,233–236] Similar to 5-hmU, 5-fdU in DNA exists as 5-fU:A (formed from A:T base pair) or 5-fU:G (formed from 5mC:G base pair). The former form can be removed by *E. coli* AlkA protein,[227,228] and the latter may be repaired by AlkA protein and a MutHLS mismatch repair system (e.g., *E. coli* mismatch uracil DNA glycosylase, Mug),[229,233] suggesting the involvement of the MMR pathway in the repair of 5-fdU. Meanwhile, repair initiated by SMUG1 can excise 5-fdU opposite any of the four nucleobases, with the highest activity toward 5-fU:C and 5-fU:T.[232] The subsequent repair process will lead to T → G and T → A transversions, which are in agreement with the T → G and T → A transversions induced by this lesion in mammalian cells. In addition, KsgA was recently reported to remove the 5-fU:C mispair in *E. coli*, and mutation in ksgA resulted in increased spontaneous mutations in the *mutM mutY* and *nth nei* background.[237] The repair of 5-fdU was also found to be modulated by a nearby apurinic/apyrimidinic (AP) site. When an AP site is located directly opposite 5-fdU, it is repaired through the long-patch BER pathway; by contrast, when the AP site is shifted it is primarily repaired by the short-patch BER pathway.[238]

Previous studies have provided significant insights about how the oxidized 5-mdC derivatives influence the efficiency and accuracy of DNA replication and transcription. An *in vitro* mutagenesis assay illustrated that, among the oxidized 5-mdC derivatives, only 5-fdC is marginally mutagenic, leading to 1–2% C → T transitions.[239] 5-hmdC, 5-fdC, and 5-cadC are slightly mutagenic in *E. coli* cells, where the C → T transition mutation occurs at frequencies of 0.17–1.12%.[240] In this vein, 5-fdC was found to block DNA replication and lead to mutation in simian COS-7 cells, with bypass efficiencies and mutation frequencies being 39–90% and 0.03–0.28%, respectively.[241] Moreover, Ji et al.[242] demonstrated that, in HEK293T human embryonic kidney epithelial cells, 5-fdC and 5-cadC constituted modest blocks to DNA replication (with a 30% reduction in bypass efficiencies) without inducing detectable mutations in human cells, whereas replicative bypass of 5-hmdC is highly accurate and efficient.

An *in vitro* assay demonstrated that the yeast and mammalian RNA polymerase II (Pol II)-mediated polymerization rates and specificity constants for GTP incorporation against 5-fC and 5-caC were reduced significantly compared with those for unmodified C template, whereas no changes were observed for 5-mC and 5-hmC templates.[243] Additionally, the substrate specificity was reduced by ~30-fold for the 5-fC-containing template in comparison with the C template.[243] Later, You et al.[242] revealed that 5-fC and 5-caC

displayed marginal mutagenic (~0.7–1.7%) and modest inhibitory (31–50%) effects on transcription mediated by T7RNAP or human RNA polymerase II (hRNAPII) *in vitro* and in HEK293T cells. In addition, 5-hmC did not compromise appreciably the efficiency or accuracy of transcription *in vitro* or in HEK293T cells.[242] The lack of pronounced deleterious effects of 5-hmC, 5-fC, and 5-caC on replication or transcription is in keeping with the potential roles of these oxidized 5-mC derivatives in epigenetic regulation.

Different from the passive DNA cytosine demethylation where 5-mdC is diluted during replication,[244,245] it has been proposed that the TET-mediated oxidation of 5-mdC to 5-fdC and 5-cadC may play an important role in active cytosine demethylation in mammals, a process that results in the loss of 5-mdC independent of DNA replication. Along this line, the excision of 5-fdC and 5-cadC from DNA by thymine DNA glycosylase (TDG) and the following action through the BER pathway may result in the restoration with unmodified cytosine.[59,246] It was found that genetic depletion or catalytic inactivation of TDG leads to embryonic lethality in mice,[220,247] indicating the significant roles of TDG in maintaining epigenetic stability during embryonic development. An alternative active cytosine demethylation pathway was also proposed: The AID (activation-induced cytidine deaminase)/APOBEC (apolipoprotein B mRNA editing enzyme, catalytic polypeptide-like) proteins can deaminate 5-hmdC to give 5-hmdU (Figure 3b), which is then removed by TDG or SMUG1 (single-stranded-selective monofunctional uracil DNA glycosylase 1) and finally restored to unmodified cytosine through BER.[65,220] Nevertheless, this mechanism is still controversial because the purified AID/APOBEC proteins exhibit no detectable activity toward 5-hmC deamination *in vitro*.[248]

3.1.2. Tandem Lesions—Multiple lines of evidence support that cdA and cdG are repaired by the NER pathway. First, cleavage products of cdA-containing duplex DNA emanating from NER activity in human cell nuclear extracts was observed, and depletion of XPA protein led to a pronounced decrease in such cleavage.[249] By contrast, no correction of the lesion by direct damage reversal or base excision repair was detected.[249] Second, genetic depletion of ERCC1 gave rise to elevated accumulation of cdA and cdG in mouse tissues.[86,91] Third, a transcriptional bypass assay revealed that cdA and cdG are substrates for the transcription-coupled NER pathway in mammalian cells.[250]

cdA and cdG were found to be strong blockades to DNA replication, and replicative bypass of these lesions are highly mutagenic. With the use of DNA containing a site-specifically inserted cdA as template, both the 5′*R*- and 5′*S*-diastereomers of cdA were observed to block primer extension by replicative polymerases, including human DNA polymerase δ and T7 DNA polymerase.[249,251] *S*-cdA and *S*-cdG were strongly blocking to DNA replication in *E. coli* and human cells and induced substantial frequencies of mutations at the lesion sites, where cdA induces A → T mutation, and cdG induces mainly G → A and G → T mutations.[252–254] Additionally, Pol η, Pol ι, and Pol ζ, but not Pol κ, assume crucial roles in promoting replication across *S*-cdA and *S*-cdG in human cells,[254] and Pol V plays a major role in bypassing these lesions in *E. coli*[252,253]

It was found that both *S*-cdA and *S*-cdG strongly inhibited transcription and induced transcriptional mutagenesis *in vitro* and in mammalian cells.[250,255] Different from the

observations made from replication studies, *S*-cdA and *S*-cdG primarily induce a 5′-A mutation during transcription in human cells, where the lesions direct human RNA polymerase II to misincorporate an adenosine nucleotide opposite the template base situated on the 5′ side of the lesions. Furthermore, when placed on the template strand of an actively transcribed gene, both *S*-cdA and *S*-cdG were primarily repaired by transcription-coupled NER pathways in mammalian cells.[250]

For the oxidatively induced intrastrand nucleobase-nucleobase cross-link lesions, d(G[8–5]C), d(G[8–5m]mC), and d(G[8–5m]T) could be recognized by *E. coli* UvrABC nuclease, suggesting the possible involvement of the NER pathway in the repair of these lesions *in vivo*.[256,257] *S. cerevisiae* DNA polymerase η (Pol η) was able to bypass d(G[8–5]C) and d(G[8–5m]T), with the 5′ guanine portion of the lesion markedly reducing the efficiency and the fidelity of nucleotide incorporation.[106,107] In line with *in vitro* replicative bypass studies, d(G[8–5]C) was found to block considerably DNA replication in *E. coli* cells, as reflected by a 20% bypass efficiency, and the lesion was significantly mutagenic *in vivo*, inducing G → T (8.7%) and G → C (1.2%) transversion mutations. In addition, Pol V was found to be responsible for the error-prone bypass of d(G[8–5]C).[107] Similar observations were made for d(G[8–5m]T), where the guanine portion of the lesion induces G → T mutation, and among the three SOS-inducible DNA polymerases in *E. coli*, Pol V is the most efficient in bypassing the lesion, and it is required for most targeted G → T transversions.[258] *In vitro* studies performed in HeLa cell extracts have demonstrated that the d(G[8-*N*3]T) lesions could be potential substrates of both NER and BER pathways.[259,260] Another recent primer extension experiment revealed that the d(G[8-*N*3]T) lesions could strongly block the A-family BF polymerase from *Bacillus stearothermophilus*, Y-family polymerases Dpo4 from *Sulfolobus sulfataricus* P2 and human Pol κ, with bypass efficiencies being <1–2%, ~8%, and 9–11%, respectively.[261] In addition, the primer extension catalyzed by Pol η was also partially inhibited (with bypass efficiency being 28–45%) by the d(G[8-*N*3]T) cross-links, and more efficient bypass of nonadjacent d(G[8-*N*3]T) lesions in the GCT sequence context was observed than the adjacent counterpart in the GT sequence context.[261243]

3.2. Inflammation-Induced DNA Damage

To date, not much is known about the repair of halogenated nucleobases. Notwithstanding the activity of the human MutT homologue (hMTH1) toward 8-Cl-dGTP,[262] human 8-oxoguanine DNA glycosylase 1 (hOGG1), endonuclease VIII-like 1 (hNEIL1), alkyladenine DNA glycosylase (hAAG), *E. coli* formamidopyrimidine DNA glycosylase (FPG), or endonuclease V (EndoV) could not cleave 8-Cl-G when paired with a C in duplex DNA.[130]

5-Cl-dU can be incorporated into DNA as a thymidine analogue. It is more readily cleaved by hSMUG1 when paired with dG than dA.[263] Relative to the T:G mispair, 5-Cl-U, when mispaired with G, is more efficiently repaired by TDG and hSMUG1.[263] No specific repair pathway has yet been established for 5-Cl-C. On the other hand, DNA glycosylase MBD4-mediated excision repair of 5-Cl-U, 5-Br-U, and 5-Br-C within CpG and mCpG sites has been demonstrated.[264,265] The lack of specific repair pathway may account for the accumulation of halogenated nucleobases in DNA.

Base-pairing energy of 5-Cl-C:G is only slightly lower than that of the C:G pair,[266] suggesting that 5-Cl-C is likely a persistent DNA lesion. It was recently reported that all families of DNA polymerases predominantly decode 5-Cl-C as C *in vitro*; meanwhile, 5-Cl-C, when placed on single-stranded M13 plasmid and replicated in *E. coli* cells, induced 3–9% C → T transition, which is as mutagenic as 8-oxo-dG in similar assays.[264] On the other hand, the 5-halogenated derivatives of cytosine may also perturb epigenetic signaling. In this vein, 5–Cl-C and 5–Br-C in a CpG sequence context can, similar to 5-mC, direct DNMT1-mediated maintenance DNA cytosine methylation and can bind to methyl-CpG-binding proteins.[265,267,268] Such interactions may result in aberrant cytosine methylation and alteration of epigenetic signaling. Hence, 5-Cl-dC may contribute to inflammation-driven cancers through both epigenetic and mutagenic mechanisms.

The accumulation of 5-Cl-dU has been shown to cause mutations, such as T:A → C:G transition, and sister chromatid exchange.[122,263,269,270] 5-Cl-dU can be incorporated into DNA as a dT analogue, and it codes as a dT in an oligonucleotide template.[263] Similar to 5-Cl-dU, 5-Br-dU is also a mutagenic analogue of thymidine, and it can mispair with guanine in DNA.[117] Pols α, κ, and η were shown to incorporate predominantly a dG opposite 5-Br-dC, indicating that 5-Br-dC itself is not a mutagenic lesion. However, 5-Br-dC can be deaminated to 5-Br-dU and further lead to mutation.[271] 8-CldG is a mutagenic adduct; Sassa and co-workers[130] showed that Pol α and Pol κ were slightly retarded at the 8-Cl-dG site, while Pol η readily bypassed the lesion. 8-Br-dG is a mutagenic lesion, and it may produce a broad spectrum of mutations at the site of inflammation. Pols α, κ, and η all incorporated the correct base opposite 8-Br-dA, indicating a low mutagenic potential of this lesion.[271] Further investigations regarding the repair of halogenated nucleosides in DNA and the impact of these lesions on the efficiency and fidelity of DNA replication in mammalian cells are needed.

Recently, Shafirovich et al.[199] revealed that dNIm was a substrate of the human BER pathway but was resistant to excision by the NER machinery when incubated with cell-free HeLa S3 cell extracts. Previous primer extension assays demonstrated that dNIm blocked significantly replication mediated by calf thymus polymerase α and *E. coli* polymerase I, but not human polymerase β.[139] In addition, replicative bypass of dNIm by these two polymerases could induce G → T and G → C transversions.[139] Along this line, by conducting cellular replication studies with the use of a single-stranded M13mp7L2 bacteriophage genome in *E. coli* AB1157 cells, Neeley et al.[272] showed that dNIm strongly blocked DNA replication, with bypass efficiency being only (7.0 ± 1.6)% in uninduced wild-type cells. However, the bypass efficiency of dNIm markedly increased to (57 ± 1)% in SOS-induced cells. In wild-type AB1157 cells, dNIm induced (8.9 ± 0.5)% G → C mutations and roughly equal frequencies of G → A and G → T mutations, at (19 ± 2)% and (22 ± 3)%, respectively.[272] Nonetheless, much lower frequencies of G → A and G → C mutations, at (13 ± 2)% and (2.5 ± 0.6)%, respectively, were found in SOS-induced cells.[272] Later, Dimitri et al.[273] found that dNIm displayed modest inhibitory effects, with bypass efficiency being (87 ± 5)% during transcription mediated by T7RNAP. However, dNIm strongly blocked transcription mediated by human RNA polymerase II (hRNAPII) in HeLa nuclear extract, with a bypass efficiency of (9 ± 5)%.[273] Lesion bypass by T7RNAP induced base misinsertions and deletions opposite the dNIm (22% A, 13% –1 deletion, 7% >

G and 1% U), while hRNAPII exhibited error-free nucleotide incorporation opposite the lesion.[273]

3.3. DNA Damage Formed from Byproducts of Lipid Peroxidation

Previous *in vitro* primer extension assays showed that both human Pol α and Pol β were primarily blocked by LPO-induced etheno DNA adduct εdA with minimal extension.[274] Pol η was capable of catalyzing a substantial amount of bypass across the lesion, where the polymerase incorporated all four nucleotides opposite εdA with different preferences. Human Pol ι, a paralogue of Pol η, was blocked by εdA with a very small amount of synthesis past εdA, which results in insertion of dCMP and, to a much lesser extent, dTMP, opposite εdA.[274] The mutagenic potential of εdA was also investigated using a single-stranded shuttle vector system in *E. coli* and in COS7 simian kidney cells. A nonmutagenic dTMP incorporation opposite εdA was found as the nearly exclusive event in *E. coli*; the lesion is, however, highly mutagenic in COS7 cells, which leads to a very high frequency of A → G transition (63%), followed by A → T (6%) and A → C (1%) transversions.[275] Different from what was observed in COS7 cells, εdA induced all three possible base substitutions at similar frequencies (1.5–3% each) in HeLa human cervical cancer cells.[276] Levine et al.[277] also reported that, when placed on the leading strand, εdA induces A → T (7%),A → C (5%), and A → G (2%) mutations in HeLa human cervical cancer cells and A → G (5%) and A → C (2%) mutations in HCT-116 human colorectal carcinoma cells. Similar to what was observed for εdA, the mutagenic properties of εdC were found to be strikingly different in *E. coli* and COS7 cells (2% in uninduced *E. coli* cells, 32% in SOS-induced *E. coli* cells, and 81% in COS7 cells).[278] 1,N^2-εdG is moderately mutagenic and directs the incorporation of the correct nucleotide (dCMP) in >80% of the replication events in *E. coli*.[279] N^2,3-εdG specifically induces a very low frequency (0.5%) of G → A transition during DNA replication in *E. coli*.[280] The above-mentioned etheno adducts can be repaired by multiple DNA repair pathways, including BER and AlkB/ALKBH family dioxygenases-mediated direct damage reversal, which were previously reviewed.[281,282]

The mutagenicity of malondialdehyde (MDA)-induced DNA adducts was measured in the *lacZ*α forward mutation assay in *E. coli*.[283] The most common type of mutations induced by MDA was base-pair substitution (76%), though frameshift mutations were detected in 16% of the induced mutants, and they comprised mainly single-nucleotide additions in runs of reiterated bases.[283] Modified genomes containing a C opposite M_1G resulted in roughly equal frequencies of G → A and G → T mutations with few G → C mutations. The (−)-strand was replicated only 20% of the time when M_1dG was present. M_1dG was also found to be a substrate for the NER pathway in *E. coli*.[284] In addition, MDA-induced mutations, such as large insertions and deletions, were found after lesion-carrying shuttle vectors undergo replication in human cells.[285] Furthermore, replication studies also demonstrated that M_1dG can induce −1 and −2 frameshift mutations when positioned in a reiterated $(CpG)_4$ sequence but not when positioned in a nonreiterated sequence in *E. coli* or COS-7 cells.[286] Recently, Singh et al.[287] revealed that AlkB could repair Acr-dG and M_1dG *in vitro*, suggesting an important role for the AlkB family of dioxygenases in protecting against the deleterious biological consequences of acrolein- and MDA-induced DNA adducts *in vivo*.

For more detailed discussion about the mutagenic consequences, replication bypass and repair of DNA lesions induced by lipid peroxidation byproducts, the readers should consult a recent review by Minko et al.[14]

4. Implications of Oxidative Stress-Induced DNA Lesions in Human Diseases

The oxidative stress-induced DNA lesions may have significant impact on human health, including the natural processes of aging, neurodegeneration, and carcinogenesis. Recently, the development of LC-MS, coupled with the isotope-dilution method for the unambiguous identification and accurate quantification of multiple DNA lesions, has provided profound insights into the involvement of DNA lesions in different pathological conditions.[15,16,288]

4.1. Direct ROS-Induced DNA Lesions

4.1.1. Single-Nucleobase Lesions—Previous data from the investigation of Chinese and Japanese patients indicated that low BER activity arising from inactivating mutations of the *NEIL1* gene may be involved in the pathogenesis of a subset of gastric cancers.[289] In addition, elevated levels of Fapy-dA and Fapy-dG were observed in the liver, kidney, and brain tissues of *Neil1*$^{-/-}$ mice relative to the wild-type animals.[24] These findings, along with the high incidence of pulmonary and hepatocellular tumors in *Nth1*$^{-/-}$*Neil1*$^{-/-}$ mice, suggest the importance of DNA glycosylase NEIL1 in maintaining genomic stability.[24]

As discussed above, the dGh and dSp lesions are highly mutagenic.[290] In the viewpoint that 8-oxo-dG is produced at high frequencies and that it is more readily oxidized than dG, the major oxidation products of 8-oxo-dG, i.e., dGh and dSp, may bear a significant impact on cellular functions. For example, the presence of dGh and dSp could influence the thermal stability and folding of the G-quadruplex,[291] and dSp lesions could disturb the structure of duplex DNA and affect nucleosome positioning.[292] dGh and dSp lesions have been detected in *E. coli*[197] and in mice,[131] though further studies are needed for systematically assessing their formation and repair in mammals.

Thymidine glycol has been suggested as a biomarker of oxidative stress and detected in urine samples of mammals.[293–295] Thymidine glycol in DNA inhibits the nuclease P1-mediated hydrolysis of its neighboring 3′ phosphodiester bond,[296–298] rendering the release of the lesion as a dinucleotide. The lesion-containing dinucleotide was thus utilized for the quantification of thymidine glycol in DNA using LC-MS/MS coupled with the stable isotope-dilution method.[47,299,300] This method has been applied for probing oxidative stress in white blood cell DNA of ovarian cancer patients[301] and *BRCA* mutation carriers[302] as well as for examining the effect of smoking cessation[303] and antioxidant usage[304] on levels of oxidatively induced DNA damage. Rather than being highly mutagenic, thymidine glycol strongly inhibits DNA replication.[203,305]

As mentioned above, 5-hmdU can be produced from oxidative stress as well as epigenetic machinery (i.e., TET-mediated oxidation of thymidine). 5-hmdU has been detected in murine and human tissues,[306] although the physiological implications are less well explored.

A number of studies have been conducted in measuring 5-fdU. Earlier quantification of 5-fdU in DNA was performed using GC-MS analysis of the modified nucleobase released from DNA with the use of formic acid or 70% (w/w) hydrogen fluoride in pyridine.[68,69] Stable isotope dilution coupled with LC-MS/MS was later developed for the quantification of 5-fdU but with a relatively poor detection limit.[307] Derivatization with Girard reagent T significantly improved the detection limit and has been applied for the detection of 5-fdU in DNA of HeLa-S3 cells[308] and *Trypanosoma brucei*.[309] 5-fdU has also been detected in various tissues of LEA and LEC rats with LC-MS/MS/MS in the negative-ion mode.[85] Higher levels of 5-fdU were observed in the liver of 3-month old LEC rats,[85] which model Wilson disease, a disease characterized by hepatitis and hepatocellular carcinoma.[310] Wilson's disease arises from mutations in ATP7B, which encodes a transporter protein required for hepatic excretion of copper ions.[310] This results in the accumulation of copper ion and increased ROS production.[311,312] This finding provides a vivid illustration of the role of oxidative DNA damage in transition metal-induced diseases such as Wilson's disease.

Global 5-hmC levels are lower in a variety of human cancers including breast, liver, lung, pancreatic, and prostate cancers than in normal tissues.[245] One mechanism to explain this is that cancer-related gain-of-function mutations in *IDH1* and *IDH2* genes cause an increase in production of the oncometabolite (*R*)-2-hydroxyglutarate ((*R*)-2-HG) instead of production of the normal product 2-oxogluterate (2-OG). In addition, cancer-related mutations in two Krebs cycle genes, fumarate hydratase (*FH*) and succinate dehydrogenase (*SDH*), led to the accumulation of their substrates, fumarate and succinate, respectively. (*R*)-2-HG, succinate, and fumarate, which are structurally similar to 2-OG, act as competitive inhibitors of 2-OG-dependent TET activity, leading to diminished levels of 5-hmC in some tumors[313–321] Additionally, Jin et al.[322] reported pronounced depletion of 5-hmdC in multiple human cancers in an *IDH* mutation-independent manner, indicating the existence of alternative mechanism(s) involved in the loss of 5-hmdC. Together, the data suggest that 5-hmdC levels may serve as a useful molecular biomarker for cancer detection and diagnosis.[322]

It has been shown that 5-hmC, 5-fC, and 5-caC may serve as epigenetic marks in addition to being intermediates for active cytosine demethylation in mammals.[62,63,88,323,324] In this vein, 5-hmC, 5-fC, and 5-caC are recognized by some specific cellular proteins critical for chromatin remodeling and transcriptional regulation.[325–331] Thus, the homeostasis of these oxidized 5-mdC derivatives is crucial for maintaining normal cellular function, whereas the loss or aberrant accumulation of these epigenetic marks may lead to deleterious biological consequences and diseases. For instance, LC-MS/MS results revealed a significantly lower level of 5-hmdC in the liver of diseased LEC rats compared to that of control LEA rats, though no difference was found in the levels of 5-mdC.[88] *In vitro* biochemical assays showed that Cu^{2+} ions could directly inhibit the activity of TET enzymes, suggesting that in LEC rats perturbation of 5-hmdC-mediated epigenetic signaling contributes to the etiology of Wilson's disease.[88]

4.1.2. Bulky Lesions—The implication of bulky DNA lesions, including cPus and the d(G[8–5m]T) intrastrand cross-link, were also investigated. Markedly elevated levels of 5′*R*- and 5′*S*-diastereomers of cdA and cdG were found in the liver of the LEC rat model of Wilson's disease[85] Moreover, the levels of these lesions increased with age in the liver and

brain of LEC rats, illustrating a correlation with disease progression.[85] cPus also accumulate in the genomic DNA of wild-type mice with age, providing further evidence of the accumulation of endogenous lesions over the lifespan of mammals and a potential contribution of these lesions to aging.[86] Mitra et al.[89] detected greater levels of cPus lesions in the skin of a murine model of human melanoma. The increase in cPus levels is ultraviolet radiation-independent but pheomelanin pigment-dependent, suggesting that pigment-driven oxidative stress and the resultant oxidative DNA damage contribute to melanoma in humans even in the absence of UV exposure.[89]

Results from a similar LC-MS^3 method revealed that the levels of d(G[8–5m]T) are elevated in tissues of LEC rats relative to LEA rats.[332] Additionally, XPA-deficient human brain and mouse liver as well as various types of tissues of ERCC1-deficient mice contain higher levels of d(G[8–5m]T).[332] In an earlier review, Brooks[81] proposed that chemically stable bulky DNA lesions, such as cPus, may play a crucial role in neurodegeneration in XP patients.[333] Since the brain is not directly exposed to sunlight, the accumulation of ROS-induced bulky DNA lesions in brains of XP patients may contribute to neuron loss in these patients. In support of this, in *Ercc1*$^{-/\Delta}$ mice, with defective nucleotide excision repair of cPus and progressive neurodegeneration,[334] the lesions accumulate more rapidly in the brain than in normal mice. However, as neurodegeneration progresses, the number of cPus decreases significantly in the brain, suggesting a direct causal role of oxidative DNA damage in the loss of neurons in the brain.[86]

A recent technique improvement by employing nanoflow liquid chromatography–nanoelectrospray ionization coupled with tandem mass spectrometry provided much better sensitivity in measuring cPus as well as LPO-induced εdA and εdG lesions in the liver and brain tissues of LEA and LEC rats.[88] Simultaneous quantification of these two different types of lesions demonstrated a preferential accumulation of direct ROS-induced cPus *in vivo*.[88] This result indicates that cPus may contribute to the etiology of oxidative stress-induced diseases to a greater extent than the etheno adducts arising from byproducts of lipid peroxidation.[88]

Earlier reviews discussed the application of LPO-induced DNA lesions as potential biomarkers for cancer risk assessment in humans with cancer-prone diseases such as chronic pancreatitis, ulcerative colitis, or Crohn's disease, as well as in patients with alcohol abuse-related chronic hepatitis, fatty liver, fibrosis, or cirrhosis.[158,335] Results from an isotope dilution-capillary LC-MS/MS method revealed a significant increase in levels of Acr-dG in Alzheimer's disease (AD) patients compared to controls in DNA isolated from the hippocampus/parahippocampal gyrus.[336] This, along with the existence of potential acrolein-derived DNA-peptide cross-links,[149] provides evidence to support the correlation between acrolein-induced DNA damage and AD pathogenesis. The LPO-induced bulky exocyclic 1,N^2-propano-dG adducts may play a significant role in driving congenital abnormalities, myelodysplasia, acute myeloid leukemia (AML), and certain solid tumors in patients suffering from Fanconi anemia (FA).[337–339] FA is an autosomal recessive disease caused by deficiency in the repair of DNA interstrand cross-links. As discussed previously, the DNA interstrand cross-links generated from the ring-open form of 1,N^2-propano-dG are likely substrates of the FA repair pathway, and if left unrepaired, these cross-links impede

replication and transcription, causing chromosomal breaks and translocations that can drive disease in FA patients.[340]

4.2. Inflammation-Induced DNA Damage

Halogenated nucleobases are commonly associated with inflammation, and 5–Cl-C is often used as a biomarker for inflammation.[131,132] Various halogenation products have been detected in mammalian cells, tissues, and fluids. Chlorinated DNA lesions such as 5-Cl-dC, 8-Cl-dG, 8-Cl-dA, and chlorinated ribonucleo-sides including 5-chlorocytidine (5-Cl-rC), 8-chloroguanosine (8-Cl-rG), and 8-chloroadenosine (8-Cl-rA) have been detected with an LC-MS/MS-based method in HOCl-treated cells and freshly isolated human white blood cells. 5-Cl-dC was the predominant DNA lesion, and 8-Cl-G and 5–Cl-C were present at higher levels in RNA than DNA.[127] Jiang et al.[341] found, from GC-MS analysis, increased levels of 5-Cl-dU in DNA from cells treated with HOCl, as well as in exudate fluid from carrageenan-induced inflammation sites, but not in the DNA from tissues at inflammation sites in rats, possibly due to the lack of proliferation in the isolated tissues.[341] 5-Cl-U has been detected in neutrophil-rich inflammatory sites[118] as well as aortic tissue[342] with isotope dilution coupled with GC-MS methods. The 5-Cl-U level in atherosclerotic aortic tissue was reported to be 10-fold higher than that in normal tissue, implying a potential role of halogenated nucleobases in atherogenesis. 8-Br-dG and 8-Cl-dG were quantitatively measured with stable isotope-dilution coupled with the LC-MS/MS method in rat liver, rat urine, and human urine samples, and elevated levels of 8-Br-dG and 8-Cl-dG were observed in urine samples of diabetic patients compared to those in healthy controls.[129] Noyon et al.[343] used LC-MS/MS for the quantification of 5-Cl-dC, 5-Cl-C, and 8-Cl-G and detected the presence of 5-Cl-C (1.0 ± 0.2 nM) in healthy human plasma. 5-Cl-C and 8-Cl-G could be detected in the cytoplasmic nucleotide pool and RNA, and 5-Cl-C is present in DNA from endothelial cells treated with HOCl.[343]

5. Conclusions and Perspectives

In this review, we summarized the chemical formation and biological consequences of a series of oxidatively induced DNA lesions. We also discussed the involvement of these lesions in the etiology of human diseases. Over the past several decades, much has been learned about the mechanisms of formation and repair of oxidative stress-induced DNA lesions. A number of shuttle vector-based studies have provided important molecule-level information about the degrees to which some of the oxidatively induced DNA lesions perturb the transmission of genetic information by inhibiting DNA replication and transcription as well as inducing mutations during these processes (Tables 1 and 2). Nevertheless, work remains to be done on assessing how other oxidatively induced DNA lesions, particularly the secondary oxidation products of dG (i.e., the dGhand dSp adducts) as well as the halogenated nucleosides induced by inflammatory processes, alter the efficiency and fidelity of DNA replication and transcription in mammalian cells.

The available data suggest that these mutagenic DNA adducts, especially the bulky DNA lesions such as exocyclic propano adducts, cPus, and nucleobase-nucleobase intrastrand cross-links, could be potential biomarkers for investigating the role of oxidative stress in

human diseases. Along this line, future work must be done to further elucidate the relationship between the levels of oxidatively induced DNA lesions and the stages of disease (e.g., cancer), which will provide important knowledge for future diagnostic applications of DNA adduct measurements.

During the past two decades, the sensitivities of mass spectrometers for measuring DNA adducts have greatly improved, and the LC-MS coupled with the stable isotope-dilution method is considered the most powerful technique for the unequivocal identification and accurate quantification of oxidatively induced DNA lesions in cells and tissues. We envision that further development of the method for high-throughput and simultaneous quantification of multiple oxidatively induced DNA lesions is necessary. Adapting methods to the measurement of lesions in ever increasingly smaller quantities of genomic DNA will also improve translation of these techniques, for example, to tissue biopsies like bronchoalveolar lavage. Improvement of LC-MS instrument performance as well as sample preparation and cleanup are both needed. For instance, the use of small internal diameter columns coupled with nLC-nESI-MS systems has already facilitated the quantitative analysis of multiple oxidatively induced DNA lesions with the use of low microgram quantity of DNA.[88,159,160,163,165] Recently, high-resolution Orbitrap mass spectrometers have been used for the detection of alkylated DNA lesions induced by carcinogens present in tobacco smoke.[344,345] Owing to their accurate mass measurement capability and high sensitivity, we expect more applications of this type of instruments for the quantification of low levels of oxidatively generated DNA lesions in cellular and tissue samples in the future. The improvement in LC-MS-based quantification techniques will also enable systematic adductomics research,[346–348] which may facilitate the discovery of novel oxidatively induced DNA lesions involved in the pathogenesis of human diseases.

Apart from the improvement in MS instrumentation, new sample preparation and cleanup techniques are also crucial for future high-throughput analysis of DNA lesions *in vivo*. For example, offline HPLC enrichment permits sensitive quantification of the 5′*R*- and 5′*S*-diastereomers of cdA and cdG.[85,86,88,89] Although offline HPLC provides effective sample cleanup and removal of the excess amount of unmodified nucleosides in the DNA digestion mixture, it is relatively time-consuming and not conducive to rapid analysis. Because of the high separation ability, ultraperformance liquid chromatography (UPLC),[349–351] nanoflow UPLC (nUPLC)-nESI coupled with high-sensitivity and high-resolution MS method may enable simultaneous and efficient quantification of multiple oxidatively induced DNA lesions in a DNA digestion mixture without offline HPLC enrichment.

Last, but not least, it is important to note that caution needs to be exerted during sample preparation (i.e., DNA extraction, enzymatic digestion of DNA, etc.) so that artificial generation of oxidatively induced DNA lesions can be minimized. In this vein, the levels of 8-oxo-dG in the DNA of pig liver or HeLa cells could vary by 2 orders of magnitude when the same samples were analyzed by a network of laboratories.[352] Thus, extreme precautions should always be taken while measuring this and other direct ROS-induced DNA lesions as well as those DNA adducts arising from byproducts of lipid peroxidation. It is crucial that the final levels of DNA lesions measured reflect the levels of DNA adducts present in

cellular and tissue DNA, not a combination of those present in initial DNA and artificially formed during sample preparation.

Acknowledgments

Funding: This work was supported by the National Institutes of Health (R01 CA101864 and P01 AG043376).

References

1. Lindahl T. Instability and decay of the primary structure of DNA. Nature. 1993; 362:709–715. [PubMed: 8469282]
2. Finkel T, Holbrook NJ. Oxidants, oxidative stress and the biology of ageing. Nature. 2000; 408:239–247. [PubMed: 11089981]
3. Balaban RS, Nemoto S, Finkel T. Mitochondria, oxidants, and aging. Cell. 2005; 120:483–495. [PubMed: 15734681]
4. Stohs SJ, Bagchi D. Oxidative mechanisms in the toxicity of metal ions. Free Radical Biol Med. 1995; 18:321–336. [PubMed: 7744317]
5. De Bont R, van Larebeke N. Endogenous DNA damage in humans: a review of quantitative data. Mutagenesis. 2004; 19:169–185. [PubMed: 15123782]
6. Evans MD, Dizdaroglu M, Cooke MS. Oxidative DNA damage and disease: induction, repair and significance. Mutat Res Rev Mutat Res. 2004; 567:1–61.
7. Ohshima H, Tatemichi M, Sawa T. Chemical basis of inflammation-induced carcinogenesis. Arch Biochem Biophys. 2003; 417:3–11. [PubMed: 12921773]
8. Winterbourn CC, Kettle AJ. Redox reactions and microbial killing in the neutrophil phagosome. Antioxid Redox Signaling. 2013; 18:642–660.
9. Rayner BS, Love DT, Hawkins CL. Comparative reactivity of myeloperoxidase-derived oxidants with mammalian cells. Free Radical Biol Med. 2014; 71:240–255. [PubMed: 24632382]
10. Panday A, Sahoo MK, Osorio D, Batra S. NADPH oxidases: an overview from structure to innate immunity-associated pathologies. Cell Mol Immunol. 2015; 12:5–23. [PubMed: 25263488]
11. Valko M, Izakovic M, Mazur M, Rhodes CJ, Telser J. Role of oxygen radicals in DNA damage and cancer incidence. Mol Cell Biochem. 2004; 266:37–56. [PubMed: 15646026]
12. Lonkar P, Dedon PC. Reactive species and DNA damage in chronic inflammation: reconciling chemical mechanisms and biological fates. Int J Cancer. 2011; 128:1999–2009. [PubMed: 21387284]
13. Marnett LJ. Lipid peroxidation—DNA damage by malondialdehyde. Mutat Res Fundam Mol Mech Mutagen. 1999; 424:83–95.
14. Minko IG, Kozekov ID, Harris TM, Rizzo CJ, Lloyd RS, Stone MP. Chemistry and biology of DNA containing 1,N^2-deoxyguanosine adducts of the α,β-unsaturated aldehydes acrolein, crotonaldehyde, and 4-hydroxynonenal. Chem Res Toxicol. 2009; 22:759–778. [PubMed: 19397281]
15. Liu S, Wang Y. Mass spectrometry for the assessment of the occurrence and biological consequences of DNA adducts. Chem Soc Rev. 2015; 44:7829–7854. [PubMed: 26204249]
16. Tretyakova N, Villalta PW, Kotapati S. Mass spectrometry of structurally modified DNA. Chem Rev. 2013; 113:2395–2436. [PubMed: 23441727]
17. von Sonntag, C. The Chemical Basis of Radiation Biology. Taylor & Francis; London: 1987.
18. Kasai H, Nishimura S. Hydroxylation of deoxyguanosine at the C-8 position by ascorbic acid and other reducing agents. Nucleic Acids Res. 1984; 12:2137–2145. [PubMed: 6701097]
19. Steenken S. Purine bases, nucleosides, and nucleotides: aqueous solution redox chemistry and transformation reactions of their radical cations and e^- and OH adducts. Chem Rev. 1989; 89:503–520.
20. Dizdaroglu M, Kirkali G, Jaruga P. Formamidopyrimidines in DNA: Mechanisms of formation, repair, and biological effects. Free Radical Biol Med. 2008; 45:1610–1621. [PubMed: 18692130]

21. Cho BP, Evans FE. Structure of oxidatively damaged nucleic acid adducts 3 Tautomerism, ionization and protonation of 8-hydroxyadenosine studied by ^{15}N NMR spectroscopy. Nucleic Acids Res. 1991; 19:1041–1046. [PubMed: 1850508]
22. Ravanat JL, Di Mascio P, Martinez GR, Medeiros MHG, Cadet J. Singlet oxygen induces oxidation of cellular DNA. J Biol Chem. 2000; 275:40601–40604. [PubMed: 11007783]
23. Egler RA, Fernandes E, Rothermund K, Sereika S, de Souza-Pinto N, Jaruga P, Dizdaroglu M, Prochownik EV. Regulation of reactive oxygen species, DNA damage, and c-Myc function by peroxiredoxin 1. Oncogene. 2005; 24:8038–8050. [PubMed: 16170382]
24. Chan MK, Ocampo-Hafalla MT, Vartanian V, Jaruga P, Kirkali G, Koenig KL, Brown S, Lloyd RS, Dizdaroglu M, Teebor GW. Targeted deletion of the genes encoding NTH1 and NEIL1 DNA *N*-glycosylases reveals the existence of novel carcinogenic oxidative damage to DNA. DNA Repair. 2009; 8:786–794. [PubMed: 19346169]
25. Dizdaroglu M. Oxidatively induced DNA damage: Mechanisms, repair and disease. Cancer Lett. 2012; 327:26–47. [PubMed: 22293091]
26. Dizdaroglu M, Coskun E, Jaruga P. Measurement of oxidatively induced DNA damage and its repair, by mass spectrometric techniques. Free Radical Res. 2015; 49:525–548. [PubMed: 25812590]
27. Dizdaroglu M. Oxidatively induced DNA damage and its repair in cancer. Mutat Res Rev Mutat Res. 2015; 763:212–245. [PubMed: 25795122]
28. Hu J, de Souza-Pinto NC, Haraguchi K, Hogue BA, Jaruga P, Greenberg MM, Dizdaroglu M, Bohr VA. Repair of formamidopyrimidines in DNA involves different glycosylases: role of the OGG1, NTH1, and NEIL1 enzymes. J Biol Chem. 2005; 280:40544–40551. [PubMed: 16221681]
29. Steenken S, Jovanovic SV. How easily oxidizable is DNA? One-electron reduction potentials of adenosine and guanosine radicals in aqueous solution. J Am Chem Soc. 1997; 119:617–618.
30. Steenken S, Jovanovic SV, Bietti M, Bernhard K. The trap depth (in DNA) of 8-oxo-7,8-dihydro-2′-deoxyguanosine as derived from electron-transfer equilibria in aqueous solution. J Am Chem Soc. 2000; 122:2373–2374.
31. Luo WC, Muller JG, Rachlin EM, Burrows CJ. Characterization of hydantoin products from one-electron oxidation of 8-oxo-7,8-dihydroguanosine in a nucleoside model. Chem Res Toxicol. 2001; 14:927–938. [PubMed: 11453741]
32. Cui L, Ye WJ, Prestwich EG, Wishnok JS, Taghizadeh K, Dedon PC, Tannenbaum SR. Comparative analysis of four oxidized guanine lesions from reactions of DNA with peroxynitrite, singlet oxygen, and γ-radiation. Chem Res Toxicol. 2013; 26:195–202. [PubMed: 23140136]
33. Niles JC, Wishnok JS, Tannenbaum SR. Spiroiminodihydantoin is the major product of the 8-oxo-7,8-dihydroguanosine reaction with peroxynitrite in the presence of thiols and guanosine photooxidation by methylene blue. Org Lett. 2001; 3:963–966. [PubMed: 11277770]
34. Niles JC, Wishnok JS, Tannenbaum SR. Spiroiminodihydantoin and guanidinohydantoin are the dominant products of 8-oxoguanosine oxidation at low fluxes of peroxynitrite: Mechanistic studies with ^{18}O. Chem Res Toxicol. 2004; 17:1510–1519. [PubMed: 15540949]
35. Fleming AM, Muller JG, Ji IS, Burrows CJ. Characterization of 2′-deoxyguanosine oxidation products observed in the Fenton-like system Cu(II)/H_2O_2/reductant in nucleoside and oligodeoxynucleotide contexts. Org Biomol Chem. 2011; 9:3338–3348. [PubMed: 21445431]
36. Suzuki T, Masuda M, Friesen MD, Ohshima H. Formation of spiroiminodihydantoin nucleoside by reaction of 8-oxo-7,8-dihydro-2′-deoxyguanosine with hypochlorous acid or a myeloperoxidase-H_2O_2-Cl^- system. Chem Res Toxicol. 2001; 14:1163–1169. [PubMed: 11559029]
37. Fleming AM, Burrows CJ. G-quadruplex folds of the human telomere sequence alter the site reactivity and reaction pathway of guanine oxidation compared to duplex DNA. Chem Res Toxicol. 2013; 26:593–607. [PubMed: 23438298]
38. Ye Y, Muller JG, Luo WC, Mayne CL, Shallop AJ, Jones RA, Burrows CJ. Formation of ^{13}C-, ^{15}N-, and ^{18}O-labeled guanidinohydantoin from guanosine oxidation with singlet oxygen. Implications for structure and mechanism. J Am Chem Soc. 2003; 125:13926–13927. [PubMed: 14611206]

39. Zhu J, Fleming AM, Orendt AM, Burrows CJ. pH-Dependent equilibrium between 5-guanidinohydantoin and iminoallantoin affects nucleotide insertion opposite the DNA lesion. J Org Chem. 2016; 81:351–359. [PubMed: 26582419]
40. Luo WC, Muller JG, Burrows CJ. The pH-dependent role of superoxide in riboflavin-catalyzed photooxidation of 8-oxo-7,8-dihydroguanosine. Org Lett. 2001; 3:2801–2804. [PubMed: 11529760]
41. Dizdaroglu M, Jaruga P. Mechanisms of free radical-induced damage to DNA. Free Radical Res. 2012; 46:382–419. [PubMed: 22276778]
42. Teoule R. Radiation-induced DNA damage and its repair. Int J Radiat Biol Relat Stud Phys Chem Med. 1987; 51:573–589. [PubMed: 3034813]
43. Castro GD, Stamato CJ, Castro JA. 5-Methylcytosine attack by free radicals arising from bromotrichloro-methane in a model system: structures of reaction products. Free Radical Biol Med. 1994; 17:419–428. [PubMed: 7835748]
44. Zuo SJ, Boorstein RJ, Teebor GW. Oxidative damage to 5-methylcytosine in DNA. Nucleic Acids Res. 1995; 23:3239–3243. [PubMed: 7667100]
45. Bienvenu C, Cadet J. Synthesis and kinetic study of the deamination of the cis diastereomers of 5,6-dihydroxy-5,6-dihydro-5-methyl-2′-deoxycytidine. J Org Chem. 1996; 61:2632–2637. [PubMed: 11667092]
46. Tremblay S, Douki T, Cadet J, Wagner JR. 2′-Deoxycytidine glycols, a missing link in the free radical-mediated oxidation of DNA. J Biol Chem. 1999; 274:20833–20838. [PubMed: 10409624]
47. Cao HC, Jiang Y, Wang YS. Kinetics of deamination and Cu(II)/H2O2/Ascorbate-induced formation of 5-methylcytosine glycol at CpG sites in duplex DNA. Nucleic Acids Res. 2009; 37:6635–6643. [PubMed: 19706732]
48. Pfeifer GP. *p53* mutational spectra and the role of methylated CpG sequences. Mutat Res Fundam Mol Mech Mutagen. 2000; 450:155–166.
49. Kanwal R, Gupta S. Epigenetic modifications in cancer. Clin Genet. 2012; 81:303–311. [PubMed: 22082348]
50. Teoule R, Bonicel A, Bert C, Cadet J, Polverel M. Identification of radioproducts resulting from breakage of thymine moiety by gamm-irradiation of Escherichia coli DNA in an aerated aqueous-solution. Radiat Res. 1974; 57:46–58. [PubMed: 10874927]
51. Teoule R, Bert C, Bonicel A. Thymine fragment damage retained in the DNA polynucleotide chain after gamma irradiation in aerated solutions. II. Radiat Res. 1977; 72:190–200. [PubMed: 918256]
52. Frenkel K, Goldstein MS, Duker NJ, Teebor GW. Identification of the cis-thymine glycol moiety in oxidized deoxyribonucleic acid. Biochemistry. 1981; 20:750–754. [PubMed: 7011371]
53. Bienvenu C, Wagner JR, Cadet J. Photosensitized oxidation of 5-methyl-2′-deoxycytidine by 2-methyl-1,4-naphthoquinone: Characterization of 5-(hydroperoxymethyl)-2′-deoxycytidine and stable methyl group oxidation products. J Am Chem Soc. 1996; 118:11406–11411.
54. Wagner JR, Cadet J. Oxidation reactions of cytosine DNA components by hydroxyl radical and one-electron oxidants in aerated aqueous solutions. Acc Chem Res. 2010; 43:564–571. [PubMed: 20078112]
55. Kasai H, Iida A, Yamaizumi Z, Nishimura S, Tanooka H. 5-Formyldeoxyuridine: a new type of DNA damage induced by ionizing-radiation and its mutagenicity to Salmonella strain TA102. Mutat Res Lett. 1990; 243:249–253.
56. Tahiliani M, Koh KP, Shen YH, Pastor WA, Bandukwala H, Brudno Y, Agarwal S, Iyer LM, Liu DR, Aravind L, Rao A. Conversion of 5-methylcytosine to 5-hydroxymethylcytosine in mammalian DNA by MLL partner TET1. Science. 2009; 324:930–935. [PubMed: 19372391]
57. Ito S, Shen L, Dai Q, Wu SC, Collins LB, Swenberg JA, He C, Zhang Y. Tet proteins can convert 5-methylcytosine to 5-formylcytosine and 5-carboxylcytosine. Science. 2011; 333:1300–1303. [PubMed: 21778364]
58. He YF, Li BZ, Li Z, Liu P, Wang Y, Tang QY, Ding JP, Jia YY, Chen ZC, Li L, Sun Y, Li XX, Dai Q, Song CX, Zhang KL, He C, Xu GL. Tet-mediated formation of 5-carboxylcytosine and its excision by TDG in mammalian DNA. Science. 2011; 333:1303–1307. [PubMed: 21817016]
59. Pastor WA, Pape UJ, Huang Y, Henderson HR, Lister R, Ko M, McLoughlin EM, Brudno Y, Mahapatra S, Kapranov P, Tahiliani M, Daley GQ, Liu XS, Ecker JR, Milos PM, Agarwal S, Rao

A. Genome-wide mapping of 5-hydroxymethylcytosine in embryonic stem cells. Nature. 2011; 473:394–397. [PubMed: 21552279]

60. Wu H, D'Alessio AC, Ito S, Wang ZB, Cui KR, Zhao KJ, Sun YE, Zhang Y. Genome-wide analysis of 5-hydroxymethylcytosine distribution reveals its dual function in transcriptional regulation in mouse embryonic stem cells. Genes Dev. 2011; 25:679–684. [PubMed: 21460036]
61. Raiber EA, Beraldi D, Ficz G, Burgess HE, Branco MR, Murat P, Oxley D, Booth MJ, Reik W, Balasubramanian S. Genome-wide distribution of 5-formylcytosine in embryonic stem cells is associated with transcription and depends on thymine DNA glycosylase. Genome Biol. 2012; 13:R69. [PubMed: 22902005]
62. Shen L, Wu H, Diep D, Yamaguchi S, D'Alessio AC, Fung HL, Zhang K, Zhang Y. Genome-wide analysis reveals TET- and TDG-dependent 5-methylcytosine oxidation dynamics. Cell. 2013; 153:692–706. [PubMed: 23602152]
63. Song CX, Szulwach KE, Dai Q, Fu Y, Mao SQ, Lin L, Street C, Li YJ, Poidevin M, Wu H, Gao J, Liu P, Li L, Xu GL, Jin P, He C. Genome-wide profiling of 5-formylcytosine reveals its roles in epigenetic priming. Cell. 2013; 153:678–691. [PubMed: 23602153]
64. Lu XY, Zhao BS, He C. TET family proteins: oxidation activity, interacting molecules, and functions in diseases. Chem Rev. 2015; 115:2225–2239. [PubMed: 25675246]
65. Guo JU, Su YJ, Zhong C, Ming GL, Song HJ. Hydroxylation of 5-methylcytosine by TET1 promotes active DNA demethylation in the adult brain. Cell. 2011; 145:423–434. [PubMed: 21496894]
66. Branco MR, Ficz G, Reik W. Uncovering the role of 5-hydroxymethylcytosine in the epigenome. Nat Rev Genet. 2012; 13:7–13.
67. Pfaffeneder T, Spada F, Wagner M, Brandmayr C, Laube SK, Eisen D, Truss M, Steinbacher J, Hackner B, Kotljarova O, Schuermann D, Michalakis S, Kosmatchev O, Schiesser S, Steigenberger B, Raddaoui N, Kashiwazaki G, Muller U, Spruijt CG, Vermeulen M, Leonhardt H, Schar P, Muller M, Carell T. Tet oxidizes thymine to 5-hydroxymethyluracil in mouse embryonic stem cell DNA. Nat Chem Biol. 2014; 10:574–581. [PubMed: 24838012]
68. Bjelland S, Eide L, Time RW, Stote R, Eftedal I, Volden G, Seeberg E. Oxidation of thymine to 5-formyluracil in DNA: mechanisms of formation, structural implications, and base excision by human cell free extracts. Biochemistry. 1995; 34:14758–14764. [PubMed: 7578084]
69. Douki T, Delatour T, Paganon F, Cadet J. Measurement of oxidative damage at pyrimidine bases in gamma-irradiated DNA. Chem Res Toxicol. 1996; 9:1145–1151. [PubMed: 8902270]
70. MurataKamiya N, Kamiya H, Muraoka M, Kaji H, Kasai H. Comparison of oxidation products from DNA components by γ-irradiation and Fenton-type reactions. J Radiat Res. 1997; 38:121–131. [PubMed: 9287465]
71. Hong H, Cao H, Wang Y, Wang Y. Identification and quantification of a guanine–thymine intrastrand cross-link lesion induced by Cu(II)/H_2O_2/ascorbate. Chem Res Toxicol. 2006; 19:614–621. [PubMed: 16696563]
72. Feig DI, Reid TM, Loeb LA. Reactive oxygen species in tumorigenesis. Cancer Res. 1994; 54:1890s–1894s. [PubMed: 8137306]
73. Lee DH, O'Connor TR, Pfeifer GP. Oxidative DNA damage induced by copper and hydrogen peroxide promotes CGàTT tandem mutations at methylated CpG dinucleotides in nucleotide excision repair-deficient cells. Nucleic Acids Res. 2002; 30:3566–3573. [PubMed: 12177298]
74. Reid TM, Loeb LA. Tandem double CCàTT mutations are produced by reactive oxygen species. Proc Natl Acad Sci U S A. 1993; 90:3904–3907. [PubMed: 8483909]
75. Newcomb TG, Allen KJ, Tkeshelashvili L, Loeb LA. Detection of tandem CCàTT mutations induced by oxygen radicals using mutation-specific PCR. Mutat Res Fundam Mol Mech Mutagen. 1999; 427:21–30.
76. Randerath K, Randerath E, Zhou GD, Li D. Bulky endogenous DNA modifications (I-compounds)—possible structural origins and functional implications. Mutat Res Fundam Mol Mech Mutagen. 1999; 424:183–194.
77. Randerath K, Reddy MV, Disher RM. Age- and tissue-related DNA modifications in untreated rats: detection by ^{32}Ppostlabeling assay and possible significance for spontaneous tumor induction and aging. Carcinogenesis. 1986; 7:1615–1617. [PubMed: 3742734]

78. Randerath K, Zhou GD, Somers RL, Robbins JH, Brooks PJ. A ^{32}P-postlabeling assay for the oxidative DNA lesion 8,5′-cyclo-2′-deoxyadenosine in mammalian tissues: Evidence that four type II I-compounds are dinucleotides containing the lesion in the 3′ nucleotide. J Biol Chem. 2001; 276:36051–36057. [PubMed: 11454870]

79. Jaruga P, Dizdaroglu M. 8,5′-Cyclopurine-2′-deoxynucleosides in DNA: mechanisms of formation, measurement, repair and biological effects. DNA Repair. 2008; 7:1413–1425. [PubMed: 18603018]

80. Chatgilialoglu C, Ferreri C, Terzidis MA. Purine 5′,8-cyclonucleoside lesions: chemistry and biology. Chem Soc Rev. 2011; 40:1368–1382. [PubMed: 21221459]

81. Brooks PJ. The case for 8,5′-cyclopurine-2′-deoxynucleosides as endogenous DNA lesions that cause neuro-degeneration in xeroderma pigmentosum. Neuroscience. 2007; 145:1407–1417. [PubMed: 17184928]

82. Dizdaroglu M. Free-radical-induced formation of an 8,5′-cyclo-2′-deoxyguanosine moiety in deoxyribonucleic acid. Biochem J. 1986; 238:247–254. [PubMed: 3800936]

83. Dirksen ML, Blakely WF, Holwitt E, Dizdaroglu M. Effect of DNA conformation on the hydroxyl radical-induced formation of 8,5′-cyclopurine 2′-deoxyribonucleoside residues in DNA. Int J Radiat Biol. 1988; 54:195–204. [PubMed: 2900276]

84. Guerrero CR, Wang J, Wang Y. Induction of 8,5′-cyclo-2′-deoxyadenosine and 8,5′-cyclo-2′-deoxyguanosine in isolated DNA by Fenton-type reagents. Chem Res Toxicol. 2013; 26:1361–1366. [PubMed: 23961697]

85. Wang J, Yuan B, Guerrero C, Bahde R, Gupta S, Wang Y. Quantification of oxidative DNA lesions in tissues of Long-Evans Cinnamon rats by capillary high-performance liquid chromatography–tandem mass spectrometry coupled with stable isotope-dilution method. Anal Chem. 2011; 83:2201–2209. [PubMed: 21323344]

86. Wang J, Clauson CL, Robbins PD, Niedernhofer LJ, Wang Y. The oxidative DNA lesions 8,5′-cyclopurines accumulate with aging in a tissue-specific manner. Aging Cell. 2012; 11:714–716. [PubMed: 22530741]

87. Kirkali G, de Souza-Pinto NC, Jaruga P, Bohr VA, Dizdaroglu M. Accumulation of (5′S)-8,5′-cyclo-2′-deoxyadenosine in organs of Cockayne syndrome complementation group B gene knockout mice. DNA Repair. 2009; 8:274–278. [PubMed: 18992371]

88. Yu Y, Guerrero CR, Liu S, Amato NJ, Sharma Y, Gupta S, Wang Y. Comprehensive assessment of oxidatively induced modifications of DNA in a rat model of human Wilson's disease. Mol Cell Proteomics. 2016; 15:810–817. [PubMed: 26362317]

89. Mitra D, Luo X, Morgan A, Wang J, Hoang MP, Lo J, Guerrero CR, Lennerz JK, Mihm MC, Wargo JA, Robinson KC, Devi SP, Vanover JC, D'Orazio JA, McMahon M, Bosenberg MW, Haigis KM, Haber DA, Wang Y, Fisher DE. An ultraviolet-radiation-independent pathway to melanoma carcinogenesis in the red hair/fair skin background. Nature. 2012; 491:449–453. [PubMed: 23123854]

90. Shaked H, Hofseth LJ, Chumanevich A, Chumanevich AA, Wang J, Wang Y, Taniguchi K, Guma M, Shenouda S, Clevers H, Harris CC, Karin M. Chronic epithelial NF-κB activation accelerates APC loss and intestinal tumor initiation through iNOS up-regulation. Proc Natl Acad Sci U S A. 2012; 109:14007–14012. [PubMed: 22893683]

91. Tilstra JS, Robinson AR, Wang J, Gregg SQ, Clauson CL, Reay DP, Nasto LA, St Croix CM, Usas A, Vo N, Huard J, Clemens PR, Stolz DB, Guttridge DC, Watkins SC, Garinis GA, Wang Y, Niedernhofer LJ, Robbins PD. NF-κB inhibition delays DNA damage–induced senescence and aging in mice. J Clin Invest. 2012; 122:2601–2612. [PubMed: 22706308]

92. Box HC, Budzinski EE, Dawidzik JB, Gobey JS, Freund HG. Free radical-induced tandem base damage in DNA oligomers. Free Radical Biol Med. 1997; 23:1021–1030. [PubMed: 9358245]

93. Box HC, Budzinski EE, Dawidzik JB, Wallace JC, Iijima H. Tandem lesions and other products in X-irradiated DNA oligomers. Radiat Res. 1998; 149:433–439. [PubMed: 9588353]

94. Box HC, Budzinski EE, Dawidzik JD, Wallace JC, Evans MS, Gobey JS. Radiation-induced formation of a crosslink between base moieties of deoxyguanosine and thymidine in deoxygenated solutions of d(CpGpTpA). Radiat Res. 1996; 145:641–643. [PubMed: 8619032]

95. Budzinski EE, Dawidzik JB, Rajecki MJ, Wallace JC, Schroder EA, Box HC. Isolation and characterization of the products of anoxic irradiation of d(CpGpTpA). Int J Radiat Biol. 1997; 71:327–336. [PubMed: 9134023]
96. Bellon S, Ravanat JL, Gasparutto D, Cadet J. Cross-Linked thymine-purine base tandem lesions: Synthesis, characterization, and measurement in γ-Irradiated Isolated DNA. Chem Res Toxicol. 2002; 15:598–606. [PubMed: 11952347]
97. Romieu A, Bellon S, Gasparutto D, Cadet J. Synthesis and UV photolysis of oligodeoxynucleotides that contain 5-(phenylthiomethyl)-2′-deoxyuridine: a specific photolabile precursor of 5-(2′-deoxyuridilyl)methyl radical. Org Lett. 2000; 2:1085–1088. [PubMed: 10804560]
98. Zhang Q, Wang Y. Independent generation of 5-(2′-deoxycytidinyl)methyl radical and the formation of a novel cross-link lesion between 5-methylcytosine and guanine. J Am Chem Soc. 2003; 125:12795–12802. [PubMed: 14558827]
99. Zhang Q, Wang Y. Generation of 5-(2′-deoxycytidyl)methyl radical and the formation of intrastrand cross-link lesions in oligodeoxyribonucleotides. Nucleic Acids Res. 2005; 33:1593–1603. [PubMed: 15767284]
100. Zhang Q, Wang Y. Independent generation of the 5-hydroxy-5,6-dihydrothymidin-6-yl radical and its reactivity in dinucleoside monophosphates. J Am Chem Soc. 2004; 126:13287–13297. [PubMed: 15479083]
101. Zhang Q, Wang Y. The reactivity of the 5-hydroxy-5,6-dihydrothymidin-6-yl radical in oligodeoxyribonucleotides. Chem Res Toxicol. 2005; 18:1897–1906. [PubMed: 16359180]
102. Zeng Y, Wang Y. Facile formation of an intrastrand cross-link lesion between cytosine and guanine upon pyrex-filtered UV light irradiation of d(BrCG) and duplex DNA containing 5-bromocytosine. J Am Chem Soc. 2004; 126:6552–6553. [PubMed: 15161273]
103. Zeng Y, Wang Y. Sequence-dependent formation of intrastrand crosslink products from the UVB irradiation of duplex DNA containing a 5-bromo-2′-deoxyuridine or 5-bromo-2′-deoxycytidine. Nucleic Acids Res. 2006; 34:6521–6529. [PubMed: 17130170]
104. Zeng Y, Wang Y. UVB-induced formation of intrastrand cross-link products of DNA in MCF-7 cells treated with 5-bromo-2′-deoxyuridine. Biochemistry. 2007; 46:8189–8195. [PubMed: 17567044]
105. Hong H, Wang Y. Formation of intrastrand cross-link products between cytosine and adenine from UV irradiation of d(BrCA) and duplex DNA containing a 5-bromocytosine. J Am Chem Soc. 2005; 127:13969–13977. [PubMed: 16201819]
106. Gu C, Wang Y. LC-MS/MS identification and yeast polymerase η bypass of a novel γ-irradiation-induced intrastrand cross-link lesion G[8–5]C. Biochemistry. 2004; 43:6745–6750. [PubMed: 15157108]
107. Jiang Y, Hong H, Cao H, Wang Y. *In vivo* formation and *in vitro* replication of a guanine-thymine intrastrand cross-link lesion. Biochemistry. 2007; 46:12757–12763. [PubMed: 17929946]
108. Hong H, Cao H, Wang Y. Formation and genotoxicity of a guanine–cytosine intrastrand cross-link lesion *in vivo*. Nucleic Acids Res. 2007; 35:7118–7127. [PubMed: 17942427]
109. Crean C, Uvaydov Y, Geacintov NE, Shafirovich V. Oxidation of single-stranded oligonucleotides by carbonate radical anions: generating intrastrand cross-links between guanine and thymine bases separated by cytosines. Nucleic Acids Res. 2008; 36:742–755. [PubMed: 18084033]
110. Yun BH, Geacintov NE, Shafirovich V. Generation of Guanine–Thymidine Cross-Links in DNA by Peroxynitrite/Carbon Dioxide. Chem Res Toxicol. 2011; 24:1144–1152. [PubMed: 21513308]
111. Madugundu GS, Wagner JR, Cadet J, Kropachev K, Yun BH, Geacintov NE, Shafirovich V. Generation of Guanine–Thymine Cross-Links in Human Cells by One-Electron Oxidation Mechanisms. Chem Res Toxicol. 2013; 26:1031–1033. [PubMed: 23734842]
112. Grivennikov SI, Greten FR, Karin M. Immunity, inflammation, and cancer. Cell. 2010; 140:883–899. [PubMed: 20303878]
113. Mangerich A, Dedon PC, Fox JG, Tannenbaum SR, Wogan GN. Chemistry meets biology in colitis-associated carcinogenesis. Free Radical Res. 2013; 47:958–986. [PubMed: 23926919]
114. Halliwell B. Phagocyte-derived reactive species: salvation or suicide? Trends Biochem Sci. 2006; 31:509–515. [PubMed: 16890439]

115. Henderson JP, Byun J, Heinecke JW. Molecular chlorine generated by the myeloperoxidase-hydrogen peroxide-chloride system of phagocytes produces 5-chlorocytosine in bacterial RNA. J Biol Chem. 1999; 274:33440–33448. [PubMed: 10559226]
116. Klebanoff SJ. Myeloperoxidase: friend and foe. J Leukocyte Biol. 2005; 77:598–625. [PubMed: 15689384]
117. Henderson JP, Byun J, Mueller DM, Heinecke JW. The eosinophil peroxidase-hydrogen peroxide-bromide system of human eosinophils generates 5-bromouracil, a mutagenic thymine analogue. Biochemistry. 2001; 40:2052–2059. [PubMed: 11329272]
118. Henderson JP, Byun J, Takeshita J, Heinecke JW. Phagocytes produce 5-chlorouracil and 5-bromouracil, two mutagenic products of myeloperoxidase, in human inflammatory tissue. J Biol Chem. 2003; 278:23522–23528. [PubMed: 12707270]
119. Gotto AM, Belkhode ML, Touster O. Stimulatory effects of inosine and deoxyinosine on the incorporation of uracil-2-^{14}C, 5-fluorouracil-2-^{14}C, and 5-bromouracil-2-^{14}C into nucleic acids by Ehrlich ascites tumor cells *in vitro*. Cancer Res. 1969; 29:807–811. [PubMed: 5775710]
120. Pal BC, Cumming RB, Walton MF, Preston RJ. Environmental pollutant 5-chlorouracil is incorporated in mouse liver and testes DNA. Mutat Res Lett. 1981; 91:395–401.
121. Morris SM. The genetic toxicology of 5-bromodeoxyuridine in mammalian cells. Mutat Res Rev Genet Toxicol. 1991; 258:161–188.
122. Morris SM. The genetic toxicology of 5-fluoropyrimidines and 5-chlorouracil. Mutat Res Rev Genet Toxicol. 1993; 297:39–51.
123. Whiteman M, Jenner A, Halliwell B. Hypochlorous acid-induced base modifications in isolated calf thymus DNA. Chem Res Toxicol. 1997; 10:1240–1246. [PubMed: 9403176]
124. Winterbourn CC, Kettle AJ. Biomarkers of myeloperoxidase-derived hypochlorous acid. Free Radical Biol Med. 2000; 29:403–409. [PubMed: 11020661]
125. Kawai Y, Morinaga H, Kondo H, Miyoshi N, Nakamura Y, Uchida K, Osawa T. Endogenous formation of novel halogenated 2′-deoxycytidine - Hypohalous acid-mediated DNA modification at the site of inflammation. J Biol Chem. 2004; 279:51241–51249. [PubMed: 15364942]
126. Kang JI, Sowers LC. Examination of hypochlorous acid-induced damage to cytosine residues in a CpG dinucleotide in DNA. Chem Res Toxicol. 2008; 21:1211–1218. [PubMed: 18826175]
127. Badouard C, Masuda M, Nishino H, Cadet J, Favier A, Ravanat JL. Detection of chlorinated DNA and RNA nucleosides by HPLC coupled to tandem mass spectrometry as potential biomarkers of inflammation. J Chromatogr B: Anal Technol Biomed Life Sci. 2005; 827:26–31.
128. Shen ZZ, Mitra SN, Wu WJ, Chen YH, Yang YW, Qin J, Hazen SL. Eosinophil peroxidase catalyzes bromination of free nucleosides and double-stranded DNA. Biochemistry. 2001; 40:2041–2051. [PubMed: 11329271]
129. Asahi T, Kondo H, Masuda M, Nishino H, Aratani Y, Naito Y, Yoshikawa T, Hisaka S, Kato Y, Osawa T. Chemical and immunochemical detection of 8-halogenated deoxyguanosines at early stage inflammation. J Biol Chem. 2010; 285:9282–9291. [PubMed: 20081197]
130. Sassa A, Kamoshita N, Matsuda T, Ishii Y, Kuraoka I, Nohmi T, Ohta T, Honma M, Yasui M. Miscoding properties of 8-chloro-2′-deoxyguanosine, a hypochlorous acid-induced DNA adduct, catalysed by human DNA polymerases. Mutagenesis. 2013; 28:81–88. [PubMed: 23076070]
131. Mangerich A, Knutson CG, Parry NM, Muthupalani S, Ye WJ, Prestwich E, Cui L, McFaline JL, Mobley M, Ge ZM, Taghizadeh K, Wishnok JS, Wogan GN, Fox JG, Tannenbaum SR, Dedon PC. Infection-induced colitis in mice causes dynamic and tissue-specific changes in stress response and DNA damage leading to colon cancer. Proc Natl Acad Sci U S A. 2012; 109:E1820–E1829. [PubMed: 22689960]
132. Knutson CG, Mangerich A, Zeng Y, Raczynski AR, Liberman RG, Kang P, Ye WJ, Prestwich EG, Lu K, Wishnok JS, Korzenik JR, Wogan GN, Fox JG, Dedon PC, Tannenbaum SR. Chemical and cytokine features of innate immunity characterize serum and tissue profiles in inflammatory bowel disease. Proc Natl Acad Sci U S A. 2013; 110:E2332–E2341. [PubMed: 23754421]
133. Dedon PC, Tannenbaum SR. Reactive nitrogen species in the chemical biology of inflammation. Arch Biochem Biophys. 2004; 423:12–22. [PubMed: 14989259]

134. Xia Y, Zweier JL. Superoxide and peroxynitrite generation from inducible nitric oxide synthase in macrophages. Proc Natl Acad Sci U S A. 1997; 94:6954–6958. [PubMed: 9192673]
135. Carreras MC, Pargament GA, Catz SD, Poderoso JJ, Boveris A. Kinetics of nitric oxide and hydrogen peroxide production and formation of peroxynitrite during the respiratory burst of human neutrophils. FEBS Lett. 1994; 341:65–68. [PubMed: 8137924]
136. Huie RE, Padmaja S. The Reaction of no With Superoxide. Free Radical Res Commun. 1993; 18:195–199. [PubMed: 8396550]
137. Juedes MJ, Wogan GN. Peroxynitrite-induced mutation spectra of pSP189 following replication in bacteria and in human cells. Mutat Res Fundam Mol Mech Mutagen. 1996; 349:51–61.
138. Burney S, Niles JC, Dedon PC, Tannenbaum SR. DNA Damage in Deoxynucleosides and Oligonucleotides Treated with Peroxynitrite. Chem Res Toxicol. 1999; 12:513–520. [PubMed: 10368314]
139. Gu F, Stillwell WG, Wishnok JS, Shallop AJ, Jones RA, Tannenbaum SR. Peroxynitrite-Induced Reactions of Synthetic Oligo 2′-Deoxynucleotides and DNA Containing Guanine: Formation and Stability of a 5-Guanidino-4-nitroimidazole Lesion. Biochemistry. 2002; 41:7508–7518. [PubMed: 12044185]
140. Misiaszek R, Crean C, Geacintov NE, Shafirovich V. Combination of Nitrogen Dioxide Radicals with 8-Oxo-7,8-dihydroguanine and Guanine Radicals in DNA: Oxidation and Nitration End-Products. J Am Chem Soc. 2005; 127:2191–2200. [PubMed: 15713097]
141. Girotti AW. Mechanisms of lipid peroxidation. J Free Radicals Biol Med. 1985; 1:87–95.
142. Halliwell B, Chirico S. Lipid peroxidation: its mechanism, measurement, and significance. Am J Clin Nutr. 1993; 57:715S–724S. [PubMed: 8475889]
143. Burcham PC. Genotoxic lipid peroxidation products: their DNA damaging properties and role in formation of endogenous DNA adducts. Mutagenesis. 1998; 13:287–305. [PubMed: 9643589]
144. Chung FL, Chen HJC, Nath RG. Lipid peroxidation as a potential endogenous source for the formation of exocyclic DNA adducts. Carcinogenesis. 1996; 17:2105–2111. [PubMed: 8895475]
145. Nair J, Barbin A, Velic I, Bartsch H. Etheno DNA-base adducts from endogenous reactive species. Mutat Res Fundam Mol Mech Mutagen. 1999; 424:59–69.
146. Winczura A, Zdżalik D, Tudek B. Damage of DNA and proteins by major lipid peroxidation products in genome stability. Free Radical Res. 2012; 46:442–459. [PubMed: 22257221]
147. Prado FM, Oliveira MCB, Miyamoto S, Martinez GR, Medeiros MHG, Ronsein GE, Di Mascio P. Thymine hydroperoxide as a potential source of singlet molecular oxygen in DNA. Free Radical Biol Med. 2009; 47:401–409. [PubMed: 19426799]
148. Blair IA. DNA adducts with lipid peroxidation products. J Biol Chem. 2008; 283:15545–15549. [PubMed: 18285329]
149. Minko IG, Kozekov ID, Kozekova A, Harris TM, Rizzo CJ, Lloyd RS. Mutagenic potential of DNA–peptide crosslinks mediated by acrolein-derived DNA adducts. Mutat Res Fundam Mol Mech Mutagen. 2008; 637:161–172.
150. Stone MP, Cho YJ, Huang H, Kim HY, Kozekov ID, Kozekova A, Wang H, Minko IG, Lloyd RS, Harris TM, Rizzo CJ. Interstrand DNA cross-links induced by α,β-unsaturated aldehydes derived from lipid peroxidation and environmental sources. Acc Chem Res. 2008; 41:793–804. [PubMed: 18500830]
151. Kozekov ID, Nechev LV, Moseley MS, Harris CM, Rizzo CJ, Stone MP, Harris TM. DNA interchain cross-links formed by acrolein and crotonaldehyde. J Am Chem Soc. 2003; 125:50–61. [PubMed: 12515506]
152. Garcia CCM, Angeli JPF, Freitas FP, Gomes OF, de Oliveira TF, Loureiro APM, Di Mascio P, Medeiros MHG. [$^{13}C_2$]-acetaldehyde promotes unequivocal formation of 1,N^2-Propano-2′-deoxyguanosine in human cells. J Am Chem Soc. 2011; 133:9140–9143. [PubMed: 21604744]
153. el Ghissassi F, Barbin A, Nair J, Bartsch H. Formation of 1,N^6-ethenoadenine and 3,N^4-ethenocytosine by lipid peroxidation products and nucleic acid bases. Chem Res Toxicol. 1995; 8:278–283. [PubMed: 7766812]
154. Bartsch H, Nair J, Owen RW. Exocyclic DNA adducts as oxidative stress markers in colon carcinogenesis: potential role of lipid peroxidation, dietary fat and antioxidants. Biol Chem. 2002; 383:915–921. [PubMed: 12222681]

155. Swenberg JA, Fedtke N, Ciroussel F, Barbin A, Bartsch H. Etheno adducts formed in DNA of vinyl chloride-exposed rats are highly persistent in liver. Carcinogenesis. 1992; 13:727–729. [PubMed: 1576725]
156. Lee SH, Arora JA, Oe T, Blair IA. 4-Hydroperoxy-2-nonenal-Induced Formation of 1,N2-Etheno-2′-deoxyguanosine Adducts. Chem Res Toxicol. 2005; 18:780–786. [PubMed: 15833039]
157. Lee SH, Oe T, Blair IA. 4,5-Epoxy-2(E)-decenal-Induced Formation of 1,N6-Etheno-2′-deoxyadenosine and 1,N2-Etheno-2′-deoxyguanosine Adducts. Chem Res Toxicol. 2002; 15:300–304. [PubMed: 11896675]
158. Nair U, Bartsch H, Nair J. Lipid peroxidation-induced DNA damage in cancer-prone inflammatory diseases: A review of published adduct types and levels in humans. Free Radical Biol Med. 2007; 43:1109–1120. [PubMed: 17854706]
159. Chen HJ, Lin WP. Simultaneous quantification of 1,N^2-propano-2′-deoxyguanosine adducts derived from acrolein and crotonaldehyde in human placenta and leukocytes by isotope dilution nanoflow LC nanospray ionization tandem mass spectrometry. Anal Chem. 2009; 81:9812–9818. [PubMed: 19899782]
160. Chen HJC. Analysis of DNA adducts in human samples: Acrolein-derived exocyclic DNA adducts as an example. Mol Nutr Food Res. 2011; 55:1391–1400. [PubMed: 21796778]
161. Chen HJC, Chiang LC, Tseng MC, Zhang LL, Ni J, Chung FL. Detection and quantification of 1,N^6-ethenoadenine in human placental DNA by mass spectrometry. Chem Res Toxicol. 1999; 12:1119–1126. [PubMed: 10604859]
162. Chen HJC, Chiu WL. Association between cigarette smoking and urinary excretion of 1,N^2-ethenoguanine measured by isotope dilution liquid chromatography-electrospray ionization/tandem mass spectrometry. Chem Res Toxicol. 2005; 18:1593–1599. [PubMed: 16533024]
163. Chen HJC, Lin GJ, Lin WP. Simultaneous quantification of three lipid peroxidation-derived etheno adducts in human DNA by stable isotope dilution nanoflow liquid chromatography nanospray ionization tandem mass spectrometry. Anal Chem. 2010; 82:4486–4493. [PubMed: 20429514]
164. Chen HJC, Lin TC, Hong CL, Chiang LC. Analysis of 3,N^4-ethenocytosine in DNA and in human urine by isotope dilution gas chromatography/negative ion chemical ionization/mass spectrometry. Chem Res Toxicol. 2001; 14:1612–1619. [PubMed: 11743744]
165. Chen HJC, Lin WP. Quantitative analysis of multiple exocyclic DNA adducts in human salivary DNA by stable isotope dilution nanoflow liquid chromatography-nanospray ionization tandem mass spectrometry. Anal Chem. 2011; 83:8543–8551. [PubMed: 21958347]
166. Chen HJC, Wu CF, Hong CL, Chang CM. Urinary excretion of 3,N^4-etheno-2′-deoxycytidine in humans as a biomarker of oxidative stress: association with cigarette smoking. Chem Res Toxicol. 2004; 17:896–903. [PubMed: 15257614]
167. Zhang S, Villalta PW, Wang M, Hecht SS. Analysis of crotonaldehyde- and acetaldehyde-derived 1,N^2-propanodeoxyguanosine adducts in DNA from human tissues using liquid chromatography electrospray ionization tandem mass spectrometry. Chem Res Toxicol. 2006; 19:1386–1392. [PubMed: 17040109]
168. Garcia CCM, Freitas FP, Di Mascio P, Medeiros MHG. Ultrasensitive simultaneous quantification of 1,N^2-etheno-2′-deoxyguanosine and 1,N^2-propano-2′-deoxyguanosine in DNA by an online liquid chromatography–electrospray tandem mass spectrometry assay. Chem Res Toxicol. 2010; 23:1245–1255. [PubMed: 20550124]
169. Loureiro APM, Marques SA, Garcia CCM, Di Mascio P, Medeiros MHG. Development of an on-line liquid chromatography-electrospray tandem mass spectrometry assay to quantitatively determine 1,N^2-Etheno-2′-deoxyguanosine in DNA. Chem Res Toxicol. 2002; 15:1302–1308. [PubMed: 12387629]
170. Nair J, Strand S, Frank N, Knauft J, Wesch H, Galle PR, Bartsch H. Apoptosis and age-dependant induction of nuclear and mitochondrial etheno-DNA adducts in Long-Evans Cinnamon (LEC) rats: enhanced DNA damage by dietary curcumin upon copper accumulation. Carcinogenesis. 2005; 26:1307–1315. [PubMed: 15790590]

171. Ma B, Villalta PW, Balbo S, Stepanov I. Analysis of a malondialdehyde–deoxyguanosine adduct in human leukocyte DNA by liquid chromatography nanoelectrospray–high-resolution tandem mass spectrometry. Chem Res Toxicol. 2014; 27:1829–1836. [PubMed: 25181548]

172. Chaudhary AK, Nokubo M, Marnett LJ, Blair IA. Analysis of the malondialdehyde-2′-deoxyguanosine adduct in rat liver DNA by gas chromatography/electron capture negative chemical ionization mass spectrometry. Biol Mass Spectrom. 1994; 23:457–464. [PubMed: 7918689]

173. Zhang Y, Chen SY, Hsu T, Santella RM. Immunohistochemical detection of malondialdehyde–DNA adducts in human oral mucosa cells. Carcinogenesis. 2002; 23:207–211. [PubMed: 11756243]

174. Leuratti C, Watson MA, Deag EJ, Welch A, Singh R, Gottschalg E, Marnett LJ, Atkin W, Day NE, Shuker DEG, Bingham SA. Detection of malondialdehyde DNA adducts in human colorectal mucosa: relationship with diet and the presence of adenomas. Cancer Epidemiol Biomarkers Prev. 2002; 11:267–273. [PubMed: 11895876]

175. Delaney JC, Essigmann JM. Biological properties of single chemical-DNA adducts: a twenty year perspective. Chem Res Toxicol. 2008; 21:232–252. [PubMed: 18072751]

176. You C, Wang Y. Mass spectrometry-based quantitative strategies for assessing the biological consequences and repair of DNA adducts. Acc Chem Res. 2016; 49:205–213. [PubMed: 26758048]

177. Shibutani S, Takeshita M, Grollman AP. Insertion of specific bases during DNA synthesis past the oxidation-damaged base 8-oxodG. Nature. 1991; 349:431–434. [PubMed: 1992344]

178. Cheng KC, Cahill DS, Kasai H, Nishimura S, Loeb LA. 8-Hydroxyguanine, an abundant form of oxidative DNA damage, causes G——T and A——C substitutions. J Biol Chem. 1992; 267:166–172. [PubMed: 1730583]

179. Wood ML, Dizdaroglu M, Gajewski E, Essigmann JM. Mechanistic studies of ionizing radiation and oxidative mutagenesis: genetic effects of a single 8-hydroxyguanine (7-hydro-8-oxoguanine) residue inserted at a unique site in a viral genome. Biochemistry. 1990; 29:7024–7032. [PubMed: 2223758]

180. Kamiya H, Miura H, Murata-Kamiya N, Ishikawa H, Sakaguchi T, Inoue H, Sasaki T, Masutanl C, Hanaoka F, Nishimura S, Ohtsuka E. 8-Hydroxyadenine (7, 8-dihydro-8-oxoadenine) induces misincorporation in *in vitro* DNA synthesis and mutations in NIH 3T3 cells. Nucleic Acids Res. 1995; 23:2893–2899. [PubMed: 7659512]

181. Kalam MA, Haraguchi K, Chandani S, Loechler EL, Moriya M, Greenberg MM, Basu AK. Genetic effects of oxidative DNA damages: comparative mutagenesis of the imidazole ring-opened formamidopyrimidines (Fapy lesions) and 8-oxo-purines in simian kidney cells. Nucleic Acids Res. 2006; 34:2845.

182. Wiederholt CJ, Greenberg MM. Fapy·dG instructs Klenow exo^{-} to misincorporate deoxyadenosine. J Am Chem Soc. 2002; 124:7278–7279. [PubMed: 12071730]

183. Tornaletti S, Maeda LS, Kolodner RD, Hanawalt PC. Effect of 8-oxoguanine on transcription elongation by T7 RNA polymerase and mammalian RNA polymerase II. DNA Repair. 2004; 3:483–494. [PubMed: 15084310]

184. Viswanathan A, Doetsch PW. Effects of nonbulky DNA base damages on Escherichia coli RNA polymerase-mediated elongation and promoter clearance. J Biol Chem. 1998; 273:21276–21281. [PubMed: 9694887]

185. Brégeon D, Doddridge ZA, You HJ, Weiss B, Doetsch PW. Transcriptional mutagenesis induced by uracil and 8-oxoguanine in Escherichia coli. Mol Cell. 2003; 12:959–970. [PubMed: 14580346]

186. Kuraoka I, Endou M, Yamaguchi Y, Wada T, Handa H, Tanaka K. Effects of endogenous DNA base lesions on transcription elongation by mammalian RNA polymerase II: Implications for transcription-coupled DNA repair and transcriptional mutagenesis. J Biol Chem. 2003; 278:7294–7299. [PubMed: 12466278]

187. Saxowsky TT, Meadows KL, Klungland A, Doetsch PW. 8-Oxoguanine-mediated transcriptional mutagenesis causes Ras activation in mammalian cells. Proc Natl Acad Sci U S A. 2008; 105:18877–18882. [PubMed: 19020090]

188. Cooke MS, Evans MD, Dizdaroglu M, Lunec J. Oxidative DNA damage: mechanisms, mutation, and disease. FASEB J. 2003; 17:1195–1214. [PubMed: 12832285]

189. Bjelland S, Seeberg E. Mutagenicity, toxicity and repair of DNA base damage induced by oxidation. Mutat Res Fundam Mol Mech Mutagen. 2003; 531:37–80.

190. Wallace SS. Biological consequences of free radical-damaged DNA bases. Free Radical Biol Med. 2002; 33:1–14. [PubMed: 12086677]

191. Henderson PT, Delaney JC, Muller JG, Neeley WL, Tannenbaum SR, Burrows CJ, Essigmann JM. The hydantoin lesions formed from oxidation of 7,8-dihydro-8-oxoguanine are potent sources of replication errors *in vivo*. Biochemistry. 2003; 42:9257–9262. [PubMed: 12899611]

192. Delaney S, Neeley WL, Delaney JC, Essigmann JM. The substrate specificity of MutY for hyperoxidized guanine lesions *in vivo*. Biochemistry. 2007; 46:1448–1455. [PubMed: 17260974]

193. Leipold MD, Workman H, Muller JG, Burrows CJ, David SS. Recognition and removal of oxidized guanines in duplex DNA by the base excision repair enzymes hOGG1, yOGG1, and yOGG2. Biochemistry. 2003; 42:11373–11381. [PubMed: 14503888]

194. McKibbin PL, Fleming AM, Towheed MA, Van Houten B, Burrows CJ, David SS. Repair of hydantoin lesions and their amine adducts in DNA by base and nucleotide excision repair. J Am Chem Soc. 2013; 135:13851–13861. [PubMed: 23930966]

195. Hazra TK, Muller JG, Manuel RC, Burrows CJ, Lloyd RS, Mitra S. Repair of hydantoins, one electron oxidation product of 8-oxoguanine, by DNA glycosylases of Escherichia coli. Nucleic Acids Res. 2001; 29:1967–1974. [PubMed: 11328881]

196. Leipold MD, Muller JG, Burrows CJ, David SS. Removal of hydantoin products of 8-oxoguanine oxidation by the Escherichia coli DNA repair enzyme, FPG. Biochemistry. 2000; 39:14984–14992. [PubMed: 11101315]

197. Hailer MK, Slade PG, Martin BD, Sugden KD. Nei deficient Escherichia coli are sensitive to chromate and accumulate the oxidized guanine lesion spiroiminodihydantoin. Chem Res Toxicol. 2005; 18:1378–1383. [PubMed: 16167829]

198. Krishnamurthy N, Zhao XB, Burrows CJ, David SS. Superior removal of hydantoin lesions relative to other oxidized bases by the human DNA glycosylase hNEIL1. Biochemistry. 2008; 47:7137–7146. [PubMed: 18543945]

199. Shafirovich V, Kropachev K, Anderson T, Liu Z, Kolbanovskiy M, Martin BD, Sugden K, Shim Y, Chen XJ, Min JH, Geacintov NE. Base and nucleotide excision repair of oxidatively generated guanine lesions in DNA. J Biol Chem. 2016; 291:5309–5319. [PubMed: 26733197]

200. Aller P, Rould MA, Hogg M, Wallace SS, Doublie S. A structural rationale for stalling of a replicative DNA polymerase at the most common oxidative thymine lesion, thymine glycol. Proc Natl Acad Sci U S A. 2007; 104:814–818. [PubMed: 17210917]

201. Dolinnaya NG, Kubareva EA, Romanova EA, Trikin RM, Oretskaya TS. Thymidine glycol: the effect on DNA molecular structure and enzymatic processing. Biochimie. 2013; 95:134–147. [PubMed: 23000318]

202. Hayes RC, Petrullo LA, Huang H, Wallace SS, Leclerc JE. Oxidative damage in DNA:lack of mutagenicity by thymine glycol lesions. J Mol Biol. 1988; 201:239–246. [PubMed: 3418701]

203. Yuan BF, Jiang Y, Wang YS, Wang YS. Efficient formation of the tandem thymine glycol/8-oxo-7,8-dihydroguanine lesion in isolated DNA and the mutagenic and cytotoxic properties of the tandem lesions in Escherichia coli cells. Chem Res Toxicol. 2010; 23:11–19. [PubMed: 20014805]

204. Bellon S, Shikazono N, Cunniffe S, Lomax M, O'Neill P. Processing of thymine glycol in a clustered DNA damage site: mutagenic or cytotoxic. Nucleic Acids Res. 2009; 37:4430–4440. [PubMed: 19468043]

205. Almohaini M, Chalasani L, Bafail D, Akopiants K, Zhou T, Yannone SM, Ramsden DA, Hartman MCT, Povirk LF. Nonhomologous end joining of complex DNA double-strand breaks with proximal thymine glycol and interplay with base excision repair. DNA Repair. 2016; 41:16–26. [PubMed: 27049455]

206. Miller H, Fernandes AS, Zaika E, McTigue MM, Torres MC, Wente M, Iden CR, Grollman AP. Stereoselective excision of thymine glycol from oxidatively damaged DNA. Nucleic Acids Res. 2004; 32:338–345. [PubMed: 14726482]

207. Yeo JC, Goodman RA, Schirle NT, David SS, Beal PA. RNA editing changes the lesion specificity for the DNA repair enzyme NEIL1. Proc Natl Acad Sci U S A. 2010; 107:20715–20719. [PubMed: 21068368]
208. Zhu CX, Lu LM, Zhang J, Yue ZW, Song JH, Zong S, Liu MH, Stovicek O, Gao YQ, Yi CQ. Tautomerization-dependent recognition and excision of oxidation damage in base-excision DNA repair. Proc Natl Acad Sci U S A. 2016; 113:7792–7797. [PubMed: 27354518]
209. Lin JJ, Sancar A. A new mechanism for repairing oxidative damage to DNA: (A)BC excinuclease removes AP sites and thymine glycols from DNA. Biochemistry. 1989; 28:7979–7984. [PubMed: 2690930]
210. Kow YW, Wallace SS, Vanhouten B. UvrABC nuclease complex repairs thymine glycol, an oxidative DNA base damage. Mutat Res DNA Repair. 1990; 235:147–156. [PubMed: 2407949]
211. Reardon JT, Bessho T, Kung HC, Bolton PH, Sancar A. *In vitro* repair of oxidative DNA damage by human nucleotide excision repair system: Possible explanation for neuro-degeneration in Xeroderma pigmentosum patients. Proc Natl Acad Sci U S A. 1997; 94:9463–9468. [PubMed: 9256505]
212. Brown KL, Roginskaya M, Zou Y, Altamirano A, Basu AK, Stone MP. Binding of the human nucleotide excision repair proteins XPA and XPC/HR23B to the 5*R*-thymine glycol lesion and structure of the *cis*-(5*R*,6*S*) thymine glycol epimer in the 5′-GTgG-3′ sequence: destabilization of two base pairs at the lesion site. Nucleic Acids Res. 2010; 38:428–440. [PubMed: 19892827]
213. Perevozchikova SA, Trikin RM, Heinze RJ, Romanova EA, Oretskaya TS, Friedhoff P, Kubareva EA. Is thymidine glycol containing DNA a substrate of *E. coli* DNA mismatch repair system? PLoS One. 2014; 9:e104963. [PubMed: 25133614]
214. Levy DD, Teebor GW. Site directed substitution of 5-hydroxymethyluracil for thymine in replicating phi-X-174am3 DNA via synthesis of 5-hydroxymethyl-2′-deoxyuridine-5′-triphosphate. Nucleic Acids Res. 1991; 19:3337–3343. [PubMed: 2062651]
215. Herrala AM, Vilpo JA. Template-primer activity of 5-(hydroxymethyl)uracil-containing DNA for prokaryotic and eukaryotic DNA and RNA polymerases. Biochemistry. 1989; 28:8274–8277. [PubMed: 2513877]
216. Mellac S, Fazakerley GV, Sowers LC. Structures of base pairs with 5-(hydroxymethyl)-2′-deoxyuridine in DNA determined by NMR spectroscopy. Biochemistry. 1993; 32:7779–7786. [PubMed: 8394115]
217. Kallen RG, Marmur J, Simon M. Occurrence of a new pyrimidine base replacing thymine in a bacteriophage DNA: 5-hydroxymethyl uracil. J Mol Biol. 1962; 5:248–250. [PubMed: 13961966]
218. Rusmintratip V, Sowers LC. An unexpectedly high excision capacity for mispaired 5-hydroxymethyluracil in human cell extracts. Proc Natl Acad Sci U S A. 2000; 97:14183–14187. [PubMed: 11121024]
219. Wibley JEA, Waters TR, Haushalter K, Verdine GL, Pearl LH. Structure and specificity of the vertebrate anti-mutator uracil-DNA glycosylase SMUG1. Mol Cell. 2003; 11:1647–1659. [PubMed: 12820976]
220. Cortellino S, Xu JF, Sannai M, Moore R, Caretti E, Cigliano A, Le Coz M, Devarajan K, Wessels A, Soprano D, Abramowitz LK, Bartolomei MS, Rambow F, Bassi MR, Bruno T, Fanciulli M, Renner C, Klein-Szanto AJ, Matsumoto Y, Kobi D, Davidson I, Alberti C, Larue L, Bellacosa A. Thymine DNA glycosylase Is essential for active DNA demethylation by linked deamination-base excision repair. Cell. 2011; 146:67–79. [PubMed: 21722948]
221. Morera S, Grin I, Vigouroux A, Couve S, Henriot V, Saparbaev M, Ishchenko AA. Biochemical and structural characterization of the glycosylase domain of MBD4 bound to thymine and 5-hydroxymethyuracil-containing DNA. Nucleic Acids Res. 2012; 40:9917–9926. [PubMed: 22848106]
222. Hashimoto H, Hong S, Bhagwat AS, Zhang X, Cheng XD. Excision of 5-hydroxymethyluracil and 5-carboxylcytosine by the thymine DNA glycosylase domain: its structural basis and implications for active DNA demethylation. Nucleic Acids Res. 2012; 40:10203–10214. [PubMed: 22962365]

223. Zarakowska E, Gackowski D, Foksinski M, Olinski R. Are 8-oxoguanine (8-oxoGua) and 5-hydroxymethyluracil (5-hmUra) oxidatively damaged DNA bases or transcription (epigenetic) marks? Mutat Res Genet Toxicol Environ Mutagen. 2014:764–765. 58–63.

224. Olinski R, Starczak M, Gackowski D. Enigmatic 5-hydroxymethyluracil: Oxidatively modified base, epigenetic mark or both? Mutat Res Rev Mutat Res. 2016; 767:59–66. [PubMed: 27036066]

225. Klungland A, Paulsen R, Rolseth V, Yamada Y, Ueno Y, Wiik P, Matsuda A, Seeberg E, Bjelland S. 5-Formyluracil and its nucleoside derivatives confer toxicity and mutagenicity to mammalian cells by interfering with normal RNA and DNA metabolism. Toxicol Lett. 2001; 119:71–78. [PubMed: 11275423]

226. Kamiya H, Murata-Kamiya N, Karino N, Ueno Y, Matsuda A, Kasai H. Induction of TàG and TaÀ transversions by 5-formyluracil in mammalian cells. Mutat Res Genet Toxicol Environ Mutagen. 2002; 513:213–222.

227. Bjelland S, Birkeland NK, Benneche T, Volden G, Seeberg E. DNA glycosylase activities for thymine residues oxidized in the methyl-troup are functions of the AlkA enzyme in Escherichia coli. J Biol Chem. 1994; 269:30489–30495. [PubMed: 7982966]

228. Masaoka A, Terato H, Kobayashi M, Honsho A, Ohyama Y, Ide H. Enzymatic repair of 5-formyluracil I. Excision of 5-formyluracil site-specifically incorporated into oligonucleotide substrates by AlkA protein (*Escherichia coli* 3-methyladenine DNA glycosylase II). J Biol Chem. 1999; 274:25136–25143. [PubMed: 10455195]

229. Terato H, Masaoka A, Kobayashi M, Fukushima S, Ohyama Y, Yoshida M, Ide H. Enzymatic repair of 5-formyluracil II. Mismatch formation between 5-formyluracil and guanine during DNA replication and its recognition by two proteins involved in base excision repair (AlkA) and mismatch repair (MutS). J Biol Chem. 1999; 274:25144–25150. [PubMed: 10455196]

230. Matsubara M, Masaoka A, Tanaka T, Miyano T, Kato N, Terato H, Ohyama Y, Iwai S, Ide H. Mammalian 5-formyluracil-DNA glycosylase. 1. Identification and characterization of a novel activity that releases 5-formyluracil from DNA. Biochemistry. 2003; 42:4993–5002. [PubMed: 12718542]

231. Masaoka A, Matsubara M, Hasegawa R, Tanaka T, Kurisu S, Terato H, Ohyama Y, Karino N, Matsuda A, Ide H. Mammalian 5-formyluracil-DNA glycosylase. 2. role of SMUG1 uracilDNA glycosylase in repair of 5-formyluracil and other oxidized and deaminated base lesions. Biochemistry. 2003; 42:5003–5012. [PubMed: 12718543]

232. Knaevelsrud I, Slupphaug G, Leiros I, Matsuda A, Ruoff P, Bjelland S. Opposite-base dependent excision of 5-formyluracil from DNA by hSMUG1. Int J Radiat Biol. 2009; 85:413–420. [PubMed: 19365746]

233. Liu PF, Burdzy A, Sowers LC. Repair of the mutagenic DNA oxidation product, 5-formyluracil. DNA Repair. 2003; 2:199–210. [PubMed: 12531390]

234. Zhang QM, Miyabe I, Matsumoto Y, Kino K, Sugiyama H, Yonei S. Identification of repair enzymes for 5-formyluracil in DNA - Nth, Nei, and MutM proteins of *Escherichia coli*. J Biol Chem. 2000; 275:35471–35477. [PubMed: 10956660]

235. Miyabe I, Zhang QM, Kino K, Sugiyama H, Takao M, Yasui A, Yonei S. Identification of 5-formyluracil DNA glycosylase activity of human hNTH1 protein. Nucleic Acids Res. 2002; 30:3443–3448. [PubMed: 12140329]

236. Yonekura S, Nakamura N, Doi T, Sugiyama H, Yamamoto K, Yonei S, Zhang Q. Recombinant *Schizosaccharomyces pombe* Nth1 protein exhibits DNA glycosylase activities for 8-oxo-7,8-dihydroguanine and thymine residues oxidized in the methyl group. J Radiat Res. 2007; 48:417–424. [PubMed: 17641464]

237. Zhang-Akiyama QM, Morinaga H, Kikuchi M, Yonekura SI, Sugiyama H, Yamamoto K, Yonei S. KsgA, a 16S rRNA adenine methyltransferase, has a novel DNA glycosylase/AP lyase activity to prevent mutations in Escherichia coli. Nucleic Acids Res. 2009; 37:2116–2125. [PubMed: 19223326]

238. Belousova EA, Vasil'eva IA, Moor NA, Zatsepin TS, Oretskaya TS, Lavrik OI. Clustered DNA lesions containing 5-formyluracil and AP Site: repair via the BER system. PLoS One. 2013; 8:e68576. [PubMed: 23936307]

239. Münzel M, Lischke U, Stathis D, Pfaffeneder T, Gnerlich FA, Deiml CA, Koch SC, Karaghiosoff K, Carell T. Improved synthesis and mutagenicity of oligonucleotides containing 5-hydroxymethylcytosine, 5-formylcytosine and 5-carboxylcytosine. Chem - Eur J. 2011; 17:13782–13788. [PubMed: 22069110]

240. Xing XW, Liu YL, Vargas M, Wang Y, Feng YQ, Zhou X, Yuan BF. Mutagenic and cytotoxic properties of oxidation products of 5-methylcytosine revealed by next-generation sequencing. PLoS One. 2013; 8:e72993. [PubMed: 24066027]

241. Kamiya H, Tsuchiya H, Karino N, Ueno Y, Matsuda A, Harashima H. Mutagenicity of 5-formylcytosine, an oxidation product of 5-methylcytosine, in DNA in mammalian cells. J Biochem. 2002; 132:551–555. [PubMed: 12359069]

242. Ji D, You C, Wang P, Wang Y. Effects of Tet-Induced oxidation products of 5-methylcytosine on DNA replication in mammalian cells. Chem Res Toxicol. 2014; 27:1304–1309. [PubMed: 24979327]

243. Kellinger MW, Song CX, Chong J, Lu XY, He C, Wang D. 5-formylcytosine and 5-carboxylcytosine reduce the rate and substrate specificity of RNA polymerase II transcription. Nat Struct Mol Biol. 2012; 19:831–833. [PubMed: 22820989]

244. Zheng G, Fu Y, He C. Nucleic acid oxidation in DNA damage repair and epigenetics. Chem Rev. 2014; 114:4602–4620. [PubMed: 24580634]

245. Lu X, Zhao BS, He C. TET family proteins: Oxidation activity, interacting molecules, and functions in diseases. Chem Rev. 2015; 115:2225–2239. [PubMed: 25675246]

246. Maiti A, Drohat AC. Thymine DNA glycosylase can rapidly excise 5-formylcytosine and 5-carboxylcytosine: potential implications for active demethylation of CpG sites. J Biol Chem. 2011; 286:35334–35338. [PubMed: 21862836]

247. Cortazar D, Kunz C, Selfridge J, Lettieri T, Saito Y, MacDougall E, Wirz A, Schuermann D, Jacobs AL, Siegrist F, Steinacher R, Jiricny J, Bird A, Schar P. Embryonic lethal phenotype reveals a function of TDG in maintaining epigenetic stability. Nature. 2011; 470:419–423. [PubMed: 21278727]

248. Nabel CS, Jia H, Ye Y, Shen L, Goldschmidt HL, Stivers JT, Zhang Y, Kohli RM. AID/APOBEC deaminases disfavor modified cytosines implicated in DNA demethylation. Nat Chem Biol. 2012; 8:751–758. [PubMed: 22772155]

249. Kuraoka I, Bender C, Romieu A, Cadet J, Wood RD, Lindahl T. Removal of oxygen free-radical-induced 5′,8-purine cyclodeoxynucleosides from DNA by the nucleotide excision-repair pathway in human cells. Proc Natl Acad Sci U S A. 2000; 97:3832–3837. [PubMed: 10759556]

250. You C, Dai X, Yuan B, Wang J, Wang J, Brooks PJ, Niedernhofer LJ, Wang Y. A quantitative assay for assessing the effects of DNA lesions on transcription. Nat Chem Biol. 2012; 8:817–822. [PubMed: 22902614]

251. Kuraoka I, Robins P, Masutani C, Hanaoka F, Gasparutto D, Cadet J, Wood RD, Lindahl T. Oxygen free radical damage to DNA: translesion synthesis by human DNA polymerase η and resistance to exonuclease action at cyclopurine deoxynucleoside residues. J Biol Chem. 2001; 276:49283–49288. [PubMed: 11677235]

252. Jasti VP, Das RS, Hilton BA, Weerasooriya S, Zou Y, Basu AK. 5′*S*)-8,5′-cyclo-2′-deoxyguanosine is a strong block to replication, a potent pol V-dependent mutagenic lesion, and is inefficiently repaired in *Escherichia coli*. Biochemistry. 2011; 50:3862–3865. [PubMed: 21491964]

253. Yuan B, Wang J, Cao H, Sun R, Wang Y. High-throughput analysis of the mutagenic and cytotoxic properties of DNA lesions by next-generation sequencing. Nucleic Acids Res. 2011; 39:5945–5954. [PubMed: 21470959]

254. You C, Swanson AL, Dai X, Yuan B, Wang J, Wang Y. Translesion synthesis of 8,5′-cyclopurine-2′-deoxynucleo-sides by DNA polymerases η, ι, and ζ. J Biol Chem. 2013; 288:28548–28556. [PubMed: 23965998]

255. Marietta C, Brooks PJ. Transcriptional bypass of bulky DNA lesions causes new mutant RNA transcripts in human cells. EMBO Rep. 2007; 8:388–393. [PubMed: 17363972]

256. Yang Z, Colis LC, Basu AK, Zou Y. Recognition and incision of gamma-radiation-induced cross-linked γ-thymine tandem lesion G[8,5-Me]T by UvrABC nuclease. Chem Res Toxicol. 2005; 18:1339–1346. [PubMed: 16167825]

257. Gu C, Zhang Q, Yang Z, Wang Y, Zou Y, Wang Y. Recognition and incision of oxidative intrastrand cross-link lesions by UvrABC nuclease. Biochemistry. 2006; 45:10739–10746. [PubMed: 16939226]

258. Raychaudhury P, Basu AK. Genetic requirement for mutagenesis of the G[8,5-Me]T cross-link in Escherichia coli: DNA polymerases IV and V compete for error-prone bypass. Biochemistry. 2011; 50:2330–2338. [PubMed: 21302943]

259. Ding S, Kropachev K, Cai Y, Kolbanovskiy M, Durandina SA, Liu Z, Shafirovich V, Broyde S, Geacintov NE. Structural, energetic and dynamic properties of guanine(C8)– thymine(N3) cross-links in DNA provide insights on susceptibility to nucleotide excision repair. Nucleic Acids Res. 2012; 40:2506–2517. [PubMed: 22135299]

260. Talhaoui I, Shafirovich V, Liu Z, Saint-Pierre C, Akishev Z, Matkarimov BT, Gasparutto D, Geacintov NE, Saparbaev M. Oxidatively Generated Guanine(C8)-Thymine(N3) Intrastrand Cross-links in Double-stranded DNA Are Repaired by Base Excision Repair Pathways. J Biol Chem. 2015; 290:14610–14617. [PubMed: 25903131]

261. Lee YA, Lee YC, Geacintov NE, Shafirovich V. Translesion synthesis past guanine(C8)-thymine(N3) intra-strand cross-links catalyzed by selected A- and Y-family polymerases. Mol BioSyst. 2016; 12:1892–1900. [PubMed: 27102383]

262. Fujikawa K, Yakushiji H, Nakabeppu Y, Suzuki T, Masuda M, Ohshima H, Kasai H. 8-chloro-dGTP, a hypochlorous acid-modified nucleotide, is hydrolyzed by hMTH1, the human MutT homolog. FEBS Lett. 2002; 512:149–151. [PubMed: 11852070]

263. Kim CH, Darwanto A, Theruvathu JA, Herring JL, Sowers LC. Polymerase incorporation and miscoding properties of 5-chlorouracil. Chem Res Toxicol. 2010; 23:740–748. [PubMed: 20104909]

264. Fedeles BI, Freudenthal BD, Yau E, Singh V, Chang SC, Li DY, Delaney JC, Wilson SH, Essigmann JM. Intrinsic mutagenic properties of 5-chlorocytosine: A mechanistic connection between chronic inflammation and cancer. Proc Natl Acad Sci U S A. 2015; 112:E4571–E4580. [PubMed: 26243878]

265. Valinluck V, Liu P, Kang JI, Burdzy A, Sowers LC. 5-Halogenated pyrimidine lesions within a CpG sequence context mimic 5-methylcytosine by enhancing the binding of the methyl-CpG-binding domain of methyl-CpG-binding protein 2 (MeCP2). Nucleic Acids Res. 2005; 33:3057–3064. [PubMed: 15917437]

266. Theruvathu JA, Yin YW, Pettitt BM, Sowers LC. Comparison of the structural and dynamic effects of 5-methylcytosine and 5-chlorocytosine in a CpG dinucleotide sequence. Biochemistry. 2013; 52:8590–8598. [PubMed: 24147911]

267. Valinluck V, Wu W, Liu PF, Neidigh JW, Sowers LC. Impact of cytosine 5-halogens on the interaction of DNA with restriction endonucleases and methyltransferase. Chem Res Toxicol. 2006; 19:556–562. [PubMed: 16608167]

268. Valinluck V, Sowers LC. Endogenous cytosine damage products alter the site selectivity of human DNA maintenance methyltransferase DNMT1. Cancer Res. 2007; 67:946–950. [PubMed: 17283125]

269. Mazrimas JA, Stetka DG. Direct evidence for the role of incorporated BUdR in the induction of sister chromatid exchanges. Exp Cell Res. 1978; 117:23–30. [PubMed: 720406]

270. Heartlein MW, O'Neill JP, Pal BC, Preston RJ. The induction of specific-locus mutations and sister-chromatid exchanges by 5-bromo- and 5-chloro-deoxyuridine. Mutat Res Fundam Mol Mech Mutagen. 1982; 92:411–416.

271. Sassa A, Ohta T, Nohmi T, Honma M, Yasui M. Mutational specificities of brominated DNA adducts catalyzed by human DNA polymerases. J Mol Biol. 2011; 406:679–686. [PubMed: 21241706]

272. Neeley WL, Delaney JC, Henderson PT, Essigmann JM. *In vivo* Bypass Efficiencies and Mutational Signatures of the Guanine Oxidation Products 2-Aminoimidazolone and 5-Guanidino-4-nitroimidazole. J Biol Chem. 2004; 279:43568–43573. [PubMed: 15299010]

273. Dimitri A, Jia L, Shafirovich V, Geacintov NE, Broyde S, Scicchitano DA. Transcription of DNA containing the 5-guanidino-4-nitroimidazole lesion by human RNA polymerase II and bacteriophage T7 RNA polymerase. DNA Repair. 2008; 7:1276–1288. [PubMed: 18555749]

274. Hang B, Chenna A, Guliaev AB, Singer B. Miscoding properties of 1,N^6-ethanoadenine, a DNA adduct derived from reaction with the antitumor agent 1,3-bis(2-chloroethyl)-1-nitrosourea. Mutat Res Fundam Mol Mech Mutagen. 2003; 531:191–203.

275. Pandya GA, Moriya M. 1,N6-Ethenodeoxyadenosine, a DNA adduct highly mutagenic in mammalian cells. Biochemistry. 1996; 35:11487–11492. [PubMed: 8784204]

276. Tolentino JH, Burke TJ, Mukhopadhyay S, McGregor WG, Basu AK. Inhibition of DNA replication fork progression and mutagenic potential of 1,N-6-ethenoadenine and 8-oxoguanine in human cell extracts. Nucleic Acids Res. 2008; 36:1300–1308. [PubMed: 18184697]

277. Levine RL, Yang IY, Hossain M, Pandya GA, Grollman AP, Moriya M. Mutagenesis induced by a single 1,N^6-ethenodeoxyadenosine adduct in human cells. Cancer Res. 2000; 60:4098–4104. [PubMed: 10945616]

278. Moriya M, Zhang W, Johnson F, Grollman AP. Mutagenic potency of exocyclic DNA adducts: marked differences between Escherichia coli and simian kidney cells. Proc Natl Acad Sci U S A. 1994; 91:11899–11903. [PubMed: 7991554]

279. Langouët S, Mican AN, Müller M, Fink SP, Marnett LJ, Muhle SA, Guengerich FP. Misincorporation of nucleotides opposite five-membered exocyclic ring guanine derivatives by *Escherichia coli* polymerases *in vitro* and *in vivo*:1,N^2-ethenoguanine, 5,6,7,9-tetrahydro-9-oxoimidazo[1,2-*a*]purine, and 5,6,7,9-tetrahydro-7-hydroxy-9-oxoimidazo[1,2-*a*]purine. Biochemistry. 1998; 37:5184–5193. [PubMed: 9548749]

280. Cheng KC, Preston BD, Cahill DS, Dosanjh MK, Singer B, Loeb LA. The vinyl chloride DNA derivative N^2,3-ethenoguanine produces GaÀ transitions in Escherichia coli. Proc Natl Acad Sci U S A. 1991; 88:9974–9978. [PubMed: 1946466]

281. Gros L, Ishchenko AA, Saparbaev M. Enzymology of repair of etheno-adducts. Mutat Res Fundam Mol Mech Mutagen. 2003; 531:219–229.

282. Zdżalik D, Domańska A, Prorok P, Kosicki K, van den Born E, Falnes PØ, Rizzo CJ, Guengerich FP, Tudek B. Differential repair of etheno-DNA adducts by bacterial and human AlkB proteins. DNA Repair. 2015; 30:1–10. [PubMed: 25797601]

283. Benamira M, Johnson K, Chaudhary A, Bruner K, Tibbetts C, Marnett LJ. Induction of mutations by replication of malondialdehyde modified M13 DNA in *Escherichia coil*: determination of the extent of DNA modification, genetic requirements for mutagenesis, and types of mutations induced. Carcinogenesis. 1995; 16:93–99. [PubMed: 7834810]

284. Fink SP, Reddy GR, Marnett LJ. Mutagenicity in *Escherichia coli* of the major DNA adduct derived from the endogenous mutagen malondialdehyde. Proc Natl Acad Sci U S A. 1997; 94:8652–8657. [PubMed: 9238032]

285. Niedernhofer LJ, Daniels JS, Rouzer CA, Greene RE, Marnett LJ. Malondialdehyde, a product of lipid peroxidation, is mutagenic in human cells. J Biol Chem. 2003; 278:31426–31433. [PubMed: 12775726]

286. VanderVeen LA, Hashim MF, Shyr Y, Marnett LJ. Induction of frameshift and base pair substitution mutations by the major DNA adduct of the endogenous carcinogen malondialdehyde. Proc Natl Acad Sci U S A. 2003; 100:14247–14252. [PubMed: 14603032]

287. Singh V, Fedeles BI, Li D, Delaney JC, Kozekov ID, Kozekova A, Marnett LJ, Rizzo CJ, Essigmann JM. Mechanism of repair of acrolein- and malondialdehyde-derived exocyclic guanine adducts by the α-ketoglutarate/Fe(II) dioxygenase AlkB. Chem Res Toxicol. 2014; 27:1619–1631. [PubMed: 25157679]

288. Tretyakova N, Goggin M, Sangaraju D, Janis G. Quantitation of DNA adducts by stable isotope dilution mass spectrometry. Chem Res Toxicol. 2012; 25:2007–2035. [PubMed: 22827593]

289. Shinmura K, Tao H, Goto M, Igarashi H, Taniguchi T, Maekawa M, Takezaki T, Sugimura H. Inactivating mutations of the human base excision repair gene NEIL1 in gastric cancer. Carcinogenesis. 2004; 25:2311–2317. [PubMed: 15319300]

290. Delaney S, Delaney JC, Essigmann JM. Chemical-biological fingerprinting: Probing the properties of DNA lesions-formed by peroxynitrite. Chem Res Toxicol. 2007; 20:1718–1729. [PubMed: 17941698]

291. Zhou J, Fleming AM, Averill AM, Burrows CJ, Wallace SS. The NEIL glycosylases remove oxidized guanine lesions from telomeric and promoter quadruplex DNA structures. Nucleic Acids Res. 2015; 43:4039–4054. [PubMed: 25813041]

292. Norabuena EM, Williams SB, Klureza MA, Goehring LJ, Gruessner B, Radhakrishnan ML, Jamieson ER, Nunez ME. Effect of the spiroiminodihydantoin lesion on nucleosome stability and positioning. Biochemistry. 2016; 55:2411–2421. [PubMed: 27074396]

293. Cathcart R, Schwiers E, Saul RL, Ames BN. Thymine glycol and thymidine glycol in human and rat urine: a possible assay for oxidative DNA damage. Proc Natl Acad Sci U S A. 1984; 81:5633–5637. [PubMed: 6592579]

294. Adelman R, Saul RL, Ames BN. Oxidative damage to DNA: relation to species metabolic rate and life span. Proc Natl Acad Sci U S A. 1988; 85:2706–2708. [PubMed: 3128794]

295. Cao EH, Wang JJ. Oxidative damage to DNA: levels of thymine glycol and thymidine glycol in neoplastic human urines. Carcinogenesis. 1993; 14:1359–1362. [PubMed: 8330350]

296. Wang Y. Bulky DNA lesions induced by reactive oxygen species. Chem Res Toxicol. 2008; 21:276–281. [PubMed: 18189366]

297. Box HC, Budzinski EE, Evans MS, French JB, Maccubbin AE. The differential lysis of phosphoester bonds by nuclease P1. Biochim Biophys Acta, Protein Struct Mol Enzymol. 1993; 1161:291–294.

298. Falcone JM, Box HC. Selective hydrolysis of damaged DNA by nuclease P1. Biochim Biophys Acta, Protein Struct Mol Enzymol. 1997; 1337:267–275.

299. Bailey DT, DeFedericis HCC, Greene KF, Iijima H, Budzinski EE, Patrzyc HB, Dawidzik JB, Box HC. A novel approach to DNA damage assessments: Measurement of the thymine glycol lesion. Radiat Res. 2006; 165:438–444. [PubMed: 16579656]

300. Greene KE, Budzinski EE, Iijima H, Dawidzik JB, DeFedericis HC, Patrzyc HB, Evans MS, Bailey DT, Freund HG, Box HC. Assessment of DNA damage at the dimer level: Measurement of the formamide lesion. Radiat Res. 2007; 167:146–151. [PubMed: 17390722]

301. Iijima H, Patrzyc HB, Budzinski EE, Freund HG, Dawidzik JB, Rodabaugh KJ, Box HC. A study of pyrimidine base damage in relation to oxidative stress and cancer. Br J Cancer. 2009; 101:452–456. [PubMed: 19603029]

302. Budzinski EE, Patrzyc HB, Dawidzik JB, Freund HG, Frederick P, Godoy HE, Voian NC, Odunsi K, Box HC. Pyrimidine base damage is increased in women with BRCA mutations. Cancer Lett. 2013; 338:267–270. [PubMed: 23583677]

303. Box HC, O'Connor RJ, Patrzyc HB, Iijima H, Dawidzik JB, Freund HG, Budzinski EE, Cummings KM, Mahoney MC. Reduction in oxidatively generated DNA damage following smoking cessation. Tob Induced Dis. 2011; 9:5.

304. Box HC, Patrzyc HB, Budzinski EE, Dawidzik JB, Freund HG, Zeitouni NC, Mahoney MC. Profiling oxidative DNA damage: Effects of antioxidants. Cancer Sci. 2012; 103:2002–2006. [PubMed: 22834775]

305. McNulty JM, Jerkovic B, Bolton PH, Basu AK. Replication inhibition and miscoding properties of DNA templates containing a site-specific cis-thymine glycol or urea residue. Chem Res Toxicol. 1998; 11:666–673. [PubMed: 9625735]

306. Liu S, Wang J, Su Y, Guerrero C, Zeng Y, Mitra D, Brooks PJ, Fisher DE, Song H, Wang Y. Quantitative assessment of Tet-induced oxidation products of 5-methylcytosine in cellular and tissue DNA. Nucleic Acids Res. 2013; 41:6421–6429. [PubMed: 23658232]

307. Frelon S, Douki T, Ravanat JL, Pouget JP, Tornabene C, Cadet J. High-performance liquid chromatography-tandem mass spectrometry measurement of radiation-induced base damage to isolated and cellular DNA. Chem Res Toxicol. 2000; 13:1002–1010. [PubMed: 11080049]

308. Hong HH, Wang YS. Derivatization with Girard reagent T combined with LC-MS/MS for the sensitive detection of 5-formyl-2′-deoxyuridine in cellular DNA. Anal Chem. 2007; 79:322–326. [PubMed: 17194156]

309. Bullard W, da Rosa-Spiegler JL, Liu S, Wang YS, Sabatini R. Identification of the glucosyltransferase that converts hydroxymethyluracil to base J in the trypanosomatid genome. J Biol Chem. 2014; 289:20273–20282. [PubMed: 24891501]

310. Wu J, Forbes JR, Chen HS, Cox DW. The LEC rat has a deletion in the copper transporting ATPase gene homologous to the Wilson disease gene. Nat Genet. 1994; 7:541–545. [PubMed: 7951327]

311. Ala A, Walker AP, Ashkan K, Dooley JS, Schilsky ML. Wilson's disease. Lancet. 2007; 369:397–408. [PubMed: 17276780]

312. Roberts EA, Schilsky ML. Diagnosis and treatment of Wilson disease: An update. Hepatology. 2008; 47:2089–2111. [PubMed: 18506894]

313. Killian JK, Kim SY, Miettinen M, Smith C, Merino M, Tsokos M, Quezado M, Smith WI, Jahromi MS, Xekouki P, Szarek E, Walker RL, Lasota J, Raffeld M, Klotzle B, Wang Z, Jones L, Zhu Y, Wang Y, Waterfall JJ, O'Sullivan MJ, Bibikova M, Pacak K, Stratakis C, Janeway KA, Schiffman JD, Fan JB, Helman L, Meltzer PS. Succinate dehydrogenase mutation underlies global epigenomic divergence in gastrointestinal stromal tumor. Cancer Discovery. 2013; 3:648–657. [PubMed: 23550148]

314. Figueroa ME, Abdel-Wahab O, Lu C, Ward PS, Patel J, Shih A, Li Y, Bhagwat N, Vasanthakumar A, Fernandez HF, Tallman MS, Sun Z, Wolniak K, Peeters JK, Liu W, Choe SE, Fantin VR, Paietta E, Löwenberg B, Licht JD, Godley LA, Delwel R, Valk PJM, Thompson CB, Levine RL, Melnick A. Leukemic IDH1 and IDH2 mutations result in a hypermethylation phenotype, disrupt TET2 function, and impair hematopoietic differentiation. Cancer Cell. 2010; 18:553–567. [PubMed: 21130701]

315. Yang H, Lin H, Xu H, Zhang L, Cheng L, Wen B, Shou J, Guan K, Xiong Y, Ye D. TET-catalyzed 5-methylcytosine hydroxylation is dynamically regulated by metabolites. Cell Res. 2014; 24:1017–1020. [PubMed: 24971736]

316. Ye D, Xiong Y, Guan KL. The mechanisms of IDH mutations in tumorigenesis. Cell Res. 2012; 22:1102–1104. [PubMed: 22453240]

317. Dang L, White DW, Gross S, Bennett BD, Bittinger MA, Driggers EM, Fantin VR, Jang HG, Jin S, Keenan MC, Marks KM, Prins RM, Ward PS, Yen KE, Liau LM, Rabinowitz JD, Cantley LC, Thompson CB, Vander Heiden MG, Su SM. Cancer-associated IDH1 mutations produce 2-hydroxyglutarate. Nature. 2009; 462:739–744. [PubMed: 19935646]

318. Ward PS, Patel J, Wise DR, Abdel-Wahab O, Bennett BD, Coller HA, Cross JR, Fantin VR, Hedvat CV, Perl AE, Rabinowitz JD, Carroll M, Su SM, Sharp KA, Levine RL, Thompson CB. The common feature of leukemia-associated IDH1 and IDH2 mutations is a neomorphic enzyme activity converting α-ketoglutarate to 2-hydroxyglutarate. Cancer Cell. 2010; 17:225–234. [PubMed: 20171147]

319. Xiao M, Yang H, Xu W, Ma S, Lin H, Zhu H, Liu L, Liu Y, Yang C, Xu Y, Zhao S, Ye D, Xiong Y, Guan KL. Inhibition of α-KG-dependent histone and DNA demethylases by fumarate and succinate that are accumulated in mutations of FH and SDH tumor suppressors. Genes Dev. 2012; 26:1326–1338. [PubMed: 22677546]

320. Schulze A, Harris AL. How cancer metabolism is tuned for proliferation and vulnerable to disruption. Nature. 2012; 491:364–373. [PubMed: 23151579]

321. Xu W, Yang H, Liu Y, Yang Y, Wang P, Kim SH, Ito S, Yang C, Wang P, Xiao MT, Liu Lx, Jiang Wq, Liu J, Zhang Jy, Wang B, Frye S, Zhang Y, Xu Yh, Lei Qy, Guan KL, Zhao Sm, Xiong Y. Oncometabolite 2-hydroxyglutarate is acompetitive inhibitor of α-ketoglutarate-dependent dioxygenases. Cancer Cell. 2011; 19:17–30. [PubMed: 21251613]

322. Jin SG, Jiang Y, Qiu R, Rauch TA, Wang Y, Schackert G, Krex D, Lu Q, Pfeifer GP. 5-hydroxymethylcytosine is strongly depleted in human cancers but its levels do not correlate with IDH1 mutations. Cancer Res. 2011; 71:7360–7365. [PubMed: 22052461]

323. Shen L, Song CX, He C, Zhang Y. Mechanism and function of oxidative reversal of DNA and RNA methylation. Annu Rev Biochem. 2014; 83:585–614. [PubMed: 24905787]

324. Song CX, He C. Potential functional roles of DNA demethylation intermediates. Trends Biochem Sci. 2013; 38:480–484. [PubMed: 23932479]

325. Spruijt CG, Gnerlich F, Smits Arne H, Pfaffeneder T, Jansen Pascal WTC, Bauer C, Münzel M, Wagner M, Müller M, Khan F, Eberl HC, Mensinga A, Brinkman Arie B, Lephikov K, Müller U, Walter J, Boelens R, van Ingen H, Leonhardt H, Carell T, Vermeulen M. Dynamic readers for 5-(hydroxy)methylcytosine and its oxidized derivatives. Cell. 2013; 152:1146–1159. [PubMed: 23434322]

326. Mellén M, Ayata P, Dewell S, Kriaucionis S, Heintz N. MeCP2 binds to 5hmC enriched within active genes and accessible chromatin in the nervous system. Cell. 2012; 151:1417–1430. [PubMed: 23260135]

327. Yildirim O, Li R, Hung JH, Chen Poshen B, Dong X, Ee LS, Weng Z, Rando Oliver J, Fazzio TG. Mbd3/NURD complex regulates expression of 5-hydroxymethylcytosine marked genes in embryonic stem cells. Cell. 2011; 147:1498–1510. [PubMed: 22196727]

328. Frauer C, Hoffmann T, Bultmann S, Casa V, Cardoso MC, Antes I, Leonhardt H. Recognition of 5-hydroxymethylcytosine by the Uhrf1 SRA domain. PLoS One. 2011; 6:e21306. [PubMed: 21731699]

329. Iurlaro M, Ficz G, Oxley D, Raiber EA, Bachman M, Booth MJ, Andrews S, Balasubramanian S, Reik W. A screen for hydroxymethylcytosine and formylcytosine binding proteins suggests functions in transcription and chromatin regulation. Genome Biol. 2013; 14:R119. [PubMed: 24156278]

330. Sun Z, Dai N, Borgaro JG, Quimby A, Sun D, Correâ Ivan R Jr, Zheng Y, Zhu Z, Guan S. A sensitive approach to map genome-wide 5-hydroxymethylcytosine and 5-formylcytosine at single-base resolution. Mol Cell. 2015; 57:750–761. [PubMed: 25639471]

331. Jin SG, Zhang ZM, Dunwell Thomas L, Harter Matthew R, Wu X, Johnson J, Li Z, Liu J, Szabó Piroska E, Lu Q, Xu Gl, Song J, Pfeifer GP. Tet3 reads 5-carboxylcytosine through its CXXC domain and is a potential guardian against neurodegeneration. Cell Rep. 2016; 14:493–505. [PubMed: 26774490]

332. Wang J, Cao H, You C, Yuan B, Bahde R, Gupta S, Nishigori C, Niedernhofer LJ, Brooks PJ, Wang Y. Endogenous formation and repair of oxidatively induced G[8–5m]T intrastrand cross-link lesion. Nucleic Acids Res. 2012; 40:7368–7374. [PubMed: 22581771]

333. Kraemer KH, Patronas NJ, Schiffmann R, Brooks BP, Tamura D, DiGiovanna JJ. Xeroderma pigmentosum, trichothiodystrophy and Cockayne syndrome: A complex genotype–phenotype relationship. Neuroscience. 2007; 145:1388–1396. [PubMed: 17276014]

334. Borgesius NZ, de Waard MC, van der Pluijm I, Omrani A, Zondag GC, van der Horst GT, Melton DW, Hoeijmakers JH, Jaarsma D, Elgersma Y. Accelerated age-related cognitive decline and neurodegeneration, caused by deficient DNA repair. J Neurosci. 2011; 31:12543–12553. [PubMed: 21880916]

335. Bartsch, H., Nair, UJ. Cancer and Inflammation Mechanisms. John Wiley & Sons, Inc; New York: 2014. Lipid peroxidation-derived DNA adducts and the role in inflammation-related carcinogenesis; p. 61-74.

336. Liu X, Lovell MA, Lynn BC. Development of a method for quantification of acrolein–deoxyguanosine adducts in DNA using isotope dilution-capillary LC/MS/MS and its application to human brain tissue. Anal Chem. 2005; 77:5982–5989. [PubMed: 16159131]

337. Moldovan GL, D'Andrea AD. How the fanconi anemia pathway guards the genome. Annu Rev Genet. 2009; 43:223–249. [PubMed: 19686080]

338. D'Andrea AD. Susceptibility pathways in Fanconi's anemia and breast cancer. N Engl J Med. 2010; 362:1909–1919. [PubMed: 20484397]

339. Kottemann MC, Smogorzewska A. Fanconi anaemia and the repair of Watson and Crick DNA crosslinks. Nature. 2013; 493:356–363. [PubMed: 23325218]

340. Tischkowitz MD, Hodgson SV. Fanconi anaemia. J Med Genet. 2003; 40:1–10. [PubMed: 12525534]

341. Jiang Q, Blount BC, Ames BN. 5-chlorouracil, a marker of DNA damage from hypochlorous acid during inflammation - A gas chromatography-mass spectrometry assay. J Biol Chem. 2003; 278:32834–32840. [PubMed: 12810714]

342. Takeshita J, Byun J, Nhan TQ, Pritchard DK, Pennathur S, Schwartz SM, Chait A, Heinecke JW. Myeloperoxidase generates 5-chlorouracil in human athero-sclerotic tissue - A potential pathway

for somatic mutagenesis by macrophages. J Biol Chem. 2006; 281:3096–3104. [PubMed: 16326702]

343. Noyon C, Delporte C, Dufour D, Cortese M, Rousseau A, Poelvoorde P, Neve J, Vanhamme L, Boudjeltia KZ, Roumeguere T, Van Antwerpen P. Validation of a sensitive LC/MSMS method for chloronucleoside analysis in biological matrixes and its applications. Talanta. 2016; 154:322–328. [PubMed: 27154681]
344. Balbo S, Villalta PW, Hecht SS. Quantitation of 7-ethylguanine in leukocyte DNA from smokers and nonsmokers by liquid chromatography-nanoelectrospray-high resolution tandem mass spectrometry. Chem Res Toxicol. 2011; 24:1729–1734. [PubMed: 21859140]
345. Zhao L, Balbo S, Wang M, Upadhyaya P, Khariwala SS, Villalta PW, Hecht SS. Quantitation of pyridyloxobutyl-DNA adducts in tissues of rats treated chronically with (R)- or (S)-N′-nitrosonornicotine (NNN) in a carcinogenicity study. Chem Res Toxicol. 2013; 26:1526–1535. [PubMed: 24001146]
346. Bessette EE, Goodenough AK, Langouët S, Yasa I, Kozekov ID, Spivack SD, Turesky RJ. Screening for DNA Adducts by data-dependent constant neutral loss-triple stage mass spectrometry with a linear quadrupole ion trap mass spectrometer. Anal Chem. 2009; 81:809–819. [PubMed: 19086795]
347. Balbo S, Hecht SS, Upadhyaya P, Villalta PW. Application of a high-resolution mass-spectrometry-based DNA adductomics approach for identification of DNA adducts in complex mixtures. Anal Chem. 2014; 86:1744–1752. [PubMed: 24410521]
348. Balbo S, Turesky RJ, Villalta PW. DNA Adductomics. Chem Res Toxicol. 2014; 27:356–366. [PubMed: 24437709]
349. Zhao YY, Wu SP, Liu S, Zhang Y, Lin RC. Ultra-performance liquid chromatography–mass spectrometry as a sensitive and powerful technology in lipidomic applications. Chem Biol Interact. 2014; 220:181–192. [PubMed: 25014415]
350. Guo J, Yun BH, Upadhyaya P, Yao L, Krishnamachari S, Rosenquist TA, Grollman AP, Turesky RJ. Multiclass carcinogenic DNA adduct quantification in formalin-fixed paraffin-embedded tissues by ultraperformance liquid chromatography–tandem mass spectrometry. Anal Chem. 2016; 88:4780–4787. [PubMed: 27043225]
351. Li H, Cui S, Wang S, Jiang X, Zhang S, Zhang R, Fu PP, Sun X. Ultrasensitive UPLC–MS/MS method for analysis of etheno-DNA adducts in human white blood cells. Free Radical Res. 2015; 49:1049–1054. [PubMed: 25968941]
352. ESCODD (European Standards Committee on Oxidative DNA Damage. Comparative analysis of baseline 8-oxo-7,8-dihydroguanosine in mammalian cell DNA, by different methods in different laboratories: an approach to consensus. Carcinogenesis. 2002; 23:2129–2133. [PubMed: 12507938]

Biographies

Yang Yu received his B.S. (2009) and M.S. (2012) degrees in Biological Technology and Microbiology from Nankai University, China. He is currently a Ph.D. candidate in the Environmental Toxicology Graduate Program at the University of California Riverside under the supervision of Professor Yinsheng Wang. At the time of writing, Yang was close to completing his dissertation research project, which involves the development of mass spectrometric methods for the quantification of different types of structurally modified DNA and the application of these methods in assessing the biological implications of DNA adducts/modifications in various living cells/organisms.

Yuxiang Cui obtained her B.S. degree in Chemistry at Nankai University and M.S. degree in Food Safety and Toxicology at the University of Hong Kong. She joined the Environmental Toxicology Graduate Program at the University of California Riverside in 2014 and is currently a Ph.D. candidate under the guidance of Professor Yinsheng Wang.

Her research projects mainly focus on the development and application of LC-MS methods for the quantitative measurement of DNA adducts.

Laura Niedernhofer is an Associate Professor in the Department of Metabolism and Aging at The Scripps Research Institute in Florida. She has a Bachelor of Sciences in Chemistry from Duke University and completed the Medical Scientist Training Program at Vanderbilt University, earning her Ph.D. in Biochemistry. She followed this with postdoctoral training in mouse genetics at the Erasmus Medical Center in Rotterdam, The Netherlands. Her area of expertise is DNA damage and repair. Dr. Niedernhofer's current research program is focused on discovering the mechanism by which DNA damage contributes to aging and age-related diseases using genetic and pharmacologic approaches.

Yinsheng Wang obtained his Ph.D. in Chemistry from Washington University in St. Louis in 2001. He is currently a professor of Chemistry and the Director for the Environmental Toxicology Graduate Program at the University of California Riverside. Yinsheng's research concentrates on the use of mass spectrometry, along with molecular biology and/or synthetic organic chemistry, to understand the occurrence and biological consequences of DNA adducts and post-translational modifications of proteins.

Abbreviations

Acr-dG	acrolein N^2-(3-oxopropyl)-dG adduct
AD	Alzheimer's disease
AID/APOBEC proteins	activation-induced cytidine deaminase/apolipoprotein B mRNA editing enzyme, catalytic polypeptide-like proteins
AML	acute myeloid leukemia
AP site	apurinic/apyrimidinic site
BER	base excision repair
cdA	8,5′-cyclo-2′-deoxyadenosine
Cro-dG	crotonaldehyde N^2-(3-oxopropyl)-dG adduct
dA	2′-deoxyadenosine
dCMP	2′-deoxycytidine 5′-monophosphate
DDE	2,4-decadienal
dGh	guanidinohydantoin 2′-deoxynucleoside
dNIm	5-guanidino-4-nitroimidazole 2′-deoxynucleoside
DODE	9,12-dioxo-(10*E*)dodecenoic acid
DOOE	5,8-dioxo-(10*E*)-octenoic acid

DSB	double strand break
dSp	guanidinohydantoin 2′-deoxynucleoside
DHPN^{18}O$_2$	^{18}O-labeled 1,4-endoperoxide of *N*,*N*′-di(2,3-dihydroxypropyl)-1,4-naphthalene-dipropanamide
EDE	4,5-epoxy-(2*E*)-decenal
EndoV	endonuclease V
FA	Fanconi anemia
Fapy-dA	4,6-diamino-5-formamidopyrimidine 2′-deoxynucleoside
Fapy-dG	2,6-diamino-4-hydroxy-5-formamidopyrimidine 2′-deoxynucleoside
Fe-NTA	ferric nitrilotriacetate
FH	fumarate hydratase
Fpg	formamidopyrimidine DNA glycosylase
G(-H)$^{\bullet}$	guanine neutral radicals
HHE	4-hydroxy-2-hexenal
hAAG	alkyladenine DNA glycosylase
hMTH1	human MutT homologue
hNEIL1	human endonuclease VIII-like 1
hOGG1	human 8-oxoguanine DNA glycosylase 1
HNE	4-hydroxy-2-nonenal
HNE-dG	HNE N^2-(3-oxopropyl)-dG adduct
HPNE	4-hydroperoxy-(2*E*)nonenal
HOBr	hypobromous acid
HOCl	hypochlorous acid
H$_2$O$_2$	hydrogen peroxide
hRNAPII	human RNA polymerase II
M$_1$dA	N^6-(3-oxopropenyl)-2′-deoxyadenosine
M$_1$dC	N^4-(3-oxopropenyl)-2′-deoxycytidine
M$_1$dG	pyrimido[1,2-α]purine-10(3*H*)-one-2′-deoxyribose
MDA	malondialde-hyde

MEFs	mouse embryonic fibroblasts
mESCs	mouse embryonic stem cells
$N^2$3-ϵdG	N^2,3-etheno-2′-deoxyguano-sine
NADPH	nicotinamide adenine dinucleotide phosphate
NER	nucleotide excision repair
ODN	oligodeoxyribonucleo-tide
ONE	4-oxo-2-nonenal
$ONOO^-$	peroxynitrite
Pol η	DNA polymerase η
PUFA	polyunsaturated fatty acids
(*R*)-2-HG	(*R*)-2-hydroxyglutarate
ROS	reactive oxygen species
SDH	succinate dehydrogenase
SOD	superoxide dismutase
T7RNAP	T7 RNA polymerase
TDG	thymine DNA glycosylase
TET	ten-eleven translocation
thymidine glycol	5,6-dihydroxy-5,6-dihydro-2′-deoxythymidine
TLC	thin-layer chromatography
UPLC	ultraperformance liquid chromatography
1N^2-ϵdG	1,N^2-etheno-2′-deoxyguanosine
2-OG	2-oxoglutarate
5-Br-dC	5-bromo-2′-deoxycytidine
5-Br-dU	5-bromo-2′-deoxyuridine
5-Br-U	5-bromouracil
5-cadC	5-carboxyl-2′-deoxycytidine
5-Cl-C	5-chlorocytosine
5-Cl-dC	5-chloro-2′-deoxycytidine
5-Cl-dU	5-chloro-2′-deoxyuridine

5-Cl-rC	5-chlorocytidine
5-Cl-U	5-chlorouracil
5-fdC	5-formyl-2′-deoxycytidine
5-fdU	5-formyl-2′-deoxyuridine
5-hmdC	5-hydroxymethyl-2′-deoxycytidine
5-hmdU	5-hydroxymethyl-2′-deoxyuridine
5-mdC	5-methyl-2′-deoxycytidine
5-OH-8-oxo-dG	5-hydroxy-substituted derivative of 8-oxo-dG
8-Br-dA	8-chloro-2′-deoxyadenosine
8-Br-dG	8-chloro-2′-deoxyadenosine
8-Cl-dA	8-chloro-2′-deoxyadenosine
8-Cl-dG	8-chloro-2′-deoxyguanosine
8-Cl-G	8-chloroguanine
8-Cl-rA	8-chloroadenosine
8-Cl-rG	8-chloroguanosine
8-nitro-dG	8-nitro-2′-deoxyguanosine
8-oxo-dA	8-oxo-7,8-dihydro-2′-deoxyadenosine
8-oxo-dG	8-oxo-7,8-dihydro-2′-deoxyguanosine
εdA	1,N^6-etheno-2′-deoxyadenosine
εdC	3,N^4-etheno-2′-deoxycytidine

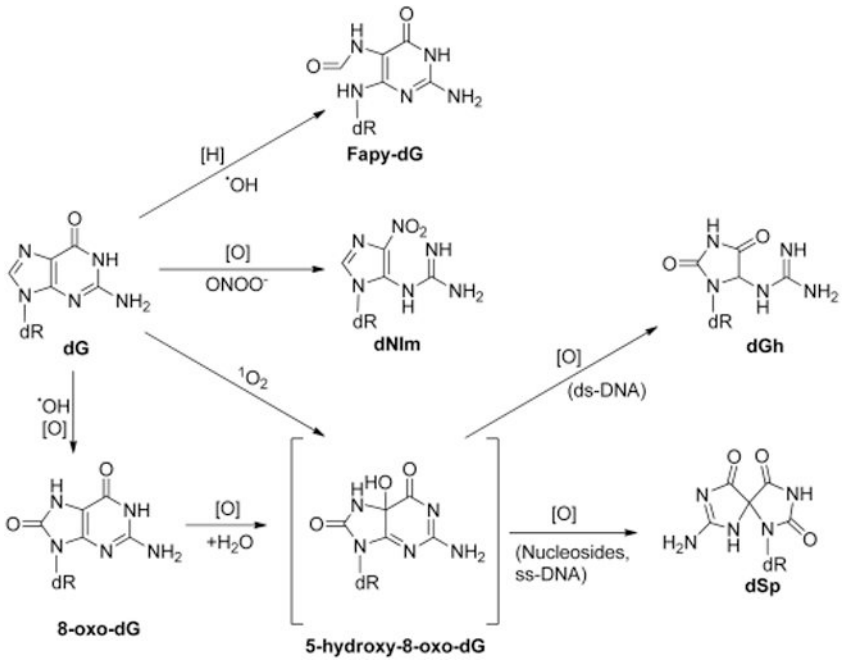

Figure 1.

ROS-induced primary and secondary oxidation products of dG. [H] and [O] represent reduction and oxidation, respectively.

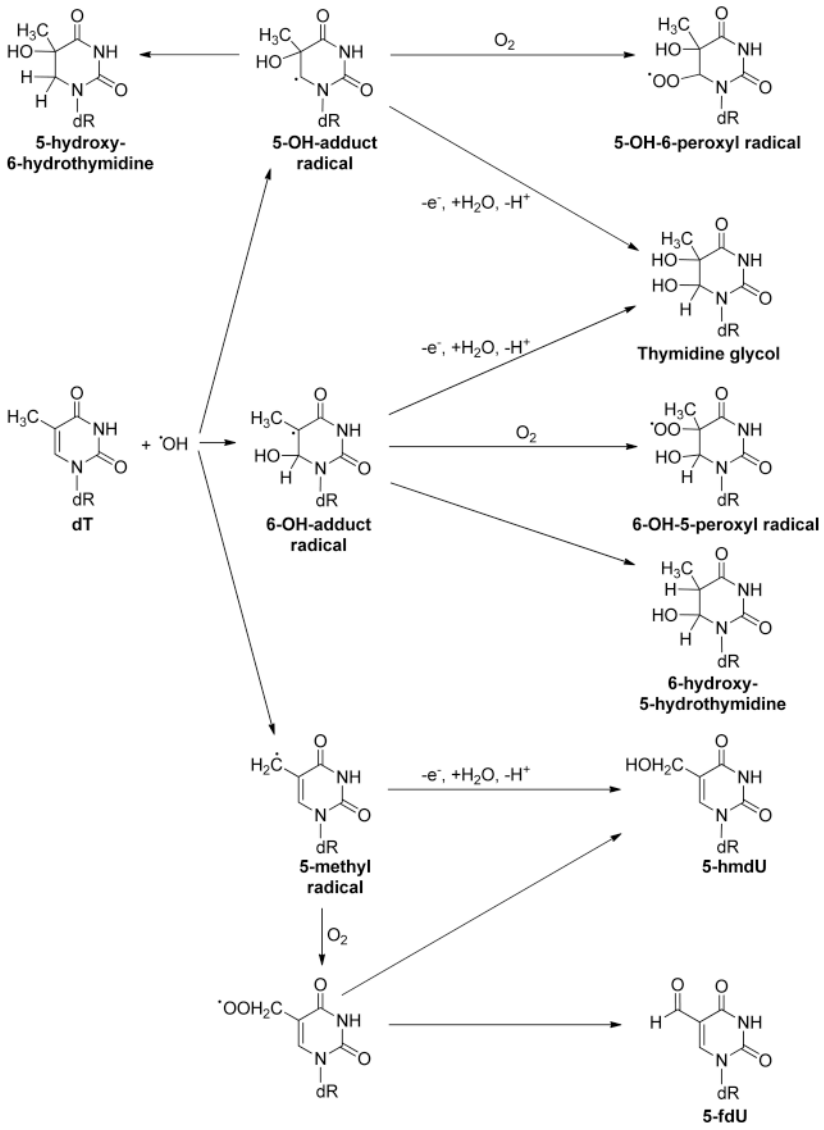

Figure 2.
Pathways for hydroxyl radical-mediated oxidation of dT.

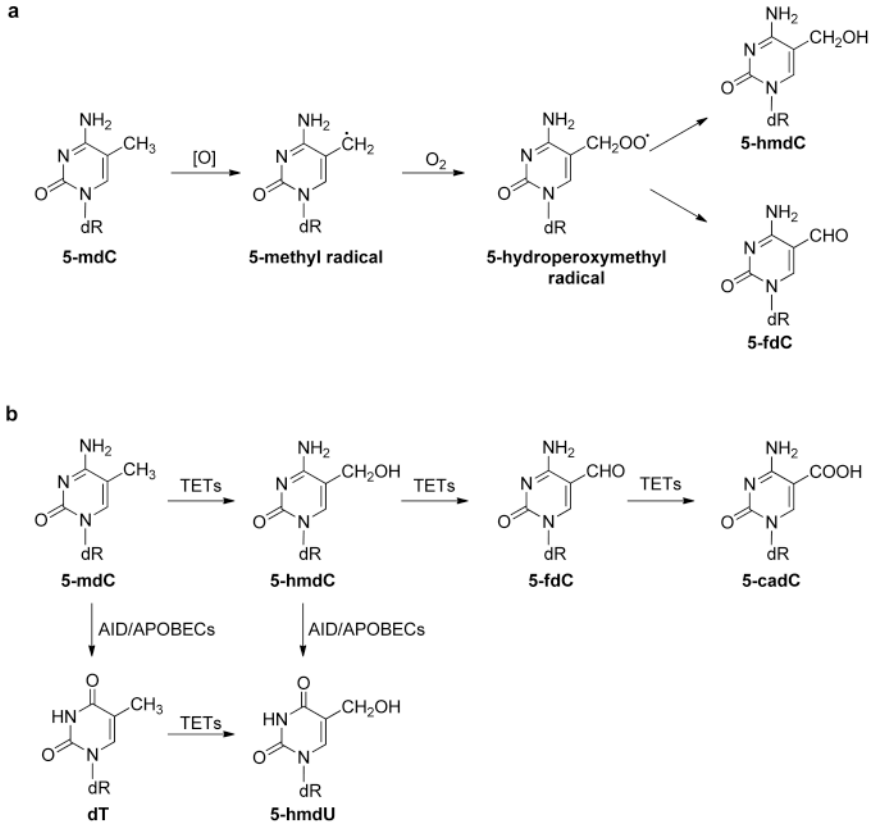

Figure 3.

Oxidation pathways of 5-mdC. (a) ROS-induced oxidation of 5-mdC; (b) TET-mediated oxidation of 5-mdC.

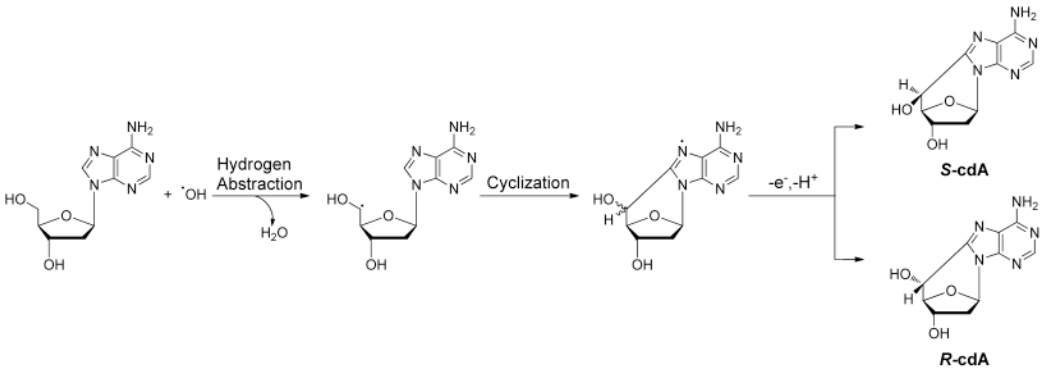

Figure 4.

Proposed mechanism for the formation of 5′*R*- and 5′*S* diastereomers of 8,5′-cyclo-2′-deoxyadenosine.

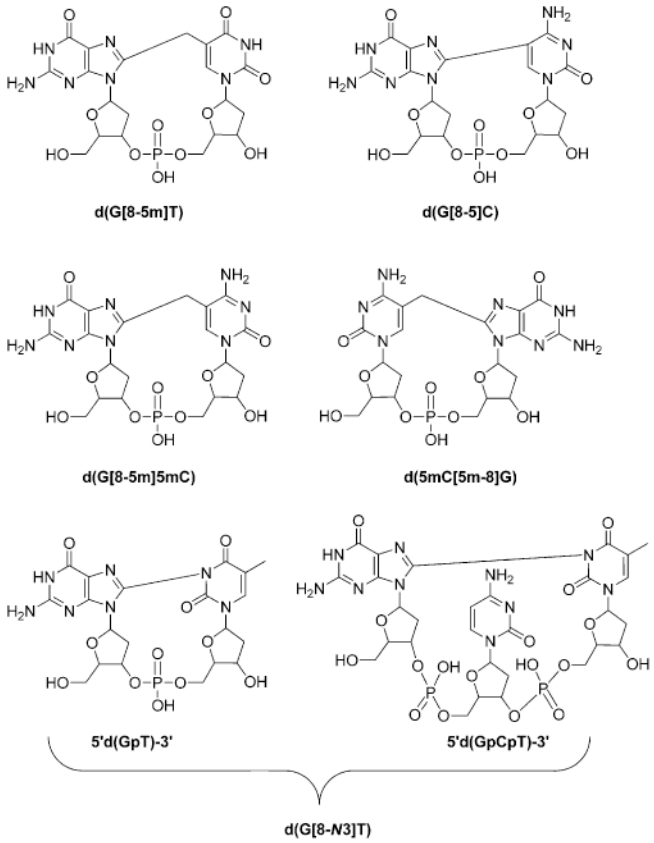

Figure 5.
Structures of ROS-induced intrastrand cross-link lesions discussed in this review.

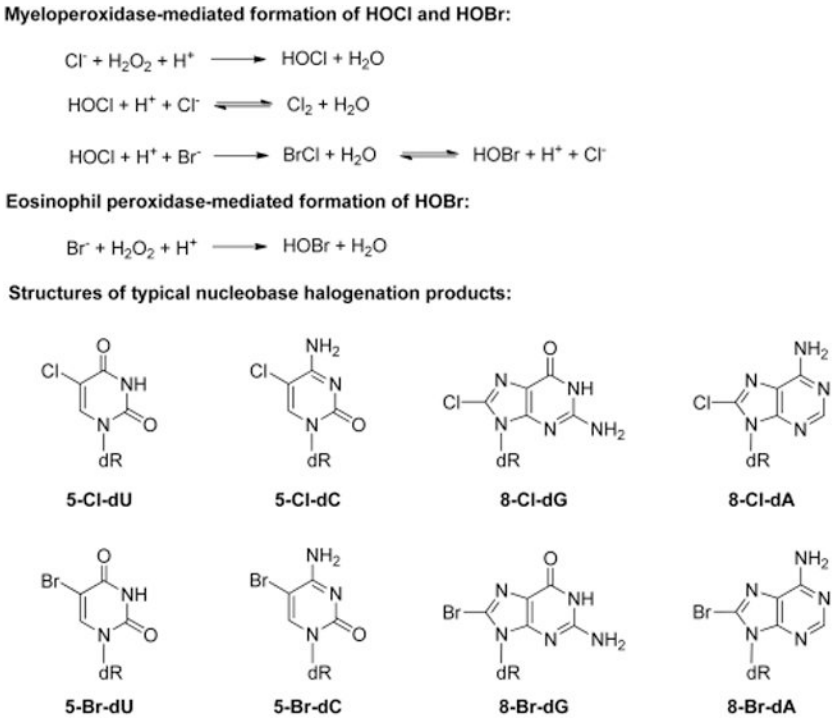

Figure 6.

Inflammation-induced formation of hypochlorous acid (HOCl) and hypobromous acid (HOBR) and major nucleobase halogenation products. Myeloperoxidase can induce the formation of both HOCl and HOBr. The mechanism for the formation of HOBr by myeloperoxidase is different from that by eosinophil peroxidase.

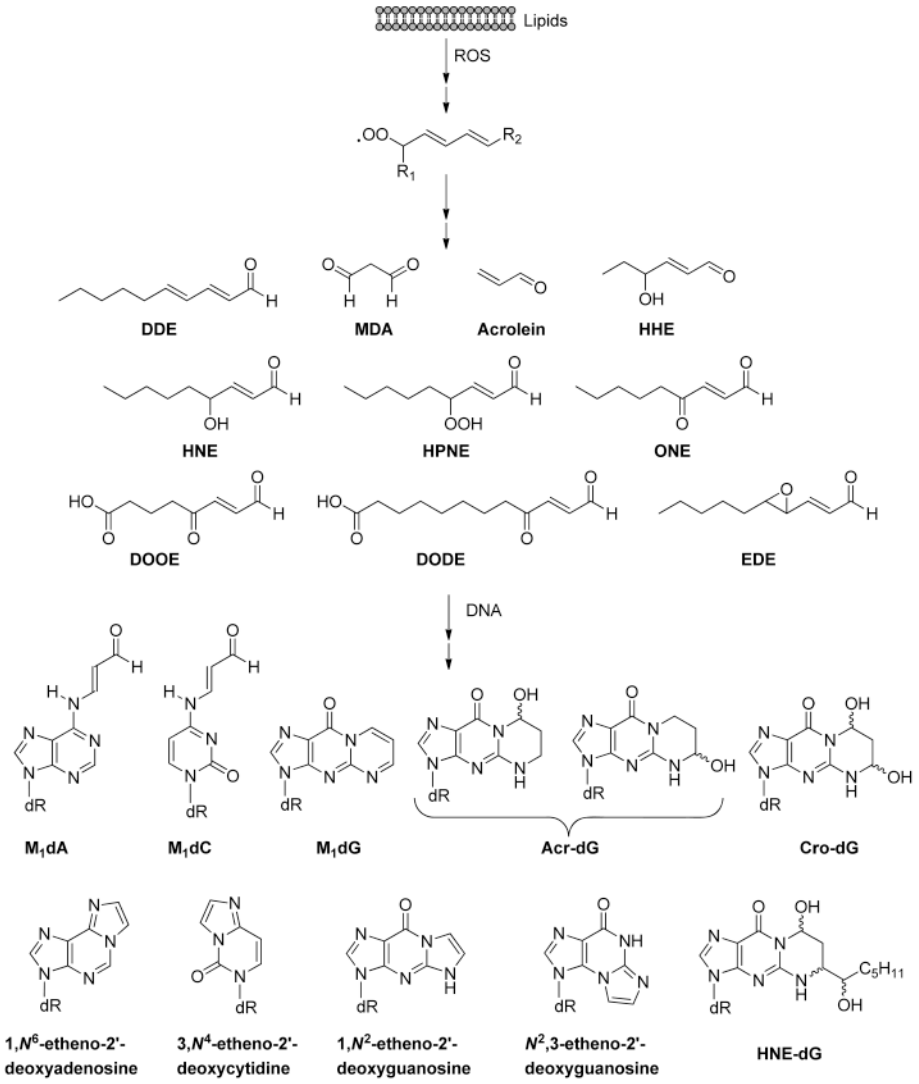

Figure 7.

Structures of representative lipid peroxidation (LPO) byproducts and DNA adducts induced by these byproducts.

Table 1

Summary of Findings Made from Cellular Replication Studies of Oxidative Stress-Induced DNA Lesions

DNA lesions	assay system	bypass efficiency	mutation type (frequency)	refererces
8-oxo-dG	M13 phage in *E. coli*	50–90%	G →T (~0.5–l%)	179
	M13 phage in *E. coli*		G →T (0.72%)	178
8-oxo-dA	double-stranded vector in NIH 3T3 cells		A → G + A → C (~1% in total)	180
Fapy-dG	single-stranded vector in COS-7 simian kidney cells		G → T (~8–30%)	181
			G → C (~2%)	
Fapy-dA	single-stranded vector in COS-7 cells		A → C (~0.4%)	181
dGh	single-stranded phage in wild-type AB1157 *E. coli* cells	~75 ± 5%	G → C (98%)	191
			G → T (2%)	
	single-stranded M13 phage in AB1157 *E. coli* cells (with MufY$^+$ or Mut Y$^-$)	~20% (MutY$^+$) ~30% (MutY$^-$)	for MutY$^+$ *E. coli*	192
			G → C (~57%)	
			G → T (~40%)	
			G → A (~3%)	
			no significant changes in mutation type or frequency were found in MutY$^-$ *E. coli* compared to MutY$^+$ *E. coli*	
dSp	single-stranded M13 phage in wild-type AB1157 *E. coli* cells	stereoisomer 1: ~9 ± 3%	stereoisomer 1:	191
			G → C (72%)	
			G → T (27%)	
		stereoisomer 2: ~9 ± 4%	stereoisomer 2:	
			G → C (57%)	
			G → T (41%)	
	single-stranded M13 phage in AB1157 *E. coli* cells (with MutY$^+$ or MutY$^-$)	MutY$^+$ strain: <20% for both stereoisomers; MutY$^-$ strain: ~30% for both stereoisomers	stereoisomer 1 (for MutY$^+$ *E. coli*): G → C (~19%)	192
			G → T (~78%)	
			G → A (~1%)	
			stereoisomer 2 (for MutY$^+$ *E. coli*):	
			G → C (~48%)	
			G → T (~49%)	
			G → A (~3%)	
			no significant changes in mutation type or frequency were found in MutY$^-$ *E. coli* compared to MutY$^+$ *E. coli*	
thymidine glycol	single-stranded M13 phage in *E. coli*	lethal	not detectable	202

DNA lesions	assay system	bypass efficiency	mutation type (frequency)	refererces
5-hmdU	ϕX-174am3 phage in *E. coli* spheroplasts		not detectable	214
5-fdU	double-stranded vectors in COS-7 simian kidney cells	not blocking	T → G + T → A (0.01–0.04% in total)	226
5-hmdC	single-stranded M13 phage in *E. coli* cells	~90–110%	C → G + C → T + C → A (0.17–1.12% in total)	240
	double-stranded vector in HEK-293T human kidney epithelial cells	~100%	not detectable	242
5-fdC	single-stranded M13 phage in *E. coli* cells	~90–110%	C → G + C → T + C → A (0.17–1.12% in total)	240
	double-stranded vector in COS-7 cells	39–90%	C → G + C → T + C → A (0.03–0.28% in total)	241
	double-stranded vector in HEK-293T cells	~70%	not detectable	242
5-cadC	single-stranded M13 phage in *E. coli* cells	~ 90–110%	C → G + C → T + C→A (0.17–1.12% in total)	240
	double-stranded vector in HEK-293T cells	~70%	not detectable	242
S-cdA	single-stranded M13 phage in *E. coli*	~10–31%	A → T (~11%)	253
	double-stranded vector in Pol η-deficient XP30RO cells and Pol η-complemented XP30RO cells	Pol η-deficient XP30RO cells: ~3%; Pol η-complemented XP30RO cells: ~5%	Pol η-deficient XP30RO cells: A →T (~S%) Pol η-complemented XP30RO cells: A → T (~9%)	254
S-cdG	single-stranded plasmid in *E. coli*	<1% without SOS induction; <5.5% with SOS induction	G→A+G→T + deletion of 5′C (~34% in total)	252
	single-stranded M13 phage in *E. coli*	~4–11%	G→A (~40% without SOS, ~20% with SOS)	253
	double-stranded vector in Pol η-deficient XP30RO cells and Pol η-complemented XP30RO cells	Pol η-deficient XP30RO cells: ~2%; Pol η-complemented XP30RO cells: ~4%	Pol η-deficient XP30RO cells: G→A (~3%)	254
			G →T (~27%);	
			Pol η-complemented XP30RO cells: G→A (~11%)	
			G →T (~32%)	
d(G[8-S]C)	single-stranded M13 phage in wild-type AB11S7 *E. coli*	20%	G →T (8.7%)	107
			G→C (1.2%)	
d(G[8-Sm]T)	single stranded pMS2 vector in *E. coli* (wild type and polymerase-deficient cells)	without SOS induction: 1.2–25%; with SOS induction: 3.1–35%	G→T (2.5% without SOS, 6.2% with SOS in wild-type cells)	258
5-Cl-dC	single-stranded M13 phage in *E. coli*	82–102%	C → T (~5%)	264
dNIm	single stranded M13mp7L2 bacteriophage genome in AB1157 *E. coli*	without SOS induction: 7%; with SOS induction: 57%	G → C (8.9%)	272
			G → A (19%)	
			G → T (22%)	
εdA	single-stranded pMS2 vector in *E. coli* and COS-7 cells		in *E. coli:* very limited mutations; in COS-7 cells:	275

DNA lesions	assay system	bypass efficiency	mutation type (frequency)	refererces
			A → G (63%)	
			A → T (6%)	
			A → C (1%)	
	single-stranded pMS2 vector and double-stranded pSBK vector in HeLa and HCT116 cells		ssDNA in HeLa cells:	277
			A → G (2%)	
			A → T (8%)	
			A → C (1%)	
			dsDNA in HeLa cells (leading strand):	
			A → G (2%)	
			A → T (7%)	
			A → C (5%)	
			dsDNA in HCT116 cells (leading strand):	
			A → G (5%)	
			A → C (2%)	
			dsDNA in HeLa cells (lagging strand):	
			A → G (5%)	
			A → T (4%)	
			A → C (1%)	
	double-stranded M13mp2S *Vori*L vectors in *E. coli*		A → C (1.6 X (10^{-4})	276
			A → G (2.9 X (10^{-4})	
			A → T (2.0 X 10^{-4})	
*e*dC	single-stranded pMS2 vector in *E. coli* or COS-7 cells		uninduced *E. coli* cells: C → A + C → T (2% in total)	278
			SOS-induced cells: C → A + C → T (32% in total)	
			COS-7 cells: C → A + C → T (81% in total)	
l,N^2-*e*dG	single-stranded M13MB19 phage in uvrA$^-$ *E. coli*		G → A (2.05%)	279
			G → T (0.74%)	
			G → C (0.09%)	
N^2,3-*e*dG	single-stranded M13G*1 phage in *E. coli*		G → A (0.5%)	280
M_1G	doubled stranded M13MB102 phage in wild-type LM102 cells *E. coli* cells	20% for the (–)-strand	G → A (0.35%)	284
			G → T (0.4%)	
			G → C (0.12%)	
	single-stranded pS189 vector and double-stranded M13MB102-1 vector in *E. coli* and COS-7 cells		−1 or −2 frameshift in *E. coli* and COS-7 with reiterated $(CpG)_4$ sequence (≤1% in total) G→A +G → T + G → C (≤2% in total)	286

Table 2

Summary of Findings Made from Cellular Transcription Studies of Oxidative Stress-Induced DNA Lesions

DNA lesions	assay system	transcription bypass efficiency	mutagenic properties	refs
8-oxo-dG	pBESTluc-fl luciferase reporter in *E. coli*	no detectable pausing or arrest	C → A (33%)	184,185
			deletion of the first base (26%)	
	pcDNA3.l(+) expression vector in mouse embryonic fibroblasts		$Ogg^{+/+}$ cells: C → A + one-nucleotide deletion (~2.6%)	187
			$Ogg^{-/-}$ cells: C → A + one-nucleotide deletion: (~10.8–13.9%)	
5-hmdC	double-stranded vector in HEK293T cells	~90–100%	not detectable	242
5-fdC	double-stranded vector in HEK293T cells	~69%	G → A (~1%)	242
5-cadC	double-stranded vector in HEK293T cells	~55%	G → A (~1%)	242
S-cdA	double-stranded vector in SV40-transformed NER-deficient XP12BE cells		5′A mutation (~30%); multiple nucleotide deletion (−7, −13, and −21 nt deletions, ~12.5%)	255
	double-stranded vectors in NER-proficient (GM00637) and NER-deficient (GM04429) human skin fibroblasts	increase with time, and up to 45% after 24 h in NER-proficient cells; no significant increase in bypass efficiency with time in NER-deficient cells	in NER-deficient cells: 5′A mutation (21%)	250
S-cdG	double-stranded vectors in NER-proficient (GM00637) and NER-deficient (GM04429) human skin fibroblasts	increase with time, and up to 45% after 24 h in NER-proficient cells; no significant increase in bypass efficiency with time in NER-deficient cells	in NER-deficient cells: 5′A mutation (32%)	250

Table 3
Levels of Oxidative Stress-Induced DNA Lesions in Cellular and Tissue DNA

DNA lesions	DNA sources	levels	refs
8-oxo-G/8-oxo-dG	mouse	~2.5–4/10^6 nucleosides in liver;	24,25
		~3–4/10^6 nucleosides in kidney;	
		~3/10^6 nucleosides in brain	
	mouse	~1–3/10^6 nucleosides in liver	27,28
	mouse	~ 1.5/10^6 nucleosides in brain;	23,26
		~3–4/10^6 nucleosides in liver;	
		~1–2/10^6 nucleosides in spleen	
8-oxD-A/8-oxo-dA	mouse	~0.3–0.5/10^6 nucleosides in brain;	23,26
		~0.2–0.4/10^6 nucleosides in liver;	
		~0.4–0.7/10^6 nucleosides in spleen	
Fapy-G/Fapy-dG	mouse	~0.6–1.2/10^6 nucleosides in liver;	24,25
		~1–2/10^6 nucleosides in kidney;	
		~0.7–1.4/10^6 nucleosides in brain	
	mouse	~6–14/10^6 nucleosides in liver	28
Fapy-A/Fapy-dA	mouse	~0.2–0.7/10^6 nucleosides in liver;	24,25
		~0.2–1.2/10^6 nucleosides in kidney;	
		~0.2–0.6/10^6 nucleosides in brain	
	mouse	~1–3/10^6 nucleosides in liver	27,28
dGh	mouse	1.08–3.14/10^8 nucleosides in colon;	131
		3.09–7.99/10^8 nucleosides in liver	
dSp	*E. coli*	~200–600/10^6 dG	197
	mouse	0.99–4.94/10^8 nucleosides in colon;	131
		2.74–20.8/10^8 nucleosides in liver	
thymine glycol/thymidine glycol	human urine	3.1 pmol/μmol of creatinine	293
	rat urine	4.8–8.9 nmol/kg per day	293
	mouse urine	8.62 nmol/kg per day	294
	monkey urine	2.07 nmol/kg per day	294
	human white blood cells	2.16 fmol/μg DNA (control); 2.83 fmol/μg DNA (ovarian cancer patients)	301
5-hmU/5-hmdU	HeLa cells	3.0/10^6 nucleosides	306
	WM-266–4	3.4/10^6 nucleosides	306
	human brain	3.9/10^6 nucleosides	306
	mouse brain	8.3/10^6 nucleosides	306
	mouse skin (red head)	6.4/10^6 nucleosides	306
	mouse skin (albino)	6.0/10^6 nucleosides	306
	LEA rat	2.6/10^6 nucleosides in liver;	85
		20.5/10^6 nucleosides in brain	
	LEC rat	3.2–8.6/10^6 nucleosides in liver;	85

DNA lesions	DNA sources	levels	refs
		12–28.3/10^6 nucleosides in brain	
	human brain	~2–3/10^6 nucleosides (control);	332
		~3–6/10^6 nucleosides (XPA-deficient)	
	mouse (control and *Ercc1*$^{-/c}$)	for control, ~6/10^6 nucleosides in liver, ~1–2/10^6 nucleosides in kidney and ~10/10^6 nucleosides in brain;	332
		For *Ercc1*$^{-/c}$, -4-20/10^6 nucleosides in liver, ~1–4/10^6 nucleosides in kidney and ~5–10/10^6 nucleosides in brain	
5-fU/5-fdU	Hela-S3 cells (exposed with edrays)	formation rate: 0.022 lesion/10^6 nucleosides/Gy	308
	LEA rat	7/10^6 nucleosides in liver;	85
		18.8/10^6 nucleosides in brain	
	LEC rat	7.8–31.4/10^6 nucleosides in liver;	85
		19.7–36.3/10^6 nucleosides in brain	
	human brain	~7–55/10^6 nucleosides (control);	332
		−10–45/10^6 nucleosides (XPA-deficient)	
	mouse (control and *Ercc1*$^{-/c}$)	for control, ~10–25/10^6 nucleosides in liver, ~5–20/10^6 nucleosides in kidney and ~9–10/10^6 nucleosides in brain;	332
		for *Ercc1*$^{-/c}$, ~10–95/10^6 nucleosides in liver, ~10–35/10^6 nucleosides in kidney and ~10–12/10^6 nucleosides in brain	
5-hmC/5-hmdC	mouse ES cells	1300/10^6 C	57
	LEA rat	339/10^6 nucleosides in liver;	88
		619/10^6 nucleosides in brain	
	LEC rat	176/10^6 nucleosides in liver;	88
		654/10^6 nucleosides in brain	
	human lung	0.078–0.182% dG in normal lung;	322
		0.033–0.096% dG in Stage-I lung squamous cell carcinoma (SCC)	
	human brain	0.817–1.175% dG in normal brain;	322
		0.028-0.753% dG in stage II/III astrocytomas	
	HeLa cells	31.2/10^6 nucleosides	306
	WM-266–4	12.2/10^6 nucleosides	306
	mouse ES cells	163/10^6 nucleosides	306
	human brain	1550/10^6 nucleosides	306
	mouse brain	560/10^6 nucleosides	306
	mouse skin (red head)	277/10^6 nucleosides	306
	mouse skin (albino)	217/10^6 nucleosides	306
5-fC/5-fdC	mouse ES cells	20/10^6 dC	57
	HeLa cells	0.67/10^6 nucleosides	306
	WM-266–4	0.69/10^6 nucleosides	306
	mouse ES cells	3.5/10^6 nucleosides	306
	human brain	1.7/10^6 nucleosides	306
	mouse brain	1.4/10^6 nucleosides	306
	mouse skin (red head)	1.2/10^6 nucleosides	306

DNA lesions	DNA sources	levels	refs
	mouse skin (albino)	0.7/10^6 nucleosides	306
5-caC/5-cadC	mouse ES cells	3/10^6 dC	57
	HeLa cells	0.27/10^6 nucleosides	306
	WM-266–4	0.29/10^6 nucleosides	306
	mouse ES cells	0.83/10^6 nucleosides	306
	human brain	0.15/10^6 nucleosides	306
	mouse brain	0.12/10^6 nucleosides	306
	mouse skin (red head)	0.21/10^6 nucleosides	306
	mouse skin (albino)	0.19/10^6 nucleosides	306
S-cdA	mouse	~0.1–0.2/10^6 nucleosides in brain;	23
		~0.2–0.35/10^6 nucleosides in liver;	26
		~0.15–0.2/10^6 nucleosides in spleen	
	LEA rat	0.11/10^6 nucleosides in liver;	85
		0.088/10^6 nucleosides in brain	
	LEC rat	0.14–0.56/10^6 nucleosides in liver;	85
		0.08–0.26/10^6 nucleosides in brain	
	mouse (control and *Csb*$^{-/-}$)	for control, ~0.05/10^6 nucleosides in brain, ~0.02/10^6 nucleosides in kidney and ~0.04/10^6 nucleosides in liver;	87
		for *Csb*$^{-/-}$, ~0.09/10^6 nucleosides in brain, ~0.06/10^6 nucleosides in kidney and ~0.08/10^6 nucleosides in liver	
	LEA rat	1.2/10^6 nucleosides in liver;	88
		1.54/10^6 nucleosides in brain	
	LEC rat	2.68/10^6 nucleosides in liver;	88
		1.41/10^6 nucleosides in brain	
	mouse (control and *Ercc1*$^{-/c}$)	for control, 0.21–0.42/10^6 nucleosides in liver, 0.26–1.25/10^6 nucleosides in kidney and 0.12–0.22/10^6 nucleosides in brain;	86
		for *Ercc1*$^{-/c}$, 0.96–4.09/10^6 nucleosides in livers, 0.19–1.81/10^6 nucleosides in kidney and 0.1–0.21/10^6 nucleosides in brain	
	mouse (albino and red head)	~0.15/10^6 nucleosides (albino); ~0.35/10^6 nucleosides (red head);	89
R-cdA	mouse	~0.025–0.035/10^6 nucleosides in brain;	23
		~0.02–0.05/10^6 nucleosides in liver;	26
		~0.04-0.05/10^6 nucleosides in spleen	
	LEA rat	0.1/10^6 nucleosides in liver;	85
		0.15/10^6 nucleosides in brain	
	LEC rat	0.18–0.48/10^6 nucleosides in liver;	85
		0.13–0.56/10^6 nucleosides in brain	
	mouse (control and Ercc1$^{-/c}$)	for control, 0.17–0.95/10^6 nucleosides in liver, 0.2–0.65/10^6 nucleosides in kidney and 0.08–0.16/10^6 nucleosides in brain;	86
		for *Ercd*$^{-/c}$, 2.54–8.37/10^6 nucleosides in liver, 0.27–0.72/10^6 nucleosides in kidney and 0.09–0.17/10^6 nucleosides in brain	
	mouse skin (albino and red head)	~0.15/10^6 nucleosides (albino); ~0.3/10^6 nucleosides (red head);	89

DNA lesions	DNA sources	levels	refs
S-cdG	mouse	~2–3.5$10^6$ nucleosides in brains	23
		~1–1.5/10^6 nucleosides in liver;	26
		~2.5–3.5/10^6 nucleosides in spleen	
	LEA rat	0.19/10^6 nucleosides in liver;	85
		0.16/10^6 nucleosides in brain	
	LEC rat	0.20–1.08/10^6 nucleosides in liver;	85
		0.14–0.43/10^6 nucleosides in brain	
	LEA rat	2.02/10^6 nucleosides in liver;	88
		2.31/10^6 nucleosides in brain	
	LEC rat	4.45/10^6 nucleosides in liver;	88
		2.21/10^6 nucleosides in brain	
	mouse (control and *Ercc*$^{-/c}$)	for control, 0.32–1.05/10^6 nucleosides in liver, 0.91–2.86/10^6 nucleosides in kidney and 0.37–0.53/10^6 nucleosides in brain;	86
		for *Ercd*$^{-/c}$, 2.03–5.64/10^6 nucleosides in liver, 0.53–2.81/10^6 nucleosides in kidney and 0.25–0.66/10^6 nucleosides in brain	
	mouse skin (albino and red head)	~0.35/10^6 nucleosides (albino); ~0.75/10^6 nucleosides (red head);	89
R-cdG	mouse	~0.5–0.8/10^6 nucleosides in brain;	23
		~0.5–0.55/10^6 nucleosides in liver;	26
		~0.5–0.6/10^6 nucleosides in spleen	
	LEA rat	0.13/10^6 nucleosides in liver;	85
		0.14/10^6 nucleosides in brain	
	LEC rat	0.16–0.54/10^6 nucleosides in liver;	85
		0.13–0.52/10^6nucleosides in brain	
	mouse (control and *Ercc1*$^{-/c}$)	for control, 0.14–1.01/10^6 nucleosides in liver, 0.35–0.73/10^6 nucleosides in kidney and 0.11–0.17/10^6 nucleosides in brain;	86
		for *Ercrf*$^{-/c}$, 2.43-7.31/10^6 nucleosides in liver, 0.28–0.73/10^6 nucleosides in kidney and 0.11–0.21/10^6 nucleosides in brain	
	mouse skin (albino and red head)	~0.15/10^6 nucleosides (albino); ~0.3/10^6 nucleosides (red head);	89
d(G[8-5]C)	Hela-S3 cells (with *γ* irradiation)	formation rate: ~0.037 lesions/10^9 nucleosides per Gy	106
d(G[8-5m]T)	Hela-S3 cells (with *γ* irradiation)	formation rate: 0.05 lesion/10^9 nucleosides/Gy	107
	LEA rat	~0.005/10^6 nucleosides in liver;	332
		~0.02/10^6 nucleosides in brain	
	LEC rat	~0.01–0.04/10^6 nucleosides in liver;	332
		~0.01–0.08/10^6 nucleosides in brain	
	mouse liver (control and XPA-deficient)	~0.005/10^6 nucleosides (control);	332
		~0.01/10^6 nucleosides (XPA-deficient)	
	human brain (control and XPA-deficient)	~0.005–0.04/10^6 nucleosides (control);	332
		~0.015–0.07/10^6 nucleosides (XPA-deficient)	

DNA lesions	DNA sources	levels	refs
	mouse (control and *Ercc1*$^{-/c}$)	for control, ~0.007~0.01/10^6 nucleosides in liver, ~0.015–0.02/10^6 nucleosides in kidney and ~0.001–0.005/10^6 nucleosides in brain; for *Ercc1*$^{-/c}$, ~0.008–0.035/10^6 nucleosides in liver, ~0.01–0.045/10^6 nucleosides in kidney and 0.001–0.007/10^6 nucleosides in brain	332
d(G[8-*N*3]T)	HeLa cells (with 266 nm laser pulse irradiation)	0.21–1.19/10^6 nucleosides	111
5–Cl-C/5-Cl-dC	mouse	3.86–7.06/10^8 nt in colon; 4.33–16.61/10^8 nt in liver	131
	human leukocyte	0.06–0.4/10^6 nucleosides	127
	human endothelial cell (treated with 300 μM HOC1)	40/10^6 dC	343
	human colon (from patients with inflammatory bowel disease)	0.002–0.294/10^6 nucleobases	132
	mouse colon (*H. hepaticus*-infected)	0.031–0.129/10^6 nucleobases	132
5–Br-C/5-Br-dC	human eosinophils	−60–225/10^6 cells	117
5–C1-U/5-CU1U	rat	20–80 pg/pouch	341
	human atherosclerotic tissue	~0.1 pmol/g tissue (normal); ~0.7 pmol/g tissue (atherosclerotic)	342
5–Br-U/5-Br-dU	human atherosclerotic tissue	~0.08 pmol/g tissue (normal); ~0.18 pmol/g tissue (atherosclerotic)	342
M_1G/M_1dG	human	0.5–1.2/10^6 nucleosides in liver; 0.05–2.8/10^6 nucleosides in white cells; 0.001–0.5/10^6 nucleosides in pancreas; 0.002–0.56/10^6 nucleosides in breast	13
	human leukocyte	64.9 fmol/mg DNA in smokers; 56.5 fmol/mg DNA in nonsmokers	171
	rat liver	0.52/10^6 nucleosides	172
	human colorectal mucosa	0.43/10^6 nucleosides for men; 4.6/10^6 nucleosides for women	174
εA/εdA	human asymptomatic colon epithelia	~0.025–0.065/10^6 nucleosides	154
	rats exposed to 600 ppm vinyl chloride (4 h/day for 5 day)	0.21/10^6 nucleosides in liver; 0.65/10^6 nucleosides in lung; 0.04/10^6 nucleosides in kidney	155
	human placenta	2.3–2.5/10^6 nucleosides	161
	human	0.282/10^6 nucleosides in placenta; 0.162/10^6 nucleosides in leukocyte;	163
	human saliva	0.22–2.1/10^6 nucleosides	165
	LEC rat liver	~0.002–0.1/10^6 nucleosides	170
	LEA rat	0.23/10^6 nucleosides in liver; 0.39/10^6 nucleosides in brain	88
	LEC rat	0.3/10^6 nucleosides in liver; 0.44/10^6 nucleosides in brain	88
1, N^2-εG/l, N^2-εdG	human IMR-90 cells	~0.02/10^6 nucleosides	152
	human urine	95 pg/mL for smokers;	

DNA lesions	DNA sources	levels	refs
		50–68 pg/mL for nonsmokers	
	human	0.085/10^6 nucleosides in placenta	163
		0.086/10^6 nucleosides in leukocyte;	
	human saliva	0.68–7.52/10^6 nucleosides	165
	Wistar rat	2.47/10^8 dG in livers;	168
		0.87/10^8 dG in lungs;	
		2.96/10^8 dG in brains	
	LEA rat	0.11/10^6 nucleosides in livers; 0.15/10^6 nucleosides in brains	88
	LEC rat	0.16/10^6 nucleosides in livers; 0.13/10^6 nucleosides in brains	88
εC/εdC	human asymptomatic colon epithelia	~0.015–0.035/10^6 nucleosides	154
	rats exposed to 600 ppm vinyl chloride (4 h/day for 5 days)	0.98/10^6 nucleosides in liver;	155
		0.3/10^6 nucleosides in lung;	
		0.29/10^6 nucleosides in kidney	
	human	0.441/10^6 nucleosides in placenta	163
		0.111/10^6 nucleosides in leukocyte;	
	human urine	104–105 pg/mL	164
	human saliva	0 –1.39/10^6 nucleosides	165
	human urine	0.45 nM for smokers;	166
		0.16 nM for nonsmokers	
	LEC rat liver	~0.035–0.25/10^6 nucleosides	170
N^2,3-εG/N^2,3-εdG	rats exposed to 600 ppm vinyl chloride (4 h/day for 5 days)	1.81/10^6 nucleosides in liver:	155
		0.21/10^6 nucleosides in lung;	
		0.31/10^6 nucleosides in kidney	
Acr-dG	human	0.78/10^6 nucleosides in leukocyte;	159
		1.08/10^6 nucleosides in placenta	
	human saliva	0.13/10^6 nucleosides	165
	human brain	5.15/10^6 nucleosides (with Alzheimer's disease);	336
		2.8/10^6 nucleosides (control)	
Cro-dG	human IMR-90 cells	~0.05/10^6 nucleosides	152
	human	0.06/10^6 nucleosides in leukocyte;	159
		0.26/10^6 nucleosides in placenta	
	human saliva	0–0.485/10^6 nucleosides	165
	human	14.57/10^9 dG in livers; 19.99/10^9 dG in lung	167
	Wistar rat	4.61/10^8 dG in liver;	168
		2.25/10^8 dG in lung;	
		5.66/10^8 dG in brain	

Table 4
Repair Mechanisms of Oxidative Stress-Induced DNA Lesions

DNA lesions/modifications	repair pathways	refs
8-oxo-dG	BER	25,27,188–190
8-oxo-dA	BER	25,27,188–190
Fapy-dG	BER	25,27,188–190
Fapy-dA	BER	25,27,188–190
dGh	BER	193,195–198
dSp	BER	193,195–198
thymidine glycol	BER	206,207,210
	NER	211
5-hmdU	BER	188,219,220
5-fdU	BER	228,230–236
5-fdC	BER	65,220,246,247
5-cadC	BER	65,220,246,247
R/*S*-cdA	NER	86,91,249,250
R/*S*-cdG	NER	86,91
d(G[8-5]C)	NER	257
d(G[8-5m]T)	NER	256,257,332
d(G[8-*N*3]T)	NER	259
	BER	260
8-Cl-dG	BER	262
5-Cl-dU	BER	263
dNIm	BER	199
εdA	AlkB/ALKBH	281,282
	BER	281
εdC	AlkB/ALKBH	281,282
	BER	281
1,N^2-εG/1,N^2-εdG	AlkB/ALKBH	281,282
	BER	281
N^2,3-εG/N^2,3-εdG	AlkB/ALKBH	282
		281
	BER	281
M_1dG	AlkB/ALKBH	287
	NER	14
Acr-dG	AlkB/ALKBH	287
	NER	14
Cro-dG	NER	14